Strategies to improve intracellular drug delivery by targeted liposomes

Marjan Fretz

Printed by PrintPartners Ipskamp B.V. Enschede

ISBN 90-393-4521-4

The research described in this thesis was performed at the Department of Pharmaceutics, Utrecht Institute of Pharmaceutical Sciences, Utrecht University, Utrecht, The Netherlands and at the Welsh School of Pharmacy, Cardiff University, Cardiff, United Kingdom

Strategies to improve intracellular drug delivery by targeted liposomes

Ontwikkeling van liposoom systemen voor intracellulaire afgifte van farmaca

(met een samenvatting in het Nederlands)

PROEFSCHRIFT

ter verkrijging van de graad van doctor aan de Universiteit Utrecht op gezag van de rector magnificus, prof. dr. W.H. Gispen, ingevolge het besluit van het college voor promoties in het openbaar te verdedigen op woensdag 16 mei 2007 des middags te 12.45 uur

door

Marjan Maria Fretz

geboren op 5 mei 1978, te ‘s Gravenhage

Promotoren: Prof. dr. G. Storm
Prof. dr. W. Jiskoot

Co-promotor: Dr. A.T. Jones

The printing of this thesis was financially supported by:

PCI Biotech

Katchem Ltd.

Merck KGaA

Utrecht University

TABLE OF CONTENTS

1

General Introduction

DRUG TARGETING

Targeted drug delivery systems aim to increase the therapeutic activity of drug molecules by facilitating and enhancing their localisation in target organs/tissue and cells (site-specific delivery) and/or to decrease their side effects by opposing and diminishing localisation at those body sites that are particularly sensitive to the toxic actions (site-avoidance delivery) (1, 2). Drug targeting can be considered at different levels within the body: 1. at the organ/tissue, 2. at the target cell and 3. at the subcellular compartment within the target cell (Figure 1). Many diseases are resident to a single organ, which makes it a challenge to develop drug targeting vehicles that deliver high concentrations of the drug within that organ. However, this level of targeting may not only affect the diseased cells, but also the healthy cells in that organ. Therefore, the second level of targeting, cell-specific targeting is often desired, for example to cancer cells within the targeted organ. The third level, subcellular targeting, is the localisation of a drug at a specific intracellular compartment within the target cell, like the cytosol, nucleus or mitochondria. For example, in the case of gene therapy targeting DNA to the nucleus to improve transgene expression (3, 4).

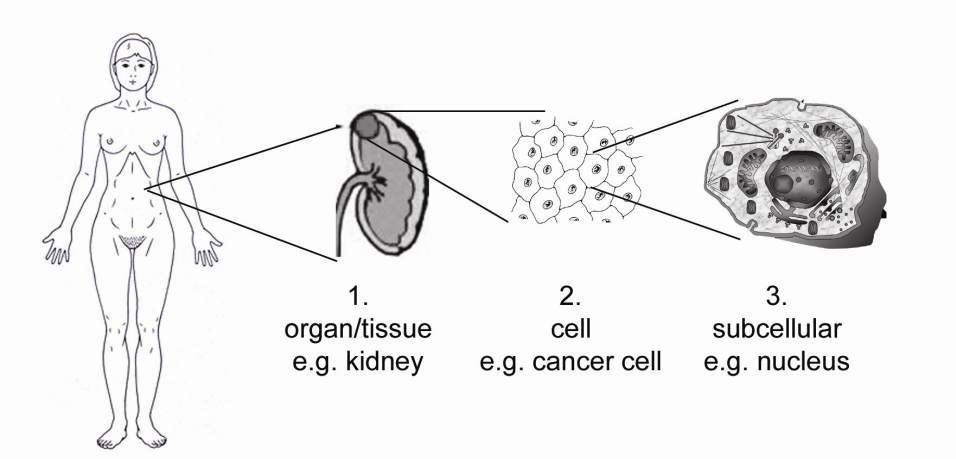

Figure 1. Different levels of drug targeting (Figure adapted from (3))

In 1986, Maeda and Matsumura proposed a novel targeting strategy to solid tumours using a *passive targeting* mechanism: the so-called enhanced permeability and retention effect (EPR effect) (5). At pathological sites, such as tumours and inflammation, the permeability of the vasculature is often enhanced. This increased permeability allows extravasation of macromolecules and colloids from the bloodstream into the diseased site. In addition, the lymphatic drainage system malfunctions in tumour tissue, causing prolonged retention of the macromolecules in the tumour interstitium. It is now well established that long-

circulating macromolecules (e.g. albumin) and particulates (including polymer conjugates, polymeric micelles and liposomes) accumulate passively in solid tumour tissue by the EPR effect, and that intravenously administered drug targeting systems can increase the tumour concentration up to a level of 70-fold (6).

The second level of targeting, i.e. cell-specific targeting deals with carrier systems presenting targeting ligands on their surface (*active targeting*). These ligands are directed against receptors or epitopes that are uniquely expressed or overexpressed on target cells. Ideally, the target antigen or receptor must be present in high density only on the target cells and has a homogeneous level of expression throughout the tumour tissue (3, 7). Some examples of receptors overexpressed by cancer cells and to be exploited by actively targeted drug delivery systems are the folate receptor (8), the transferrin receptor (9) and the epidermal growth factor receptor (10). Cellular adhesion molecules which are present on angiogenic blood vessels are also utilised for targeting cancer and rheumatoid arthritis (11, 12). Targeting ligands can be antibodies or antibody fragments, proteins, peptides and saccharides (3, 7).

Binding of ligands and ligand-exposing targeting systems to their receptor may result in internalisation. Whether this is desirable depends on the therapeutic aim. For example, cellular internalisation is essential to achieve therapeutic activity of immunotoxins. However, for antibody-directed enzyme-prodrug therapy (ADEPT), internalisation should not occur as the targeted enzyme needs to remain extracellular to convert the corresponding prodrug (14).

CELLULAR UPTAKE AND PROCESSING

Most macromolecules, like proteins and (ribo)nucleic acids, and macromolecular and particulate drug carrier systems have limited cell entrance due to cell membrane passage difficulties. Cellular uptake of these molecules is restricted to endocytosis. Different endocytosis pathways have been identified, e.g. clathrin- and caveolae-mediated endocytosis and macropinocytosis (15). Via which endocytic route the macromolecule or drug delivery vehicle will be taken up by the cell, depends on several factors, like the size of the system, the presence and type of targeting ligand and cell type. Upon endocytosis, drugs are processed from early to late endosomes with lysosomes as final destination. The harsh environment of the lysosomes with low pH and destructive enzymes will cause inactivation and degradation of most macromolecules and particles. Unless the target lies within the endocytic pathway (e.g. in the case of lysosomal storage diseases), strategies need to be explored to enable the drug to reach the cytosol in its active form (16). Besides rather invasive strategies that circumvent endocytosis, such as microinjection, electroporation and the use of detergents (17), approaches with ‘smart’ drug carrier systems with endosomal escape mechanisms are being studied. Examples include carriers systems composed of pH-responsive polymers such as poly(ethyleneimine) (PEI) (18), poly(alkylacrylic acid) (19,

20) and poly(amidoamines) (21, 22) and the use of pH-sensitive peptides like peptides derived from the influenza virus haemagglutinin (23, 24) and the synthetically designed GALA peptide (25). Literature also describes the use of pH-sensitive lipids in lipoplex and liposome formulations (26). Circumventing endocytosis by using cell-penetrating peptides is discussed in a later section.

When arrived in the cytoplasm, the (macromolecular) drug needs to find its subcellular target site. In the case of gene therapy, the DNA drug needs to be transported to and into the nucleus. Nuclear localisation signals (NLS) are being investigated to achieve this (27, 28). Also, motifs targeting mitochondria have been reported useful to target e.g proapoptotic drugs to the mitochondria (29).

LIPOSOMES AS TARGETED DRUG CARRIER SYSTEM

Liposomes are nano-sized artificial vesicles composed of one or more (phospho)lipid bilayers enclosing aqueous compartments. In the 1960s they were used as model membranes (30, 31). Interest for drug delivery purposes arose a decade later (32). A major feature of liposomes is that hydrophilic (in the inner aqueous compartment), lipophilic (in the hydrophobic compartment of the lipid bilayer) and amphiphilic drugs can be encapsulated. Liposomes alter the pharmacokinetics of a drug and give protection against degradation. First generation liposomes, also referred to as conventional liposomes, which are 'just' plain phospholipid vesicles with cholesterol, did not show the expected in vivo results. They often had poor stability in plasma and unexpectedly high levels of the liposomes and encapsulated drug were found in the liver and spleen. Due to opsonisation, the reticulo-endothelial system (RES) rapidly removes the liposomes from the bloodstream (33, 34). Coating the liposomes with hydrophilic polymers, like poly(ethylene glycol) (PEG) was introduced to stabilise the liposomes and to enhance their circulation time (e.g. up to a half life of 45 hrs in humans). Those liposomes are now called 'sterically stabilised liposomes' or 'stealth liposomes'. Owing to the passive targeting effect, enhanced localisation of stealth liposomes in tumour tissue and other pathological sites can be achieved (35-37).

To further improve cellular specificity and facilitate cellular uptake of liposomes, specific ligands have been attached to liposomes, such as antibodies or antibody fragments, folic acid, EGF and peptides. Those liposomes are generally referred to as targeted liposomes or immunoliposomes when (fragments of) antibodies are used as targeting ligand. Initially, targeting moieties were directly coupled to the phospholipid bilayer, however, after the development of sterically stabilised liposomes, ligands are often coupled to the distal ends of the PEG-coating. Both in vitro and in vivo results have shown that such ligand-targeted liposomes can increase the therapeutic efficacy of encapsulated drugs compared to non-targeted liposomes. The active targeting strategy with liposomes is adequately reviewed in (38-41). Different types of liposomes are shown in Figure 2.

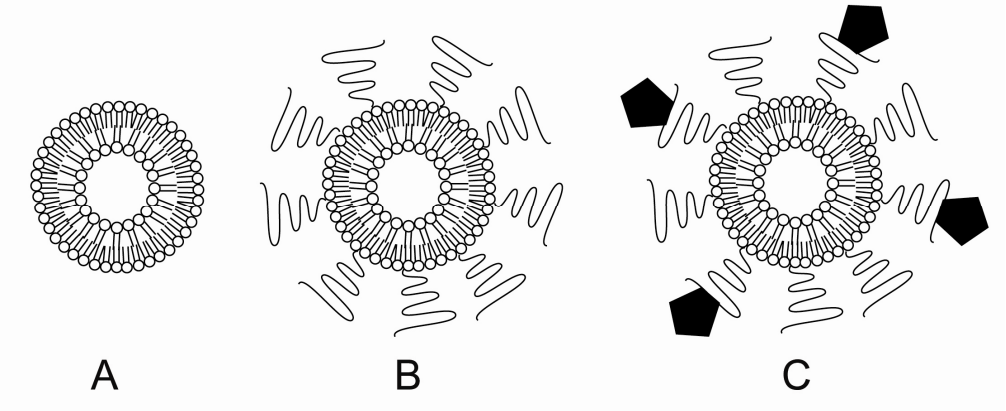

Figure 2. Different lipsome types. Conventional (A), pegylated liposomes (B) and ligand targeted liposomes (C)

After binding of the actively targeted liposomes to their target cell surface, various processes may lead intracellular drug delivery. First, drugs may be released from cell-bound liposomes into the extracellular space, followed by subsequent diffusion of the released drug molecules over the plasma membrane. This extracellular release might be triggered by heat, light or enzymes (42). Second, lipophilic compounds embedded in the lipid bilayer may be transferred from the liposome bilayer to the plasma membrane of the cell (43, 44). Third, internalisation via endocytosis leads to localisation in the endosomal/lysosomal compartment. For large hydrophilic drug molecules, like proteins, peptides and nucleic acids, only the third option is feasible, since the physiochemical properties of the macromolecules will hamper their diffusion over the plasma membrane. And since the target of these molecules is often intracellular this is a major problem. Target cell binding of targeted liposomes will also not always result in internalisation of the liposomes, which obviously impedes the therapeutic efficacy as well (45). Whether targeted liposomes are internalised or not depends on the target antigen, target cell type and other factors that are not fully understood yet. Even if liposomes are internalised via endocytosis, therapeutic activity is not guaranteed as degradation of the liposome and its encapsulated drugs can occur in the endosomes/lysosomes. Therefore, several strategies are under investigation to design pH-sensitive liposome systems that enable endosomal escape of the liposomal contents. The use of pH-dependent membrane- destabilising lipids is widely studied and a variety of different lipids are used with this approach. These lipids undergo a phase transition at the low pH environment in the endo-/ lysosomes and they promote fusion with and/or destabilisation of the endosomal membrane. This approach is reviewed in (26). A second approach makes use of the incorporation of fusogenic proteins or peptides into the liposomes. Those proteins and peptides, mostly derived from pathogens like viruses and

bacteria, also destabilise membranes in a pH dependent manner (46-48). Recently, Torchilin *et al.* showed that endocytosis could be circumvented by coupling of so-called cell-penetrating peptides (CPP) to the surface of liposomes, which appeared to induce direct translocation of the liposome particles over the plasma membrane (49). This approach, also investigated in this thesis, is discussed in the next section.

CELL-PENETRATING PEPTIDES

The interest for the use of cell-penetrating peptides (CPP) in drug delivery was evoked when it was found that conjugation of these peptides to fluorochromes (50), peptides (51), proteins (52, 53), oligonucleotides (54) and even colloidal systems like superparamagnetic nanoparticles (55) or liposomes (49, 56), leads to transportation of the cargo into the cytoplasm of the cell. Studies at low temperature and in the presence of metabolic inhibitors suggested that the uptake mechanism was energy-independent, which excluded occurrence of endocytosis. The proposed uptake mechanism was called translocation or transduction and seemed to be non-saturable, very fast (within minutes), and independent of energy and cell type. The CPP and cargo were proposed to be directly transported from the extracellular space into the cytoplasm and frequently into the nucleus of the cells. (50). Especially macromolecules like peptides, protein and nucleic acids, labile in the endo-/lysosomal vesicles, would benefit from this uptake mechanism. However, doubts were raised about the CPP-mediated translocation process as uptake mechanism when Lundberg and Johansson described the redistribution of CPP after cell fixation. They found that the (sub)cellular distribution of the peptides changed completely when live cells were compared to methanol-fixed cells (57). The fixation-induced redistribution was then described by others (58, 59) and the general nature of the translocation mechanism was being questioned more and more. This was supported by literature reporting that the uptake of CPP could be abolished by endocytosis inhibitors like low temperature and cytochalasin D when live cell imaging was used (58). In spite of the current assumption for endocytosis as CPP uptake mechanism, recently also reports were published on possible uptake mechanisms other than endocytosis. Zaro and Chen developed a cellular fractionation method and with this method they showed that nona-arginine and guanidinated nona-lysine were preferentially transduced to the cytosolic compartment, whereas nona-lysine was internalised via endocytosis (60). The importance of a guanidinium group for translocation was already proposed earlier by Mitchell *et al*. They compared polyarginine with other polycationic homopolymers like polylysine, polyhistidine and polyornithine. Flow cytometry and live cell confocal microscopy showed that polyarginine internalised by Jurkat cells much more efficiently than the other polypeptides. Microscopy data demonstrated that polyarginine was distributed throughout the whole cell and did not show any distinct endocytic localisation (61). Rothbard *et al.* speculated that the polarity of the polyarginine is changed through association with cell surface headgroups bearing negative charges, which produces a less

polar ion pair capable of diffusing through the plasma membrane. Additionally, they hypothesised that the membrane potential might be the driving force behind the translocation mechanism. This was supported by findings that reduction of the membrane potential resulted in extensive decrease in the amount of cell-associated peptide (62). Recently, the influence of the cargo (size) was also investigated; conjugation of larger cargoes, (e.g. peptides, proteins and quantum dots) to CPP seems to alter the mode of cellular uptake and translocation properties (63, 64).
Before CPP are to be used as drug delivery tools, the cellular uptake mechanism of both free CPP and CPP conjugated to a cargo should be investigated in more detail.

PHOTOCHEMICAL INTERNALISATION

One method currently explored to achieve better intracellular delivery of drugs is a technique called photochemical internalisation (PCI). Photosensitisers are used to induce rupture of the endosomal membrane and to achieve subsequent release of endocytosed material into the cytoplasm Photosensitisers are compounds that upon illumination with light of a specific wavelength can go from their ground state to an excited state. From this excited state, the energy can be transferred to other molecules, like oxygen leading to the formation of singlet oxygen which is a highly reactive oxygen species. The photosensitiser (PS) is then converted back to its ground state (Figure 3 adapted from (65)).

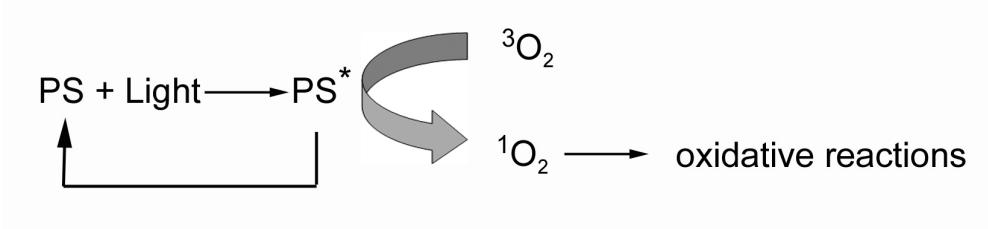

Figure 3. Photochemical reactions after illumination of photosensitiser (PS)

Singlet oxygen is a powerful oxidising agent, which can oxidise various biomolecules, like proteins, lipids and DNA. Singlet oxygen has a very short half life (< 0.1 ms) and a short range of action (10-20 nm). Consequently only molecules close to the singlet oxygen will be oxidised upon illumination (66). Depending on the nature of the photosensitiser the cellular uptake mechanism may be either endocytosis, passive or active transport over the plasma membrane. Upon addition to the cells, the amphiphilic photosensitisers $TPPS_{2a}$ (meso-tetraphenylporphine with two sulphonate groups on adjacent phenyl rings) and $AlPcS_{2a}$ (aluminium phtalocyanine with two sulphonate groups on adjacent phthalate rings) first incorporate into the plasma membrane, and subsequently they mainly localise in the

endosomal membrane via endocytosis (67). Figure 4 shows the chemical structures of both photosensitisers.

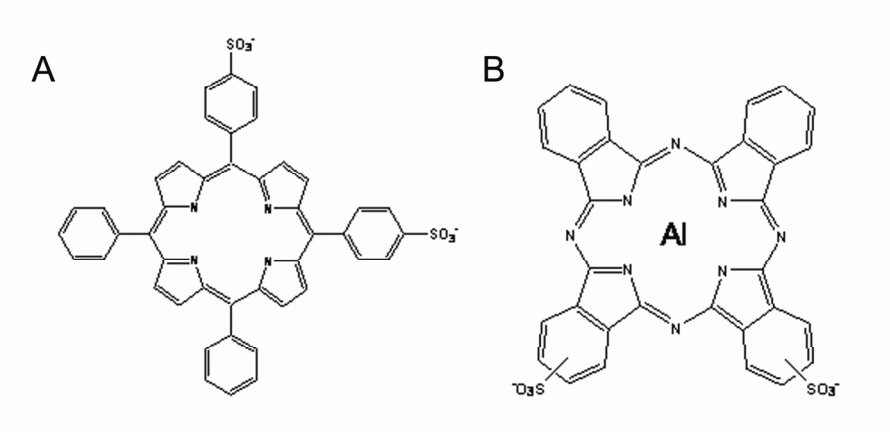

Figure 4. Chemical structures of $TPPS_{2a}$ (A) and $AlPcS_{2a}$ (B)

Photochemical internalisation was discovered when Berg *et al.* observed that illumination of cells containing photosensitiser in their endosomal membranes leads to redistribution of the photosensitiser from the endocytic vesicle membrane to the cytosol. Furthermore, the presence of lysosomal enzymes was detected in the cytoplasm, indicating release of endo-/lysosomal contents. One very attractive feature of this technique is that PCI can occur without the induction of extensive cell death (67, 68). The principle of PCI is shown in Figure 5 (Figure is reproduced from (69)).

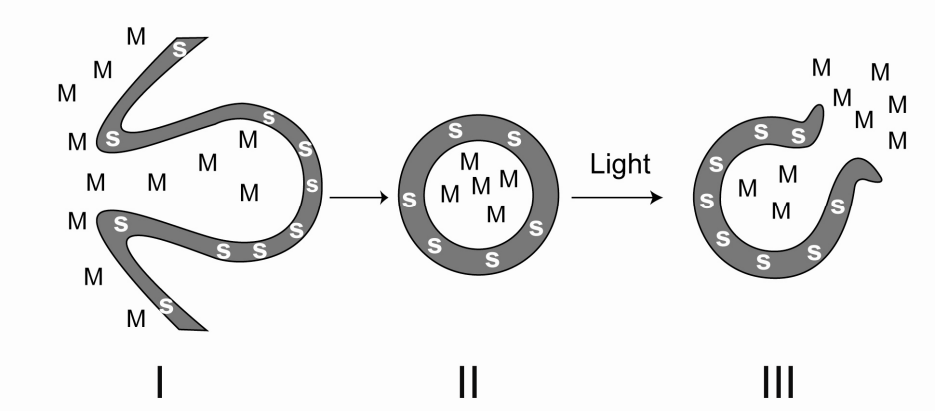

Figure 5. The principle of PCI. (I) The photosensitiser (S) localises in the plasma membrane and molecule (M) is taken up by endocytosis. (II) S and M end up in the endosomal membrane and lumen, respectively. (III) Illumination leads to excitation of S, which ultimately leads to damage and rupture of the endosomal membrane, resulting in release of M into the cytoplasm.

PCI has been studied for the delivery of many several molecules that normally would not be able to enter the cytoplasm of cells because they lack the capability to cross cellular membranes. The principle and use of PCI for drug delivery purposes is reviewed in (69). Selbo *at al.* demonstrated that the use of PCI enhanced the potency of the plant toxin gelonin in inhibiting cellular protein synthesis by a factor of 300 (70). In addition, the low-molecular weight drug bleomycin (71), antigenic peptides (72), immunotoxins (73, 74), peptide nucleic acids (75) and even colloidal carriers for gene delivery (76-78) have been successfully delivered into the cytosol of in vitro cultured cells via PCI. In addition to successful PCI-enhanced cytosolic delivery in vitro, PCI also has shown to promote cytosolic delivery in vivo (71, 79, 80). The combination of PCI and the low molecular weight drug bleomycin after i.p. co-administration of both photosensitiser and bleomycin resulted in significant anti-tumour activity and even 60% cure in two different tumour models. It was shown that combining PCI and bleomycin worked synergistic (71). Similar results were obtained with the combination of PCI and the plant toxin gelonin in two other tumour models. In the latter studies, the photosensitiser $AlPcS_{2a}$ was administered i.p., while the toxin was administered via intratumoural injection (79, 80). The combination of the drug and the photosensitiser in one delivery system might be more advantageous.

BORON NEUTRON CAPTURE THERAPY

The principle of boron neutron capture therapy (BNCT) as cancer treatment was first proposed by Locher in 1936 (82). The principle is based on the nuclear caption and fission reactions that occur when the stable boron-10 isotope is irradiated with low energy thermal neutrons. This reaction yields two high energy fission particles i.e. α-particles (^{4}He) and recoiling lithium (^{7}Li) nuclei (83). The principle of BNCT is shown in Figure 6.

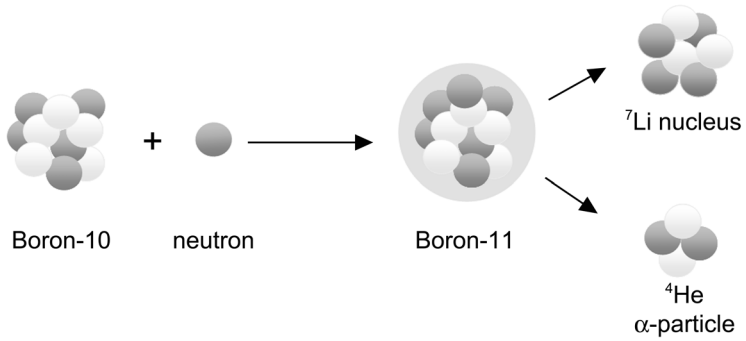

Figure 6. Principle of BNCT

Since the destructive effect of ^{4}He and ^{7}Li particles has a range of only ~10 μm, which is approximately the diameter of a mammalian cell, toxicity will be confined to cells containing boron-10 (83-85). To become a successful therapy for cancer, relatively large amounts of Boron-10 need to be delivered into tumour cells. The estimated amount for successful therapy is ~ 20 μg Boron-10/g tumour tissue, which corresponds to approximately 10^{9} Boron-10 atoms per tumour cell. The subcellular distribution of these Boron-10 atoms is even more important. The therapeutic effect will be best when the Boron-10 is localised in or in close proximity to the nucleus (84). Over the years, several strategies have been pursued to make BNCT successful (Figure 7).

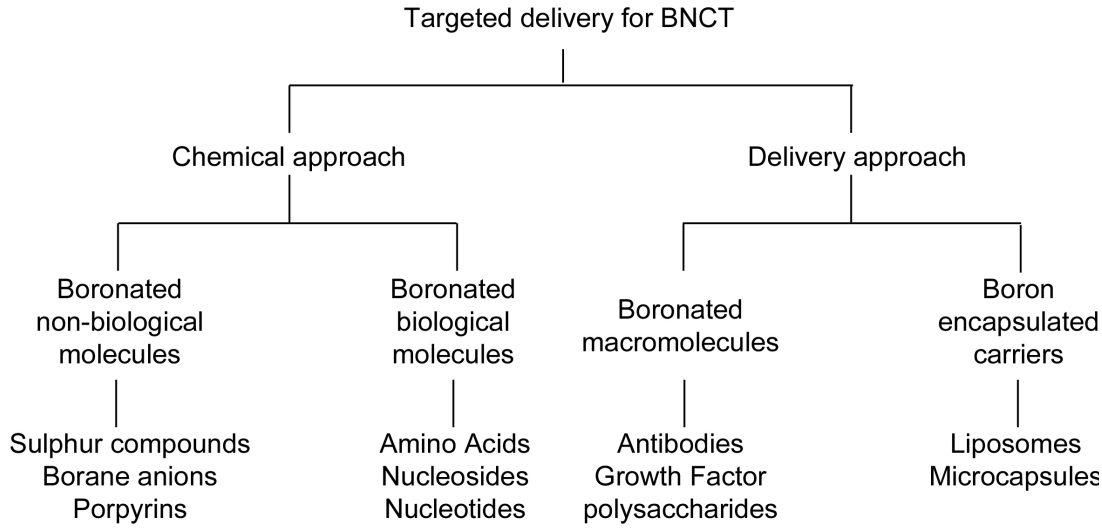

Figure 7. Strategies for BNCT (adapted from (65)).

One of those strategies is to design Boron-10-containing compounds, which localise preferentially and in large quantities in tumour tissue. Up to now, only two compounds seem to be reasonably successful regarding tumour localisation, namely mercaptoundecahydrododecaborate (BSH; $Na_2B_{12}H_{11}SH$) (86) and borono-phenylalanine (BPA) (87). However, BNCT with these compounds has not been satisfactory and tumour accumulation needs to be improved (88). Other low molecular weight boronated compounds have been designed, e.g. boronated nucleosides (89), boronated porhyrins (90) and DNA interchelating agents (91) and others (see for reviews references (92, 93)).

A second strategy is linking boron compounds to a macromolecular carrier, reviewed in (94). Although utilisation of antibodies seemed an attractive approach, the number of boron atoms required to attach to a single antibody for successful therapy, gives rise to loss of the

specificity of the antibody (65, 94). A boronated dextran conjugate designed to have high tumour accumulation by the EPR effect has been described (95). To increase the specificity of this conjugate, EGF was coupled to it as a targeting moiety (96, 97). Furthermore, boronated PAMAM dendrimers linked to different targeting ligands have also been described (98, 99).

Liposomes have also been studied for the delivery of boron compounds (reviewed in (94, 100, 101). To a great extent these studies dealt with BSH loaded in conventional and sterically stabilised liposomes. Biodistribution and efficacy studies in mice have shown promising results (102, 103)(104, 105). Also other boron-containing agents have been encapsulated in the aqueous core of the liposomes, such as BPA (106), borane anions (102, 107, 108) and boronated acridines (109). Furthermore, hydrophobic boronated compounds embedded in the lipid bilayer of liposomes have been studied (110-112). To increase the tumour cell specificity and favor the subcellular distribution of the boron encapsulated in liposomes, several ligand-targeted liposomal systems are being developed for BNCT (reviewed in (100) and (113-115)). Recently, Maruyama *et al.* demonstrated in tumour-bearing mice that encapsulation of BSH into transferrin-PEG liposomes (Tf-lips) resulted in superior tumour accumulation compared to PEG-liposomes lacking transferrin. Tf-liposomes maintained relatively high boron-10 levels over at least 72 hrs after i.v. injection. However, upon neutron radiation, tumour growth was inhibited to the same extent as compared to PEG-liposomes (116). Although this work illustrates the progress made in the (targeted) liposomal BNCT delivery field, improvements with respect to selective tumour cell targeting and intracellular delivery are still highly needed.

AIMS AND OUTLINE OF THE THESIS

The primary aim of this thesis was to improve intracellular drug delivery by applying targeted liposome systems. Two strategies are investigated to accomplish this: the use of so-called cell-penetrating peptides (CPP) (chapters 3 – 5) and photochemical internalisation (PCI) (chapter 6). In addition, targeted liposomes are investigated as intracellular drug delivery vehicles for improving boron neutron capture therapy (BNCT).

Chapter 2 briefly reviews approaches currently studied our laboratory to achieve cytosolic delivery of liposomal macromolecules.

Better understanding of the uptake mechanism and subcellular distribution of CPP and possible cargoes must be obtained before these peptides can be efficiently utilised for drug delivery purposes. Therefore, chapter 3 addresses the influence of incubation temperature, peptide concentration and plasma membrane cholesterol on the intracellular distribution of the CPP octaarginine in the human haematopoietic cell line KG1a. In chapter 4 the uptake mechanism of TAT-peptide modified liposomes by human ovarian carcinoma cells is studied. To circumvent possible fixation artefacts, all studies are done using live cells. Chapter 5 deals with the influence of the macropinocytosis inhibitors amiloride and its derivative 5-(*N*-ethyl-*N*-isopropyl) amiloride (EIPA) on the intracellular distribution of CPP and the implications of these findings.

The second strategy to improve cytosolic delivery of liposome encapsulated molecules is PCI. In chapter 6 the effect of PCI on the enhancement of the degree of cytosolic delivery of liposomally targeted proteins is examined

The last experimental part of this thesis is devoted to the potential use of targeted liposomes for the intracellular delivery of BNCT compounds. Chapter 7 illustrates the importance of receptor expression for the effectiveness of targeted liposomes for boron neutron capture therapy.

The last chapter of this thesis, chapter 8, provides a summarising discussion on the results obtained.

REFERENCES

1. M. Yokoyama. Drug targeting with nano-sized carrier systems. *J Artif Organs.* **8:** 77-84 (2005)
2. Gardner (1987) *Drug delivery systems*.
3. R. Duncan (2005) in *Encyclopedia of Molecular Cell Biology and Molecular Medicine*, ed. Meyers, R. A. (Wiley-VCH Verlag, Weinheim), pp. 163-204.
4. A. G. Schatzlein. Targeting of synthetic gene delivery systems. *J Biomed Biotechnol.* **2:** 149-58 (2003)
5. Y. Matsumura and H. Maeda. A new concept for macromolecular therapeutics in cancer chemotherapy: mechanism of tumouritropic accumulation of proteins and the antitumour agent smanc. *Cancer Res.* **46:** 6387-92 (1986)
6. H. Maeda, J. Wu, T. Sawa, Y. Matsumura and K. Hori. Tumour vascular permeability and EPR effect in macromolecular therapeutics: a review. *J Control Release.* **65:** 271-84 (2000)
7. T. M. Allen. Ligand-targeted therapeutics in anticancer therapy. *Nat Rev Cancer.* **2:** 750-63 (2002)
8. A. R. Hilgenbrink and P. S. Low. Folate receptor-mediated drug targeting: from therapeutics to diagnostics. *J Pharm Sci.* **94:** 2135-46 (2005)
9. T. R. Daniels, T. Delgado, G. Helguera and M. L. Penichet. The transferrin receptor part II: targeted delivery of therapeutic agents into cancer cells. *Clin Immunol.* **121:** 159-76 (2006)
10. J. Mendelsohn. Targeting the epidermal growth factor receptor for cancer therapy. *J Clin Oncol.* **20:** 1S-13S (2002)
11. G. A. Koning, R. M. Schiffelers, M. H. Wauben, R. J. Kok, E. Mastrobattista, G. Molema, T. L. ten Hagen and G. Storm. Targeting of angiogenic endothelial cells at sites of inflammation by dexamethasone phosphate containing RGD peptide liposomes inhibits experimental arthritis. *Arthritis Rheum.* **54:** 1055-60 (2006)
12. K. Temming, R. M. Schiffelers, G. Molema and R. J. Kok. RGD-based strategies for selective delivery of therapeutics and imaging agents to the tumour vasculature. *Drug Resist Updat.* **8:** 381-402 (2005)
13. F. Nilsson, L. Tarli, F. Viti and D. Neri. The use of phage display for the development of tumour targeting agents. *Adv Drug Deliv Rev.* **43:** 165-96 (2000)
14. P. D. Senter and C. J. Springer. Selective activation of anti-cancer prodrugs by monoclonal antibody enzyme conjugates. *Adv Drug Deliv Rev.* **53** (2001)
15. S. D. Conner and S. L. Schmid. Regulated portals of entry into the cell. *Nature.* **422:** 37-44 (2003)
16. D. Sheff. Endosomes as a route for drug delivery in the real world. *Adv Drug Deliv Rev.* **56:** 927-930 (2004)
17. S. Mehier-Humbert and R. H. Guy. physical methods for gene transfer: improving the kinetics of gene delivery into cells. *Adv Drug Deliv Rev.* **57:** 733-753 (2005)
18. A. Akinc, M. Thomas, A. M. Klibanov and R. Langer. Exploring polyethyleneimine-mediated DNA transfection and the proton sponge hypothesis. *J Gene Med.* **7:** 657-663 (2005)
19. C. A. Lackey, O. W. Press, A. S. Hoffman and P. S. Stayton. A biomimetic pH-responsive polymer directs endosomal release and intracellular delivery of an endocytosed antibody complex. *Bioconjug Chem.* **13:** 996-1001 (2002)
20. R. A. Jones, C. Y. Cheung, F. E. Black, J. K. Zia, P. S. Stayton, A. S. Hoffman and M. R. Wilson. Poly(2-alkylacrylic acid) polymers deliver molecules to the cytosol by pH-sensitive disruption of endosomal vesicles. *Biochem J.* **372:** 65-75 (2003)
21. S. Richardson, P. Ferruti and R. Duncan. Poly(amidoamine)s as potential endosomolytic polymers: evaluation in vitro and body distribution in normal and tumour-bearing animals. *J Drug Target.* **6:** 391-404 (1999)
22. P. C. Griffiths, A. Paul, Z. Khayat, K. W. Wan, S. M. King, I. Grillo, R. Schweins, P. Ferruti, J. Franchini and R. Duncan. Understanding the Mechanism of Action of Poly(amidoamine)s as Endosomolytic Polymers: Correlation of Physicochemical and Biological Properties. *Biomacromolecules.* **5:** 1422-1427 (2004)
23. T. Stegmann, F. P. Booy and J. Wilschut. Effects of low pH on influenza virus. Activation and inactivation of the membrane fusion capacity of the hemagglutinin. *J Biol Chem.* **262:** 17744-9 (1987)
24. T. Stegmann. Membrane fusion mechanisms: the influenza hemagglutinin paradigm and its implications for intracellular fusion. *Traffic.* **1:** 598-604 (2000)

25. W. Li, F. Nicol and F. C. Szoka Jr. GALA: a designed synthetic pH-responsive amphipathic peptide with application in drug and gene delivery. *Adv Drug Deliv Rev.* **56:** 999-1021 (2004)
26. S. Simoes, J. N. Moreira, C. Fonseca, N. Duzgunes and M. C. de Lima. On the formulation of pH-sensitive liposomes with long circulation times. *Adv Drug Deliv Rev.* **56:** 947-65 (2004)
27. V. Escriou, M. Carriere, D. Scherman and P. Wils. NLS bioconjugates for targeting therapeutic genes to the nucleus. *Adv Drug Deliv Rev.* **55:** 295-306 (2003)
28. M. A. Van der Aa, E. Mastrobattista, R. S. Oosting, W. E. Hennink, G. A. Koning and D. J. Crommelin. The nuclear pore complex: the gateway to succesful non-viral gene delivery. *Pharm Res.* **23:** 447-459 (2006)
29. V. Weissig, G. De Souza and V. P. Torchilin (2002) in *Biomedical aspects of drug targeting*, eds. Muzykantov, V. & Torchilin, V. P. (Kluwer Academic publishers, Dordrecht), pp. 473-495.
30. A. D. Bangham. Membrane models with phospholipids. *Prog Biophys Mol Biol.* **18:** 29-95 (1968)
31. A. D. Bangham, M. M. Standish and J. C. Watkins. Diffusion of univalent ions across the lamellae of swollen phospholipids. *J Mol Biol.* **13:** 238-52 (1965)
32. G. Gregoriadis. Drug entrapment in liposomes. *FEBS Lett.* **36:** 292-6 (1973)
33. J. H. Senior. Fate and behavior of liposomes in vivo: a review of controlling factors. *Crit Rev Ther Drug Carrier Syst.* **3:** 123-193 (1987)
34. S. Schenkman, P. S. Aroujo, R. Dijkman, F. H. Quina and H. Chaimovich. Effects of temperature and lipid composition on the serum albumin induced aggregation and fusion of small unilamellar vesicles. *Biochim Biophys Acta.* **649:** 633-647 (1981)
35. D. Papahadjopoulos, T. M. Allen, A. Gabizon, E. Mayhew, K. Matthay, S. K. Huang, K. D. Lee, M. C. Woodle, D. D. Lasic, C. Redemann and et al. Sterically stabilised liposomes: improvements in pharmacokinetics and antitumour therapeutic efficacy. *Proc Natl Acad Sci U S A.* **88:** 11460-4 (1991)
36. M. C. Woodle. Controlling liposome blood clearance by surface-grafted polymers. *Adv Drug Deliv Rev.* **32:** 139-52 (1998)
37. M. C. Woodle and D. D. Lasic. Sterically stabilised liposomes. *Biochem Biophys Acta.* **1132:** 171-99 (1992)
38. E. Mastrobattista, G. A. Koning and G. Storm. Immunoliposomes for the targeted delivery of antitumour drugs. *Adv Drug Deliv Rev.* **40:** 103-127 (1999)
39. K. Maruyama, O. Ishida, T. Takizawa and K. Moribe. Possibility of active targeting to tumour tissues with liposomes. *Adv Drug Deliv Rev.* **40:** 89-102 (1999)
40. P. Sapra. Ligand-targeted liposomal anticancer drugs. *Prog Lipid Res.* **42:** 439-462 (2003)
41. P. Sapra, P. Tyagi and T. M. Allen. Ligand-targeted liposomes for cancer treatment. *Curr Drug Deliv.* **2:** 369-381 (2005)
42. T. L. Andresen, S. S. Jensen and K. Jorgensen. Advanced strategies in liposomal cancer therapy: problems and prospect of active and tumour specific drug release. *Prog Lipid Res.* **44:** 68-97 (2005)
43. G. A. Koning, H. W. Morselt, M. J. Velinova, J. Donga, A. Gorter, T. M. Allen, S. Zalipsky, J. A. Kamps and G. L. Scherphof. Selective transfer of a lipophilic prodrug of 5-fluorodeoxyuridine from immunoliposomes to colon cancer cells. *Biochim Biophys Acta.* **1420:** 153-67 (1999)
44. G. A. Koning, J. A. Kamps and G. L. Scherphof. Efficient intracellular delivery of 5-fluorodeoxyuridine into colon cancer by targeted immunoliposomes. *Cancer Detect Prev.* **26:** 299-307 (2002)
45. E. Mastrobattista. Comparison of immunoliposomes targeting to three different receptors expressed by human ovarian carcinoma (OVCAR-3) cells. *Dissertation thesis.* (2001)
46. E. Mastrobattista, G. A. Koning, L. Van Bloois, A. C. Filipe, W. Jiskoot and G. Storm. Functional Characterization of an Endosome-disruptive Peptide and Its Application in Cytosolic Delivery of Immunoliposome-entrapped Proteins. *J Biol Chem.* **277:** 27135-43 (2002)
47. T. Kakudo, S. Chaki, S. Futaki, I. Nakase, K. Akaji, T. Kawakami, K. Maruyama, H. Kamiya and H. Harashima. Transferrin-modified liposomes equipped with a pH-sensitive fusogenic peptide: an artificial viral-like delivery system. *Biochemistry.* **43:** 5618-28 (2004)
48. C. J. Provoda, E. M. Stier and K. D. Lee. Tumour cell killing enabled by listeriolysin O-liposome-mediated delivery of the protein toxin gelonin. *J Biol Chem.* (2003)
49. V. P. Torchilin, R. Rammohan, V. Weissig and T. S. Levchenko. TAT peptide on the surface of liposomes affords their efficient intracellular delivery even at low temperature and in the presence of metabolic inhibitors. *Proc Natl Acad Sci U S A.* **98:** 8786-91 (2001)

50. E. Vives, P. Brodin and B. Lebleu. A truncated HIV-1 Tat protein basic domain rapidly translocates through the plasma membrane and accumulates in the cell nucleus. *J Biol Chem.* **272:** 16010-7 (1997)
51. E. Vives and B. Lebleu (2002) in *Cell-penetrating peptides: processes and applications*, ed. Langel, U. (CRC Press, Boca Raton), pp. 3-21.
52. S. Fawell, J. Seery, Y. Daikh, C. Moore, L. L. Chen, B. Pepinsky and J. Barsoum. Tat-mediated delivery of heterologous proteins into cells. *Proc Natl Acad Sci U S A.* **91:** 664-8 (1994)
53. S. R. Schwarze, A. Ho, A. Vocero-Akbani and S. F. Dowdy. In vivo protein transduction: delivery of a biologically active protein into the mouse. *Science.* **285:** 1569-72 (1999)
54. A. Astriab-Fisher, D. Sergueev, M. Fisher, B. R. Shaw and R. L. Juliano. Conjugates of antisense oligonucleotides with the Tat and antennapedia cell-penetrating peptides: effects on cellular uptake, binding to target sequences, and biologic actions. *Pharm Res.* **19:** 744-54 (2002)
55. M. Lewin, N. Carlesso, C. H. Tung, X. W. Tang, D. Cory, D. T. Scadden and R. Weissleder. Tat peptide-derivatized magnetic nanoparticles allow in vivo tracking and recovery of progenitor cells. *Nat Biotechnol.* **18:** 410-4 (2000)
56. Y. L. Tseng, J. J. Liu and R. L. Hong. Translocation of liposomes into cancer cells by cell-penetrating peptides penetratin and tat: a kinetic and efficacy study. *Mol Pharmacol.* **62:** 864-72 (2002)
57. M. Lundberg and M. Johansson. Positively charged DNA-binding proteins cause apparent cell membrane translocation. *Biochem Biophys Res Commun.* **291:** 367-71 (2002)
58. J. P. Richard, K. Melikov, E. Vives, C. Ramos, B. Verbeure, M. J. Gait, L. V. Chernomordik and B. Lebleu. Cell-penetrating peptides: A re-evaluation of the mechanism of cellular uptake. *J Biol Chem.* (2002)
59. S. Futaki. Oligoarginine vectors for intracellular delivery: design and cellular uptake mechanisms. *Biopolymers.* **84:** 241-49 (2006)
60. J. L. Zaro and W. C. Shen. Quantitative comparison of membrane transduction and endocytosis of oligopeptides. *Biochem Biophys Res Commun.* **307:** 241-7 (2003)
61. D. J. Mitchell, D. T. Kim, L. Steinman, C. G. Fathman and J. B. Rothbard. Polyarginine enters cells more efficiently than other polycationic homopolymers. *J Peptide Res.* **56:** 318-25 (2000)
62. J. B. Rothbard, T. C. Jessop, R. S. Lewis, B. A. Murray and P. A. Wender. Role of membrane potential and hydrogen bonding in the mechanism of translocation of guanidinium-rich peptides into cells. *J Am Chem Soc.* **126:** 9506-07 (2004)
63. J. R. Maiolo, M. Ferrer and E. A. Ottinger. Effect of cargo molecules on the cellular uptake of arginine-rich cell-penetrating peptides. *Biochem Biophys Acta.* **1712:** 161-72 (2005)
64. G. Tunnemann, R. M. Martin, S. Haupt, C. Patsch, F. Edenhofer and M. C. Cardoso. Cargo-dependent mode of uptake and bioavailability of TAT-containing proteins and peptides in living cells. *Faseb J.* **20:** 1775-84 (2006)
65. S. C. Mehta and D. R. Lu. Targeted drug delivery for boron neutron capture therapy. *Pharm Res.* **13:** 344-51 (1996)
66. I. E. Kochevar and R. W. Redmond. Photosensitized production of singlet oxygen. *Methods Enzymol.* **319:** 20-8 (2000)
67. K. Berg and J. Moan. Lysosomes as photochemical target. *Int J Cancer.* **59:** 814-822 (1994)
68. J. Moan, K. Berg, H. Anholt and K. Madslien. Sulfonated aluminium phtalocyanines as sensitizers for photochemotherapy. Effects of small light doses on localisation, dye fluorescence and photosensitivity in V79 cells. *Int J Cancer.* **58:** 865-70 (1994)
69. A. Hogset, L. Prasmickaite, P. K. Selbo, M. Hellum, B. O. Engesaeter, A. Bonsted and K. Berg. Photochemical in drug and gene delivery. *Adv Drug Deliv Rev.* **56:** 95-115 (2004)
70. P. K. Selbo, K. Sandvig, V. Kirveliene and K. Berg. Release of gelonin from endosomes and lysosomes to cytosol by photochemical internalisation. *Biochim Biophys Acta.* **1475:** 307-13 (2000)
71. K. Berg, A. Dietze, O. Kaalhus and A. Hogset. Site-specific drug delivery by photochemical internalisation enhances the antitumour effect of bleomycin. *Clin Cancer Res.* **11:** 8476-85 (2005)
72. K. Berg, P. K. Selbo, L. Prasmickaite, T. E. Tjelle, K. Sandvig, J. Moan, G. Gaudernack, O. Fodstad, S. Kjolsrud, H. Anholt, G. H. Rodal, S. K. Rodal and A. Hogset. Photochemical internalisation: a novel technology for delivery of macromolecules into cytosol. *Cancer Res.* **59:** 1180-3 (1999)
73. P. K. Selbo, G. Sivam, O. Fodstad, K. Sandvig and K. Berg. Photochemical internalisation increases the cytotoxic effect of the immunotoxin MOC31-gelonin. *Int J Cancer.* **87:** 853-9 (2000)
74. A. Weyergang, P. K. Selbo and K. Berg. Photochemically stimulated drug delivery increases the cytotoxicity and specificity of EGF-saporin. *J Control Release.* **111:** 165-173 (2006)

75. M. Folini, K. Berg, E. Millo, R. Villa, L. Prasmickaite, M. G. Daidone, U. Benatti and N. Zaffaroni. Photochemical internalisation of a peptide nucleic acid targeting the catalytic subunit of human telomerase. *Cancer Res.* **63:** 3490-4 (2003)
76. L. Prasmickaite, A. Hogset, V. M. Olsen, O. Kaalhus, S. O. Mikalsen and K. Berg. Photochemically enhanced gene transfection increases the cytotoxicity of the herpes simplex virus thymidine kinase gene combined with ganciclovir. *Cancer Gene Ther.* **11:** 514-23 (2004)
77. A. Hogset, L. Prasmickaite, M. Hellum, B. O. Engesaeter, V. M. Olsen, T. E. Tjelle, C. J. Wheeler and K. Berg. Photochemical transfection: a technology for efficient light-directed gene delivery. *Somat Cell Mol Genet.* **27:** 97-113 (2002)
78. B. O. Engesaeter, A. Bonsted, K. Berg, A. Hogset, O. Engebraten, O. Fodstad, D. T. Curiel and G. M. Maelandsmo. PCI-enhanced adenoviral transduction employs the known uptake mechanism of adenoviral particles. *Cancer Gene Ther.* **12:** 439-48 (2005)
79. A. Dietze, O. Peng, P. K. Selbo, O. Kaalhus, C. Muller, S. Brown and K. Berg. Enhanced photodynamic destruction of transplantable fibrosarcoma using photochemical internalisation of gelonin. *Br J Cancer.* **92:** 2004-9 (2005)
80. P. K. Selbo, G. Sivam, O. Fodstad, K. Sandvig and K. Berg. In vivo documentation of photochemical internalisation, a novel approach to site specific cancer therapy. *Int J Cancer.* **92:** 761-6 (2001)
81. N. Nishiyama, A. Iriyama, W. D. Jang, K. Miyata, K. Itaka, Y. Inoue, H. Takahashi, Y. Yanagi, Y. Tamaki, H. Koyama and K. Kataoka. Light-induced gene transfer from packaged DNA enveloped in dendrimeric photosensitizer. *Nat Mater.* **4:** 934-41 (2005)
82. G. L. Locher. Biological effects and therapeutic possibilities of neutron. *Am J Roentogenol Radium Ther.* **36:** 1-13 (1936)
83. A. H. Soloway, W. Tjarks, B. A. Barnum, F. G. Rong, R. F. Barth, I. M. Codogni and J. G. Wilson. The Chemistry of Neutron Capture Therapy. *Chem Rev.* **98:** 1515-1562 (1998)
84. D. Gabel, S. Foster and R. G. Fairchild. The Monte Carlo simulation of the biological effect og the 10B(n, alpha)7Li reaction in cells and its implication for boron neutron capture therapy. *Radiat Res.* **111:** 14-25 (1987)
85. R. G. Fairchild, S. B. Kahl, B. H. Laster, J. Kalef-Ezra and E. A. Popenoe. In vitro determination of uptake, distribution, biological efficacy, and toxicity of boronated compounds for neutron capture therapy: a comparison of phorphyrins with sulfhydryl boron hydrides. *Cancer Res.* **50:** 4860-4865 (1990)
86. A. H. Soloway, H. Hatanaka and M. A. Davis. Penetration of brain and brain tumour. VII. Tumour-binding sulfhydryl boron compounds. *J Med Chem.* **10:** 714-717 (1967)
87. Y. Mishima, C. Honda, M. Ichihashi, H. Obara, J. Hiratsuka, H. Fukuda, H. Karashima, T. Kobayashi, K. Kanda and K. Yoshino. First cure of primary malignant melanoma in man by single thermal neutron capture using melanoma-seeking 10B compound. *Lancet.* **II** (1989)
88. R. F. Barth, A. H. Soloway, J. H. Goodman, R. A. Gahbauer, n. Gupta, T. E. Blue, W. Yang and W. Tjarks. Boron neutron capture therapy of brain tumours: an emerging therapeutic modality. *Neurosurgery.* **44:** 433-450 (1999)
89. W. Tjarks, J. Wang, S. Chandra, W. Ji, J. Zhou, A. J. Lunato, C. Boyer, Q. Li, E. V. Usova, S. Eriksson, G. H. Morrison and G. Y. Cosquer. Synthesis and biological evaluation of boronated nucleosides for boron neutron capture therapy (BNCT) of cancer. *Nucleosides Nucleotides Nucleic Acids.* **20:** 695-8 (2001)
90. C. P. Ceberg, A. Brun, S. B. Kahl, M. S. Koo, B. R. Persson and S. L.G. A comparative study on the pharmacokinetics and biodistribution of boronated porphyrin (BOPP) and sulfhydryl boron hydride (BSH) in the RG2 rat glioma model. *J Neurosurg.* **83** (1995)
91. L. Gedda, H. Ghaneolhosseini, P. Nilsson, K. Nyholm, J. Pettersson, S. Sjoberg and J. Carlsson. The influence of lipophilicity on the binding of boronated DNA-interchelating compounds in human spheriods. *Anticancer Drug Des.* **15:** 277-86 (2000)
92. M. F. Hawthorne. New horizons for therapy based on the boron neutron capture reaction. *Mol Med Today.* **4:** 174-81 (1998)
93. S. Sjoberg, J. Carlsson, H. Ghaneolhosseini, L. Gedda, T. Hartman, J. Malmquist, C. Naeslund, P. Olsson and W. Tjarks. Chemistry and biology of some low molecular weight boron compounds for boron neutron capture therapy. *J Neurooncol.* **33:** 41-52 (1997)

94. G. Wu, R. F. Barth, W. Yang, R. J. Lee, W. Tjarks, M. V. Backer and J. M. Backer. Boron containing macromolecules and nanovehicles as delivery agents for neutron capture therapy. *Anticancer Agents Med Chem.* **6:** 167-84 (2006)
95. A. Holmberg and L. Meurling. Preparation of sulfydrylborane-dextran conjuagtes for boron neutron capture therapy. *Bioconjug Chem.* **4:** 570-3 (1993)
96. L. Gedda, P. Olsson, J. Ponten and J. Carlsson. Development and in vitro studies of epidermal growth factor-dextran conjugates for boron neutron capture therapy. *Bioconjug Chem.* **7:** 584-91 (1996)
97. P. Olsson, L. Gedda, H. Goike, L. Liu, V. Collins, J. Ponten and J. Carlsson. Uptake of a boronated epidermal growth factor-dextran conjugate in CHO xenografts with and without human EGF-receptor expression. *Anticancer Drug Des.* **13:** 279-89 (1998)
98. G. Wu, R. F. Barth, W. Yang, M. Chatterjee, W. Tjarks, M. J. Ciesielski and R. A. Fenstermaker. Site-specific conjugation of boron-containing dendrimers to anti-EGF receptor monoclonal antibody cetuximab (IMC-C225) and its evaluation as a potential delivery agent for neutron capture therapy. *Bioconjug Chem.* **15:** 185-94 (2004)
99. R. F. Barth, D. M. Adams, A. H. Soloway, F. Alam and M. V. Darby. Boronated starburst dendrimer-monoclonal antibody immunoconjugates: evaluation as a potential delivery system for neutron capture therapy. *Bioconjug Chem.* **5:** 58-66 (1994)
100. J. Carlsson, E. B. Kullberg, J. Capala, S. Sjoberg, K. Edwards and L. Gedda. Ligand liposomes and boron neutron capture therapy. *J Neurooncol.* **62:** 47-59 (2003)
101. M. F. Hawthorne and K. Shelly. Liposomes as drug delivery vehicles for boron agents. *J Neurooncol.* **33:** 53-8 (1997)
102. K. Shelly, D. A. Feakes, M. F. Hawthorne, P. G. Schmidt, T. A. Krisch and W. F. Bauer. Model studies directed towards the boron neutron-capture therapy of cancer: boron delivery to murine tumours with liposomes. *Proc Natl Acad Sci U S A.* **89:** 9039-9043 (1992)
103. S. C. Mehta, J. C. Lai and D. R. Lu. Liposomal formulations containing sodium mercaptoundecahydrododecaborate (BSH) for boron neutron capture therapy. *J Microencapsul.* **13:** 269-79 (1996)
104. H. Yanagie, K. Maruyama, T. Takizawa, O. Ishida, K. Ogura, T. Matsumoto, Y. Sakurai, T. Kobayashi, A. Shinohara, J. Rant, J. Skvarc, R. Ilic, G. Kuhne, M. Chiba, Y. Furuya, H. Sugiyama, T. Hisa, K. Ono, H. Kobayashi and M. Eriguchi. Application of boron-entrapped stealth liposomes to inhibition of growth of tumour cells in the in vivo boron neutron-capture therapy model. *Biomed Pharmacother.* (2005)
105. H. Yanagie, H. Kobayashi, Y. Takeda, I. Yoshizaki, Y. Nonaka, S. Naka, A. Nojiri, H. Shinnkawa, Y. Furuya, H. Niwa, K. Ariki, H. Yasuhara and M. Eriguchi. Inhibition of growth of human breast cancer cells in culture by neutron capture using liposomes containing 10B. *Biomed Pharmacother.* **56:** 93-9 (2002)
106. P. Perugini and F. Pavanetto. Liposomes containing boronophenylalanine for boron neutron capture therapy. *J Microencapsul.* **15:** 473-83 (1998)
107. D. A. Feakes, R. C. Waller, D. K. Hathaway and V. S. Morton. Synthesis and in vivo murine evaluation of Na4[1-(1'-B10H9)-6-SHB10H8] as a potential agent for boron neutron capture therapy. *Proc Natl Acad Sci U S A.* **96:** 6406-10 (1999)
108. G. C. Krijger, M. M. Fretz, U. D. Woroniecka, O. M. Steinebach, W. Jiskoot, G. Storm and G. A. Koning. Tumour cell and tumour vasculature targeted liposomes for neutron capture therapy. *Radiochim Acta.* **93:** 589-593 (2005)
109. M. Johnsson, N. Bergstrand and K. Edwards. Optimization of drug loading procedures and characterization of liposomal formulations of two novel agents intended for boron neutron capture therapy (BNCT). *J Liposome Res.* **9:** 53-79 (1999)
110. D. A. Feakes, K. Shelly and M. F. Hawthorne. Selective boron delivery to murine tumours by lipophilic species incorporated in the membranes of unilamellar liposomes. *Proc Natl Acad Sci U S A.* **92:** 1367-70 (1995)
111. J. J. Sudimack, D. Adams, J. Rotaru, S. Shukla, J. Yan, M. Sekido, R. F. Barth, W. Tjarks and R. J. Lee. Folate receptor-mediated liposomal delivery of a lipophilic boron agent to tumour cells in vitro for neutron capture therapy. *Pharm Res.* **19:** 1502-8 (2002)
112. Y. Miyajima, H. Nakamura, Y. Kuwata, J. D. Lee, S. Masunaga, K. Ono and K. Maruyama. Transferrin-loaded nido-carborane liposomes: tumour-targeting boron delivery system for neutronn capture therapy. *Bioconjug Chem.* **17:** 1314-1320 (2006)

113. E. Bohl Kullberg, N. Bergstrand, J. Carlsson, K. Edwards, M. Johnsson, S. Sjoberg and L. Gedda. Development of EGF-conjugated liposomes for targeted delivery of boronated DNA-binding agents. *Bioconjug Chem.* **13:** 737-43 (2002)
114. Q. Wei, E. B. Kullberg and L. Gedda. Trastuzumab-conjugated boron-containing liposomes for tumour-cell targeting; development and cellular studies. *Int J Oncol.* **23:** 1159-65 (2003)
115. X. Q. Pan, H. Wang, S. Shukla, M. Sekido, D. M. Adams, W. Tjarks, R. F. Barth and R. J. Lee. Boron-containing folate receptor-targeted liposomes as potential delivery agents for neutron capture therapy. *Bioconjug Chem.* **13:** 435-42 (2002)
116. K. Maruyama, O. Ishida, S. Kasaoka, T. Takizawa, N. Utoguchi, A. Shinohara, M. Chiba, H. Kobayashi, M. Eriguchi and H. Yanagie. Intracellular targeting of sodium mercaptoundecahydrododecaborate (BSH) to solid tumours by transferrin-PEG liposomes, for boron neutron-capture therapy (BNCT). *J Control Release.* **98:** 195-207 (2004)

2

Strategies for cytosolic delivery of liposomal macromolecules

Marjan M. Fretz, Enrico Mastrobattista, Gerben A. Koning
Wim Jiskoot and Gert Storm

Published in the International Journal of Pharmaceutics. 298: 305-309 (2005)

ABSTRACT

Potential approaches to achieve cytosolic delivery of liposomal macromolecules are presented. These approaches include: 1) the co-encapsulation of fusogenic peptides into targeted drug-containing liposomes, 2) coupling of the HIV-1 derived cell penetrating peptide TAT to the surface of liposomes and 3) photochemical internalisation, based on photochemically inducible permeabilisation of endocytic vesicles

INTRODUCTION

Despite the potential of many macromolecules such as nucleic acids, proteins and peptides to serve as therapeutic agents, the *in vivo* efficacy can be severely comprised by their unfavourable physicochemical characteristics. One major obstacle is the negative effect of their generally large size and hydrophilic nature on cellular uptake. As the target site of these therapeutics is often located in the cytoplasm, such molecules may not reach their target without a delivery system facilitating cytosolic delivery (1). Many different drug delivery systems have been investigated for this purpose. Of these, liposomes have attracted considerable attention. Liposomes are able to provide protection and targeting of the encapsulated macromolecule and may facilitate cellular internalisation. Currently, several (targeted) liposome systems are under investigation for this purpose (2-5).

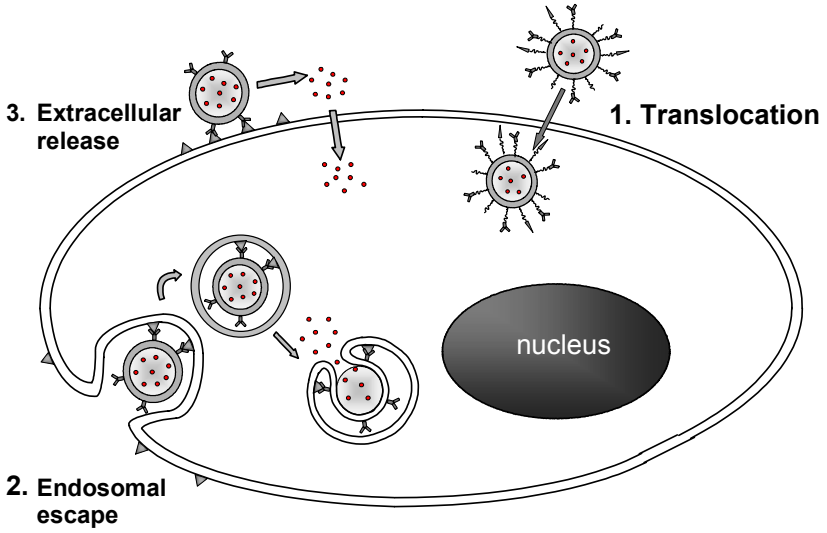

Figure 1 Schematic representation of potential pathways to achieve cytosolic delivery of liposomal macromolecules

Figure 1 illustrates three different pathways by which cytosolic delivery of liposomal macromolecules may be obtained.

Extracellular release and subsequent diffusion of the drug over the plasma membrane (Figure 1, route 1) is possible for molecules that are able to cross the plasma membrane. Generally, this route is, as just discussed, not an option for macromolecules.

Cellular uptake of liposomes can occur via endocytosis after which they end up in the lysosomes. In the lysosomal compartment the liposomes will be subjected to the acidic environment and degrading enzymes present there, resulting in degradation of the liposomes including their macromolecular contents. For that reason, utilisation of mechanisms that

allow endosomal escape may provide an effective way to achieve cytosolic delivery (Figure 1, route 2).
So-called cell penetrating peptides (CPP) have been reported to accomplish direct cytosolic delivery when attached to various cargoes including liposomes (6, 7) as illustrated in Figure 1, route 3. CPPs are supposed to be able to translocate the cargo over the plasma membrane thereby circumventing endocytosis. This results in direct cytosolic delivery (8).
Here, we present approaches studied in our laboratory to achieve cytosolic delivery of liposomal macromolecules, including co-encapsulation of fusogenic peptides, surface coupling of CPP and photochemical internalisation.

CO-ENCAPSULATION OF FUSOGENIC PEPTIDES

By destabilising the endosomal membrane, endocytosed material may be released in the cytoplasm. This endosomal escape mechanism is for example exploited by certain viruses, e.g. the influenza virus (9). After endocytosis of the influenza viral particle, the N-terminal domain of viral protein haemagglutinin subunit HA2 induces membrane destabilisation in the lysosomes. Upon acidification, this peptide domain becomes protonated, causing a conformational change from random coil to alpha helix (10, 11). Due to this conformational change, the fusion peptide is inserted into the endosomal membrane and destabilises it (12, 13).
Synthetic analogues of this fusion peptide have been used in non-viral gene delivery systems to improve the transfection efficiency (14-16).
We examined whether co-encapsulation of the influenza virus derived synthetic diINF-7 could enhance the cytosolic delivery of liposome-entrapped proteins. Using circular dichroism, the pH-induced conformational change was verified. The alpha helical content increased from 15% to 31% when the pH was lowered from 7.4 to 5.2. In addition, we showed that the fusogenic behaviour of the peptide was pH-dependent; diINF-7 induced leakage of liposome-encapsulated calcein was much more efficient at pH 5.2 than at pH 7.4.
For application as a mediator of cytosolic delivery, the peptide was co-encapsulated with the catalytic A-domain of diphtheria toxin (DTA). DTA inhibits protein synthesis when delivered in the cytoplasm, resulting in cell death. Liposomes targeted to the epidermal growth factor receptor (EGFR) of tumour cells showed cytotoxicity only when both the diINF-7 peptide and DTA were encapsulated, whereas targeted liposomes containing either DTA or diINF-7 did not have any cytotoxic effect (4).

SURFACE COUPLING OF CELL-PENETRATING PEPTIDES

The coupling of so-called cell-penetrating peptides (CPP) to cargoes of different sizes would enable the cargo to directly enter the cytoplasm (8). Recently, this concept was questioned since redistribution of fluorescently labeled CPP was observed in fixed cells due to the fixation procedure (17, 18).

We studied the uptake mechanism of TAT-peptide modified liposomes in living cells. In this study, it was clear that the coupling of TAT-peptide to the liposomes greatly enhanced the cellular binding and subsequent uptake of the liposomes. However, when the cellular distribution of fluorescent TAT-modified liposomes in fixed cells was compared to the distribution in living cells, significant differences were observed. Instead of a diffuse cytosolic fluorescence seen in fixed cells, living cells displayed punctuate intracellular spots, indicating endocytosis. This was supported by the observation that the liposomal labels co-localised with Lysotracker Red, a marker for endosomes and lysosomes. In addition, when endocytosis was inhibited by lowering the temperature to 4°C, by iodoacetamide or by cytochalasin D resulting that only plasma membrane binding was observed while intracellular fluorescence was absent. We concluded that TAT-peptide modified liposomes are taken up by endocytosis rather than plasma membrane translocation (19). This study is more extensively explained in chapter 4 of this thesis.

PHOTOCHEMICAL INTERNALISATION

Recently, a novel photochemical technique, named photochemical internalisation (PCI), was developed for inducing release of molecules from endocytic vesicles (20). In this technique, photosensitising compounds (so-called photosensitisers) are applied for endosomal escape. Upon illumination of these photosensitisers, highly reactive oxygen species are formed. Depending on their physicochemical properties, the photosensitiser can preferentially localise in endosomal membranes. Upon illumination and formation of the reactive oxygen species, the endosomal membrane is damaged and molecules present will be released in the cytosol. PCI has been shown to induce endosomal release of toxins (21, 22), immunotoxins (23) and non-viral gene delivery systems (21, 24) *in vitro*. In the near future, we will explore the use of PCI for the cytosolic delivery of liposomal macromolecules, which is described in chapter 6 of this thesis.

CONCLUSION

Despite the ability of targeted liposomes to interact specifically with certain cell types, the cytosolic delivery of the liposomal drug contents is often inefficient, an observation which particularly holds true for macromolecular compounds like DNA and proteins. After cellular uptake via endocytosis the liposomes will enter the acidic lysosomal compartment in which the liposomes with their entrapped drugs are degraded. Here we have described several approaches to improve the cytosolic delivery of therapeutic macromolecules entrapped in liposomes.

Co-encapsulation of the fusogenic peptide diINF-7 into immunoliposomes enables the cytosolic delivery of liposomal proteins. Although surface modification of liposomes with the cell penetrating peptide TAT did not lead to translocation of the liposome particles over the plasma membrane, the cellular uptake via endocytosis was greatly enhanced compared

to non-modified liposomes. In combination with endosomal escape enhancers, like the diINF-7 peptide, this system could be advantageous. Furthermore, the recent developed technique photochemical internalisation may also prove useful for the cytosolic delivery of liposomal macromolecules.

REFERENCES

1. B. Lebleu. Delivering information-rich drugs--prospects and challenges. *Trends Biotechnol.* **14:** 109-10 (1996)
2. S. Simoes, V. Slepushkin, N. Duzgunes and M. C. Pedroso de Lima. On the mechanisms of internalization and intracellular delivery mediated by pH-sensitive liposomes. *Biochim Biophys Acta.* **1515:** 23-37 (2001)
3. M. Mandal and K. D. Lee. Listeriolysin O-liposome-mediated cytosolic delivery of macromolecule antigen in vivo: enhancement of antigen-specific cytotoxic T lymphocyte frequency, activity, and tumor protection. *Biochim Biophys Acta.* **1563:** 7-17 (2002)
4. E. Mastrobattista, G. A. Koning, L. Van Bloois, A. C. Filipe, W. Jiskoot and G. Storm. Functional Characterization of an Endosome-disruptive Peptide and Its Application in Cytosolic Delivery of Immunoliposome-entrapped Proteins. *J Biol Chem.* **277:** 27135-43 (2002)
5. T. Kakudo, S. Chaki, S. Futaki, I. Nakase, K. Akaji, T. Kawakami, K. Maruyama, H. Kamiya and H. Harashima. Transferrin-modified liposomes equipped with a pH-sensitive fusogenic peptide: an artificial viral-like delivery system. *Biochemistry.* **43:** 5618-28 (2004)
6. Y. L. Tseng, J. J. Liu and R. L. Hong. Translocation of liposomes into cancer cells by cell-penetrating peptides penetratin and tat: a kinetic and efficacy study. *Mol Pharmacol.* **62:** 864-72 (2002)
7. V. P. Torchilin, R. Rammohan, V. Weissig and T. S. Levchenko. TAT peptide on the surface of liposomes affords their efficient intracellular delivery even at low temperature and in the presence of metabolic inhibitors. *Proc Natl Acad Sci U S A.* **98:** 8786-91 (2001)
8. M. Lindgren, M. Hallbrink, A. Prochiantz and U. Langel. Cell-penetrating peptides. *Trends Pharmacol Sci.* **21:** 99-103 (2000)
9. J. M. White. Viral and cellular membrane fusion proteins. *Annu Rev Physiol.* **52:** 675-97 (1990)
10. R. W. Doms, A. Helenius and J. White. Membrane fusion activity of the influenza virus hemagglutinin. The low pH-induced conformational change. *J Biol Chem.* **260:** 2973-81 (1985)
11. J. J. Skehel, P. M. Bayley, E. B. Brown, S. R. Martin, M. D. Waterfield, J. M. White, I. A. Wilson and D. C. Wiley. Changes in the conformation of influenza virus hemagglutinin at the pH optimum of virus-mediated membrane fusion. *Proc Natl Acad Sci U S A.* **79:** 968-72 (1982)
12. T. Stegmann, J. M. Delfino, F. M. Richards and A. Helenius. The HA2 subunit of influenza hemagglutinin inserts into the target membrane prior to fusion. *J Biol Chem.* **266:** 18404-10 (1991)
13. C. Harter, P. James, T. Bachi, G. Semenza and J. Brunner. Hydrophobic binding of the ectodomain of influenza hemagglutinin to membranes occurs through the "fusion peptide". *J Biol Chem.* **264:** 6459-64 (1989)
14. S. M. Van Rossenberg, K. M. Sliedregt-Bol, N. J. Meeuwenoord, T. J. Van Berkel, J. H. Van Boom, G. A. Van Der Marel and E. A. Biessen. Targeted lysosome disruptive elements for improvement of parenchymal liver cell-specific gene delivery. *J Biol Chem.* **277:** 45803-10 (2002)
15. E. Wagner. Application of membrane-active peptides for nonviral gene delivery. *Adv Drug Deliv Rev.* **38:** 279-289 (1999)
16. N. J. Zuidam, G. Posthuma, E. T. de Vries, D. J. Crommelin, W. E. Hennink and G. Storm. Effects of physicochemical characteristics of poly(2-(dimethylamino)ethyl methacrylate)-based polyplexes on cellular association and internalization. *J Drug Target.* **8:** 51-66 (2000)
17. M. Lundberg and M. Johansson. Positively charged DNA-binding proteins cause apparent cell membrane translocation. *Biochem Biophys Res Commun.* **291:** 367-71 (2002)
18. E. Vives. Cellular uptake [correction of utake] of the Tat peptide: an endocytosis mechanism following ionic interactions. *J Mol Recognit.* **16:** 265-71 (2003)
19. M. M. Fretz, G. A. Koning, E. Mastrobattista, W. Jiskoot and G. Storm. OVCAR-3 cells internalize TAT-peptide modified liposomes by endocytosis. *Biochim Biophys Acta.* **1665:** 48-56 (2004)
20. A. Hogset, L. Prasmickaite, P. K. Selbo, M. Hellum, B. O. Engesaeter, A. Bonsted and K. Berg. Photochemical internalisation in drug and gene delivery. *Adv Drug Deliv Rev.* **56:** 95-115 (2004)
21. K. Berg, P. K. Selbo, L. Prasmickaite, T. E. Tjelle, K. Sandvig, J. Moan, G. Gaudernack, O. Fodstad, S. Kjolsrud, H. Anholt, G. H. Rodal, S. K. Rodal and A. Hogset. Photochemical internalization: a novel technology for delivery of macromolecules into cytosol. *Cancer Res.* **59:** 1180-3 (1999)
22. P. K. Selbo, K. Sandvig, V. Kirveliene and K. Berg. Release of gelonin from endosomes and lysosomes to cytosol by photochemical internalization. *Biochim Biophys Acta.* **1475:** 307-13 (2000)
23. P. K. Selbo, G. Sivam, O. Fodstad, K. Sandvig and K. Berg. Photochemical internalisation increases the cytotoxic effect of the immunotoxin MOC31-gelonin. *Int J Cancer.* **87:** 853-9 (2000)

24. A. Hogset, L. Prasmickaite, M. Hellum, B. O. Engesaeter, V. M. Olsen, T. E. Tjelle, C. J. Wheeler and K. Berg. Photochemical transfection: a technology for efficient light-directed gene delivery. *Somat Cell Mol Genet.* **27:** 97-113 (2002)

3

Temperature, concentration and cholesterol dependent translocation of L- and D-octaarginine across the plasma and nuclear membrane of CD34+ leukaemia cells

Marjan M. Fretz, Neal A. Penning, Saly Al-Taei, Shiroh Futaki, Toshihide Takeuchi, Ikuhiko Nakase, Gert Storm and Arwyn T. Jones

Accepted for publication in the Biochemical Journal

ABSTRACT

Delineating the mechanisms by which cell penetrating peptides such as HIV-TAT peptide, oligoarginines and penetratin gain access to cells has recently received intense scrutiny. Heightened interest in these entities stems from their abilities to enhance cellular delivery of associated macromolecules such as genes and proteins, suggesting they may have widespread applications as drug delivery vectors. Proposed uptake mechanisms include energy-independent plasma membrane translocation and energy-dependent vesicular uptake and internalisation through endocytic pathways. Here we investigated the effects of temperature, peptide concentration and plasma membrane cholesterol levels on the uptake of a model cell penetrating peptide, octaarginine (L-R8) and its D-enantiomer (D-R8) in $CD34^+$ leukaemia cells. We find that at 4-12˚C, L-R8 uniformly labels the cytoplasm and nucleus but in cells incubated with D-R8 there is additional labeling of the nucleolus, that is still prominent at 30˚C incubations. At temperatures between 12-30˚C, the peptides are also localised to endocytic vesicles, that consequently appear as the only labeled structures in cells incubated at 37˚C. Small increases in the extracellular peptide concentration in 37˚C incubations result in a dramatic increase in the fraction of the peptide that is localised to the cytosol and promoted the binding of D-R8 to the nucleolus. Enhanced labeling of the cytosol, nucleus and nucleolus was also achieved by extraction of plasma membrane cholesterol with methyl-ß-cyclodextrin. The data argues for two, temperature-dependent, uptake mechanism for these peptides and for the existence of a threshold concentration for endocytic uptake that when exceeded promotes direct translocation across the plasma membrane.

INTRODUCTION

The scientific literature describes an ever-increasing library of peptides that mediate the lysis of biological membranes or have capacities to translocate through these structures in the absence of increasing porosity to other molecules. An example of the former is mellitin, but recently more attention has been focused on cell penetrating peptides (CPP), also called protein transduction domains, such as the TAT peptide from the HIV-TAT protein and penetratin from the *Drosophila melanogaster* homeobox protein Antennapedia (1). A particular interest in these CPPs derives from their abilities in *vitro* and in *vivo* to overcome cellular barriers such as the plasma membrane, and deliver therapeutic macromolecular cargo, including genes and proteins, into cells (2-5)

A prerequisite to efficient utilization of these peptides as delivery vectors is an enhanced understanding of (a) their interaction with cell surface components - proteins, carbohydrate, lipids, (b) their mechanism of uptake - endocytosis, direct translocation, and (c) their intracellular fate - delivery to lysosomes, dynamics in the cytosol and delivery to the nucleus. Since the discovery that a number of CPP effects is due to fixation artifacts (6, 7), the concept that cellular entry was via direct plasma membrane translocation has been somewhat superceded by models showing that entry is via some form of endocytic route, and that translocation occurs across membranes of the endo-lysosomal system or even the endoplasmic reticulum (7-11). These studies mostly relate to microscopical and flow cytometry analysis of the peptides as fluorescent conjugates, their attachment to larger cargo will undoubtedly affect their interactions with cells and their translocation capacities (12, 13).

Studies from our laboratories and others, using oligoarginine (R7-R9) and HIV-TAT peptides have shown, however, that despite the use of stringent methods to remove plasma membrane associated peptides with trypsin and heparin, a significant fraction enters cells and nucleus at 4˚C (11, 12, 14, 15). Uptake of fluorescent HIV-TAT and octaarginine (R8) peptides in the nonadherent leukaemic KG1a cell line was not inhibited by placing the cells on ice, but the labeling was diffusely localised throughout the cells compared with only vesicular labeling at 37˚C (11). Similar observations have been demonstrated in a number of adherent cell lines (12, 14, 15). Other studies in HUVEC and macrophages show that 4˚C incubations inhibited uptake by ~75% compared with incubations performed at 37˚C (10), and claims also exist for no uptake at 4˚C (9). Though there is disparity over the extent of cellular association at 4˚C there is general uniformity with respect to the fact that a significant fraction enters cells in the absence of endocytic mechanisms. Recent data also suggests that R8 was able to enhance delivery of liposomes at both 37 and 4˚C (16).

Model membrane systems have also been utilised to investigate the translocation capacities of these peptides and as expected this process is dependent on peptide sequence and the lipid composition of the membranes (17-21). These studies have allowed for proposals for the mechanism by which the peptides interact with and traverse membrane systems and

favored models suggest they are driven via a potential difference following membrane destabilization, that they induce the formation of inverted micelles or that they themselves mediate pore formation.

To further investigate the effects of temperature on cellular peptide uptake, we have performed quantitative and qualitative analysis with the model CPP R8-Alexa488 and its D-enantiomer in a leukaemia cell line. We find that peptide localization is sensitive to cholesterol sequestration, peptide concentration, and the incubation temperature, such that a reduction in endocytosis at low temperatures is paralleled by an increase in peptide translocation through the plasma membrane.

EXPERIMENTAL METHODS

Materials

Maleimide-C5-Alexa488 and Alexa488-transferrin (Alexa488-Tf) were from Invitrogen (Paisley, UK), DRAQ5 dye was a kind gift from Biostatus (Shepshed, UK). N-acetylcysteine and methyl-β-cyclodextrin (MβCD) were purchased from Sigma (Poole, UK).

Peptide synthesis

The two peptides used in this study were generated by 9-fluorenylmethyloxycarbonyl (Fmoc) solid phase synthesis and labeled at the C-terminal cysteine using Maleimide-C5-Alexa488 sodium salt as fluorescent dye as previously described (11). Purification and characterization was achieved by HPLC and MALDI-TOF mass spectrometry respectively. The final peptide products were L-R8-Alexa488 containing naturally abundant L-arginine [NH_2-$(Arg)_8$-Gly-Cys(Alexa 488)-amide] or D-R8-Alexa488 [NH_2-$(_D$-$Arg)_8$-Gly-Cys(Alexa 488)-amide].

Cell culture

The haematopoietic cell line KG1a was maintained at confluency of 0.5 – 2 x 10^6 cells/ml in RMPI 1640 supplemented with 10% fetal calf serum, 100 IU/ml penicillin and 100 µg/ml streptomycin at 37°C with 5% CO_2 in humidified air. All cell culture reagents were obtained from Invitrogen (Paisley, UK).

Fluorescence microscopy

KG1a cells (0.5 x 10^6) were washed once with complete RPMI 1640 medium (CM) and equilibrated for 15 min in complete medium set to temperatures 4 (ice), 12, 19, 30 and 37˚C. The medium was then replaced by 200 µl fresh equilibrated complete medium containing 2-10 µM of L-or D-R8-Alexa488 or 100 nM Alexa488-Tf and incubated at these temperatures for 1 h. The cells were washed twice with ice-cold PBS and once with serum free RMPI 1640 medium without phenol red, serum or antibiotics (imaging medium), and resuspended in approximately 20 µl of imaging medium. In some experiments, DRAQ5 dye was used to label the nucleus and this was added at room temperature (10 µM) for 3 min prior to the last washing step.

Finally, 2 µl of the cell suspension was transferred to a well of a 10-well multispot microscope slide (Hendley, Essex, UK), that was then layered with a coverslip. Live cells were then immediately analysed by fluorescent microscopy. Wide field fluorescent images were obtained on a Leica DMIRB inverted fluorescent microscope equipped with a 63x oil immersion objective and QIMAGING RETIGA 1300 camera (Burnaby, BC, Canada). The acquired images were processed with Improvision Openlab 5.0.2 software (Coventry, U.K).

Confocal microscopy was performed on a Leica TCS-SP2 RS confocal laser-scanning microscope equipped with an Ar and HeNe laser and a 63x oil immersion objective. Leica LCS Lite software was used to merge and stack individual confocal sections through the z-axis to generate maximum projection images.
In one designated experiment, cells were incubated with 2 μM L-R8-Alexa488 for 1 h and following washing were fixed in 3% (w/v) paraformaldehyde for 15 min prior to further washes and analysis by fluorescence microscopy.

Flow cytometry
KG1a cells (0.5 x 10^6) were equilibrated and incubated for 1 h with 2 μM L- or D-R8-Alexa488 at different temperatures as described above. Alternatively, cells were washed in ice cold CM and incubated with 0.25 – 5 μM L- or D-R8-Alexa488 for 1 h at 4°C. The cells were washed three times with ice-cold PBS, resuspended in 200 μl of PBS and Alexa488 fluorescence was measured using a Becton & Dickinson FACScalibur analyser. In some experiments, following peptide incubation, the cells were washed once with PBS, incubated with 0.25 mg/ml trypsin solution for 5 min at 37°C, washed once with ice-cold PBS and finally twice with PBS containing 14 μg/ml heparin. Live cells were gated on Forward Scatter and Side Scatter and 10,000 viable cells were analysed.

Analysis of binding and uptake of activated and inactivated Alexa488-C5-maleimide
Unconjugated (activated) Alexa488-C5-maleimide was dissolved in methanol to a concentration of 1.78 mM. For inactivation, 375 μl of the solution was incubated at room temperature for 4 h with a 4-fold molar excess of N-acetylcysteine (10 mg/ml in PBS). The solution was then stored at -20°C until use. For cell studies, KG1a cells (0.5 x 10^6) were equilibrated on ice or at 37˚C, washed and further incubated on ice or at 37˚C in CM containing 2 μM activated or inactivated dye. Finally the cells were washed two times with imaging medium and analysed, as described, by fluorescent microscopy.

Binding and uptake of peptides and transferrin by MβCD-treated cells
MβCD was dissolved in PBS to 76 mM and diluted to 5 mM in serum free medium (SFM). KG1a cells (0.5 x 10^6) were washed once with SFM, resuspended in 200 μl SFM containing 5 mM MβCD and incubated under tissue culture conditions for 30 min. Control cells were treated as above but in the absence of MβCD. The cells were then washed with SFM and incubated for 1 h at 37˚C with 2 μM L- or D-R8-Alexa488 or 100 nM Tf-Alexa488 in SFM. The cells were washed twice with SFM, resuspended in imaging medium and analysed by fluorescence microscopy.

Cell viability studies

KG1a cells (4 x 10^4 cells/well in a total volume of 200 µl) were seeded in 96-well plates and incubated with 0 - 50 µM L- or D-R8-Alexa488 for 24 h under tissue culture conditions. Cell viability was then assessed using MTT assays (22). Briefly, 20 µl MTT, 5.5 mg/ml in SFM, was directly added to each well giving a final concentration of 0.5 mg/ml. The cells were then incubated for 4 h under tissue culture conditions. The plates were centrifuged at 1000 x *g* for 5 min prior to removing the supernatant and then adding 100 µl DMSO. The samples were finally incubated at 37°C for 30 min prior to quantifying the absorbance at 550 nm.

RESULTS

Comparative analysis of the subcellular distribution of L- and D-R8-Alexa488.

We previously reported on the distinct labeling patterns of L-R8-Alexa488 in the $CD34^+$ leukaemic KG1a cell line when incubations were performed either on ice (here referred to as 4˚C) or at 37˚C (11). As shown in Figure 1A, confocal microscopy of cells incubated for 1 h at 4˚C with 2 µM L-R8-Alexa488 reveals the peptide to be localised throughout the cell including the nucleus and this compares with vesicular labeling only, when identical experiments are performed at 37˚C (Figure 1C).

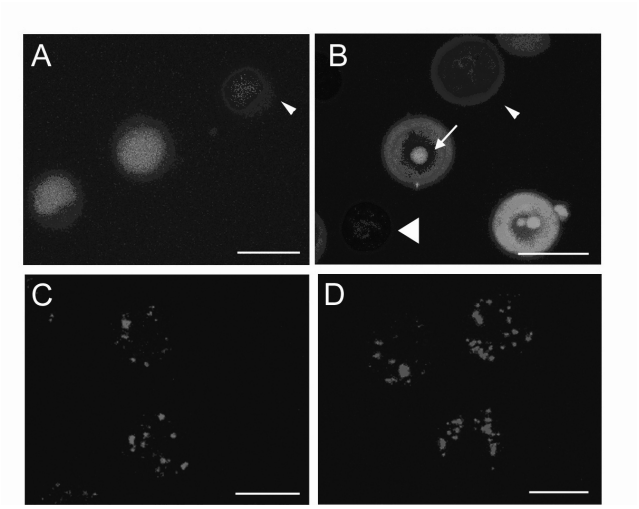

Figure 1. Cellular distribution of L- and D-R8-Alexa488 in KG1a cells at 4 and 37°C (A-D) KG1a cells were incubated for 1 h with 2 µM L- (A, C) or D-R8-Alexa488 (B, D) at either 4°C (A-B) or 37°C (C-D), prior to analysis by confocal microscopy. Shown are maximum projections of 35 z-stacks (~ 500 nm/ and 2 to 4 s/section) for each condition. A and B were also labeled with DRAQ5 dye as described in experimental. Arrows in B indicate peptide labeling of nucleolus, small arrowhead show a cell showing low peptide labeling, large arrowhead shows a cell with undetectable levels of peptide fluorescence. Scale bars 10 µm.

Our ability to label the nucleus of these live cells with the DRAQ5 probe also supports our previous observations showing heterogeneity with respect to the intensity of peptide labeling when peptide incubations are performed at this temperature (11). To obtain these images we captured multiple sections through the z-axis and then overlaid the data to create a single merged maximum projection image.

We performed identical experiments with the D-enantiomer of R8, and similar to the L form, the peptide localises to vesicles at 37˚C (Figure 1D). When the cells were incubated with D-R8-Alexa488 at 4˚C, we observed diffuse labeling that was less apparent in the

nucleus but much more prominent in the nucleolus (Figure 1B). This image also highlights the heterogeneity of peptide labeling at 4˚C, from high to undetectable.
In order to refute the possibility that these effects are caused by extracellular protease-mediated degradation of the peptide, with resulting release and internalisation of free fluorophore, we initially incubated the cells at 4 or 37˚C with the activated Alexa488 maleimide dye that is used to link to the terminal cysteine of the peptide (Figure 2A).

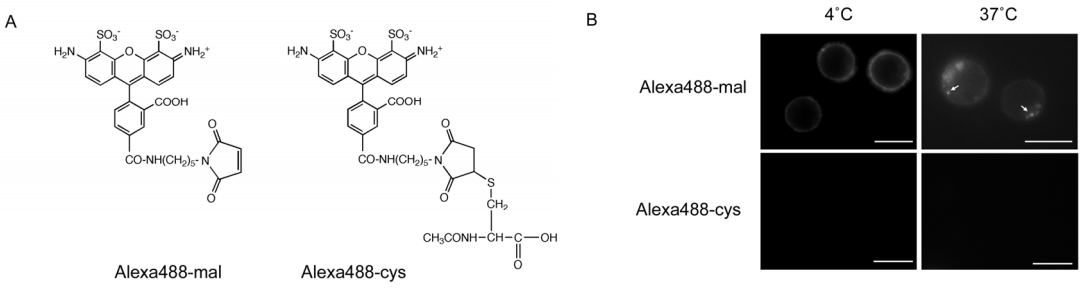

Figure 2 Cellular distribution of activated and inactivated Alexa488-C5-maleimide
(A) Chemical structures of activated (Alexa488-mal) and inactivated Alexa488-C5-maleimide (Alexa488-cys), following its conjugation to N-acetylcysteine. (B) Cellular distribution of Alexa488-mal and Alexa488-cys. KG1a cells were incubated with 2 μM label for 1 h at 4 or 37˚C prior to washing and analysis by fluorescence microscopy. Arrows depict vesicular labeling that was only observed with Alexa488-mal at 37˚C. Scale bars 10 μm.

At 4˚C the fluorescence of this compound was confined to the plasma membrane and when identical experiments were performed at 37˚C, intracellular vesicles were also labeled (Figure 2B). However, compared to experiments performed with the equivalent concentrations of Alexa488-R8 (Figure 1), much higher exposure times were required to observe these structures. This suggested that at both temperatures, the activated dye was conjugating to plasma membrane sulfhydryl groups and that these conjugates remained on this structure in the absence of endocytosis at 4˚C but were internalised at 37˚C. We therefore inactivated the maleimide functional group with N-acetylcysteine and observed that even the relatively high exposure times utilized to see the activated dye at 37˚C were not sufficient to label the cells at either temperature (Figure 2B). Thus the fluorescence observed in Figure 1 was a product of R8-mediated delivery to endosomes at 37˚C or to the cytosol, nucleus and nucleolus at 4˚C. We performed identical experiments with a control peptide NH_2-(Gly-Ser)$_4$-Gly-Cys(Alexa 488)-amide and at 2 μM this was undetectable in cells using fluorescence microscopy (data not shown).

Effects of temperature on subcellular distribution and cellular fluorescence profiles for L- and D-R8-Alexa488.

Similar microscopy experiments were then performed with L- and D-R8-Alexa488 at temperatures between 4 and 37˚C. Figure 3 shows that L-R8-Alexa488 diffusely labels the entire cell when incubations are performed at ≤ 19˚C, but at higher temperatures to 30˚C, the diffuse fluorescence is accompanied by vesicular labeling. In cells incubated with the D-R8 peptide there was similar but additional nucleolar labeling at all temperatures ≤ 30˚C; at 37˚C cellular labeling of both peptides was confined to vesicular structures. We also performed the same experiments with Alexa488-Transferrin (Alexa488-Tf), that at 4˚C is expected to only bind the transferrin receptor at the plasma membrane but not be internalised, and at higher temperatures will be endocytosed into clathrin coated vesicles and endosomes (23, 24). As expected, this protein labeled only the plasma membrane at ≤12˚C, but at higher temperatures, plasma membrane labeling was accompanied by vesicular labeling that increased in intensity as the temperature was increased to 37˚C. Thus, these octaarginine-based peptides behaved quite differently from each other and from Tf when they were incubated with cells at temperatures ≤30˚C. The data also suggest that unlike Tf, the peptides have at least two independent, but temperature-dependent uptake mechanisms. Similar differences in cellular distribution of peptides Tat P59W, R7 and R7W, were also noted in adherent cells when incubations are performed at 4˚C or 37˚C (12, 15), thus suggesting this differential labeling is not a feature unique to these leukaemia cells. We previously showed using flow cytometry that cellular fluorescence profiles of cells incubated with R8 at 4˚C differ from those incubated at 37˚C (11, 14).

We therefore performed flow cytometry analysis with cells incubated with 2 μM L- and D-R8-Alexa488 at the same selected temperatures between 4 and 37˚C. The results shown in Figure 4 show clear temperature dependent profiles, but the L and D forms gave very similar results. Two peaks were observed for both peptides after 4 to 12˚C incubations but at 19˚C the lower peak is much more apparent with a concomitant broadening of the high peak. Only one peak is observed for both peptides when incubated with cells at 30 to 37˚C.

Again, Alexa488-Tf was used for comparative analysis, and only one fluorescence peak, with the expected increasing intensity with increasing concentration, was observed at all temperatures (Figure 4). For this ligand, the data allows for easy quantification of cell-associated fluorescence, but this is not the case for quantification of cell-associated L- or D-R8-Alexa488 at <30˚C. This is why the profiles are shown here rather than just the geometric mean values. Interestingly, previous studies in Jurkat T-cells also showed two peaks of fluorescence, but the cells were incubated with a much higher concentration (12.5 μM) of R9 at 25 ˚C (25).

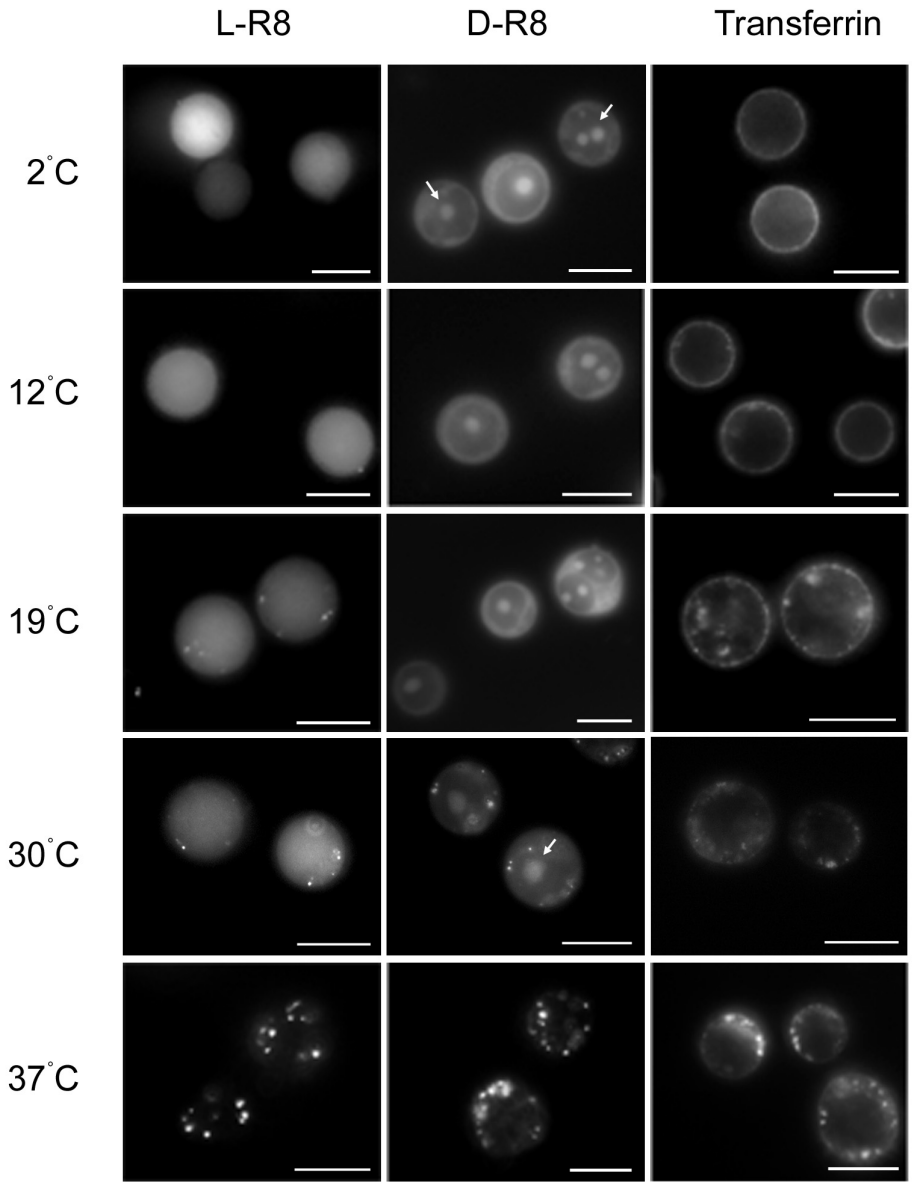

Figure 3. Temperature-dependent cellular distribution of R8-Alexa488 peptides and Alexa488-Tf. KG1a cells were incubated at 4 - 37˚C for 1 h with 2 µM L- or D-R8-Alexa488 or 100 nM Alexa488-Tf prior to washing and analysis by fluorescence microscopy. Arrows depict labeling of the nucleolus that is unique to D-R8-Alexa488 at ≤30 ˚C. Scale bars 10 µm.

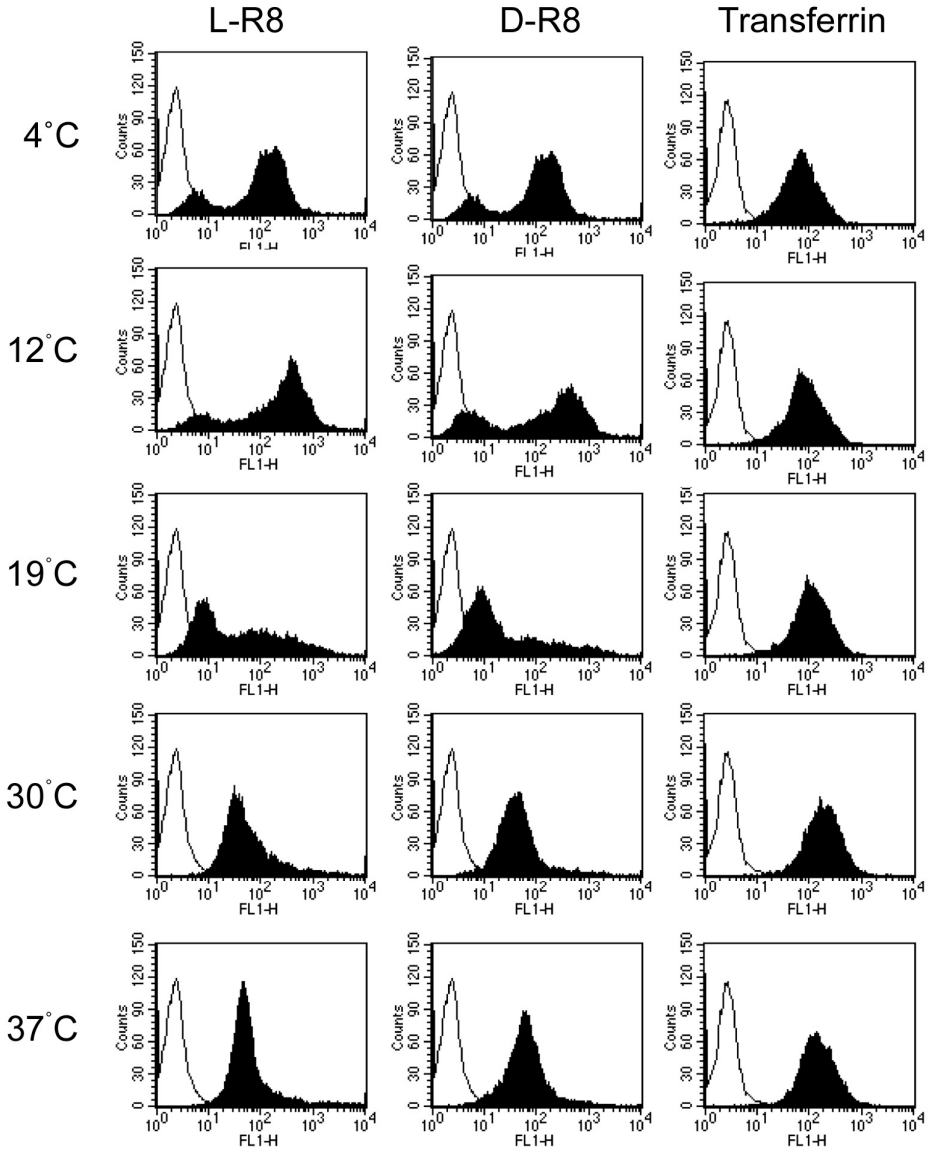

Figure 4. Temperature-dependent cellular fluorescence profiles for R8-Alexa488 peptides and Alexa488-Tf. KG1a cells were incubated at 4 - 37˚C for 1 h with 2 μM L- or D-R8-Alexa488 or 100 nM Alexa488-Tf prior to washing and analysis by flow cytometry. Unfilled peaks represent untreated cells

In conclusion, the data from this section suggest that endocytosis of peptides and transferrin occurs at a reasonably uniform rate throughout the cell population but that differences exist with respect to the capacity of the cells to associate with the peptides at temperatures < 37˚C.

Effects of concentration on subcellular distribution and cellular fluorescence profiles for L- and D-R8-Alexa488.

We then investigated whether the cellular fluorescence profiles that we observed at 4˚C were sensitive to the concentration of the peptides in the medium. Cells were incubated with 0.25 – 5 µM peptide for 1 h prior to washing and immediate analysis by flow cytometry or, following the peptide incubations, they were further treated with trypsin and washed with heparin solutions. These additional steps have been shown to reduce plasma membrane labeling that contributes significantly to the fluorescence values in adherent cells (7).

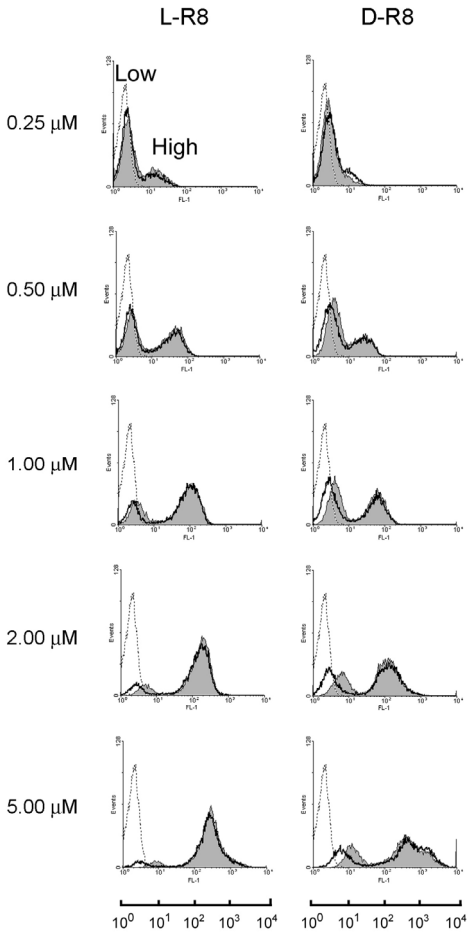

Figure 5. Concentration-dependent cellular fluorescence profiles for R8-Alexa488 peptides. KG1a cells were incubated for 1 h with 0.25 to 5.0 µM L- or D-R8-Alexa488 at 4°C. The cells were then washed and either immediately analysed by flow cytometry (filled grey) or were further treated with trypsin and heparin prior to analysis (unfilled peaks). Dotted lines represent untreated cells. In all experiments performed at 4˚C, two peaks of fluorescence of varying intensities were obtained, and designated Low and High. The geometric mean values of the two designated peaks were calculated for all conditions and these contributed with repeat experiments to generate Table 1.

The data in Figure 5 shows that L- and D-R8-Alexa488 generated two peaks of fluorescence at all concentrations, and irrespective of whether the cells were further subjected to trypsin and heparin treatment. These were designated Low and High and the mean intensity of both generally increased as the peptide concentration was increased; this was accompanied by an increase in the fraction of cells that appeared in the High peak. Trypsinisation appeared to have minimal effects on the fluorescent profiles but at >2 μM there was a visible reduction in the geometric mean of the low peaks. To analyse this further, the geometric means of the separate peaks at all studied concentrations were quantified and the results in Table 1 demonstrate that the fluorescence of the low peaks are significantly reduced ($P < 0.05$) by trypsin/heparin treatment at concentrations ≥ 0.5 μM for L-R8 or ≥ 1 μM for D-R8. However there was no significant decrease in the fluorescence of the high peak when the peptide concentration was ≥ 0.5 μM, and even at 0.25 μM peptide concentration, ≥ 75% of the fluorescence in the high peak fraction was insensitive to trypsin/heparin treatment.

Table 1 Analysis of fluorescence peaks obtained from incubating cells with increasing concentrations of R8-Alexa488 peptides. KG1a cells were incubated with 0.25 – 5.0 μM L- or D-R8-Alexa488 for 1 h at 4 °C. The cells were then washed and either immediately analysed by flow cytometry (PBS) or further treated with trypsin and heparin prior to analysis (trypsin/heparin). Two peaks of fluorescence were observed and designated Low and High (Figure 5). Shown are the geometric mean values for the Low and High peaks for all depicted concentrations. Data represent mean and SD from two individual experiments performed in duplicate. Statistical analysis for comparing the geometric means of untreated versus treated fluorescence cells was performed using students t-test. (*) Decreased relative to PBS control $P < 0.05$

L-R8

Peptide concentration (μM)	Low		High	
	PBS	Trypsin/heparin	PBS	Trypsin/heparin
0.25	2.76 ± 0.14	2.78 ± 0.45	17.20 ± 0.45	16.10* ± 0.26
0.50	3.12 ± 0.13	2.94 ± 0.12	39.99 ± 3.27	37.87 ± 2.35
1.00	3.89 ± 0.23	3.16* ± 0.22	98.88 ± 4.60	93.64 ± 2.74
2.00	4.78 ± 0.28	3.51* ± 0.19	175.14 ± 10.61	165.90 ± 14.05
5.00	9.44 ± 1.21	4.69* ± 0.47	357.73 ± 62.42	338.55 ± 46.47

D-R8

Peptide concentration (μM)	Low		High	
	PBS	Trypsin/heparin	PBS	Trypsin/heparin
0.25	3.18 ± 0.12	2.94 ± 0.19	15.73 ± 1.27	12.46* ± 0.57
0.50	4.09 ± 0.18	3.07* ± 0.05	28.71 ± 5.20	30.77 ± 4.56
1.00	4.80 ± 0.51	3.17* ± 0.17	83.14 ± 19.10	76.78 ± 17.98
2.00	6.07 ± 0.17	3.82* ± 0.28	147. 86 ± 16.75	155.025 ± 13.61
5.00	11.83 ± 1.69	6.18* ± 1.05	430.48 ± 63.94	521.81 ± 105.11

We do not currently have an explanation as to why a particular cell should fall into the Low or High peak population. It is conceivable that the low peak represents cells with the peptide located within the extracellular matrix of the plasma membrane or even embedded in the lipid bilayer and that this fraction is only partially sensitive to trypsin and heparin treatment. When cells were incubated for 1 h at 4˚C with L-R8-Alexa488, washed and then incubated for a further 1 hour at 4˚C or at 37˚C, there was no significant effect on cellular fluorescence profiles or low and high peak values (data not shown).

The possibility also exists that the loss of the low peak at higher peptide concentrations is a result of fluorescence quenching and that for L-R8, fluorescence could be further diminished by proteolysis. This is however unlikely as the intensity of the low peaks is enhanced with increasing peptide concentrations but do not increase in intensity upon trypsinisation and heparin washing and neither do they shift to baseline levels. Parallel experiments of peptide association versus cell cycle status may help define characteristics that predispose the cells to having different capacities to associate with or internalise these peptides.

Fluorescence microscopy was then utilised to determine whether increasing the peptide concentration from our standard 1 to 2 μM affected the subcellular labeling pattern when incubations were performed at 37˚C. Cells were therefore incubated with 2 to 10 μM peptide for 1 h, washed and then analysed.

Figure 6A shows that increasing the concentration from 2 to only 5 μM resulted in a dramatic increase in the fraction of the peptide that was localised to the cytosol. Vesicular labeling was still evident at this higher concentration, up to 10 μM, but this was somewhat masked by the strong diffuse labeling. In cells incubated with 10 μM D-R8-Alexa488 the nucleolus was also prominently labeled but L-R8-Alexa488 failed to label these structures even at these higher concentrations. In all our experiments we were unable to observe the presence of L-R8-Alexa488 in the nucleolus but clear nucleolar labeling was observed when cells, incubated with 2 μM peptide at 4 or 37˚C, were fixed with paraformaldehyde prior to microscopical analysis (Figure 6B and data not shown).

These data strongly suggest that endocytosis as an uptake mechanism, and visible by fluorescence microscopy, is only dominant to a specific peptide concentration. At levels higher than this threshold, the peptide also enters cells by an alternative mechanism. It is highly unlikely that this very strong cytoplasmic labeling at 5 to 10 μM is caused by endocytosis and then translocation from the endo-lysosomal system as similar data was obtained when the peptide incubations were reduced to 10 min (Figure 6C).

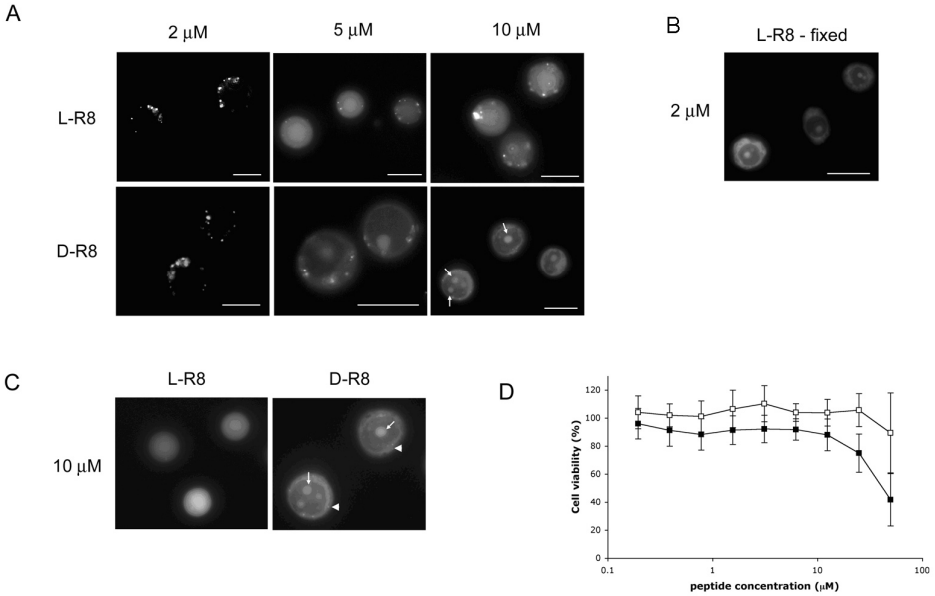

Figure 6. Concentration-dependent cellular distribution and toxicity profiles for R8-Alexa488 peptides (**A**) KG1a cells were incubated with 2, 5 or 10 μM L- or D-R8-Alexa488 for 1 h at 37°C prior to washing and analysis by fluorescence microscopy. Arrows depict labeling of the nucleolus; scale bars 10 μm. (**B**) KG1a cells were incubated with 2 μM L-R8-Alexa488 for 1 h at 37 °C. After washing, cells were fixed with paraformaldehyde prior to analysis by fluorescence microscopy. (**C**) KG1a cells were incubated with 10 μM L- or D-R8-Alexa488 for 10 min at 37°C prior to washing and analysis by fluorescence microscopy. Arrows depict labeling of the nucleolus, arrowheads show faint vesicular labeling **(D)** Cell viability of KG1a cells in the presence of increasing concentrations of R8-Alexa488 peptides. KG1a cells were incubated with 0 - 50 μM L-R8-Alexa488 (open squares) or D-R8-Alexa488 (filled squares) for 24 h prior to performing MTT assays. Cell viability is expressed as the percentage of viable cells relative to untreated controls. Data are from a two experiments performed in quadruplicate and values represent mean ± SD.

Vesicular labeling in these shorter incubations was however less pronounced. Equally it is unlikely that at low peptide concentrations at 37˚C that translocation from cytosol to endosomes and lysosomes is significant, as incubations performed at 4˚C in the presence of peptide followed by 37˚C incubations without peptides, had no effects on the pattern of labeling (Data not shown).

At concentrations ≥ 5 μM, it is conceivable that some of the observed effects were due to peptide induced membrane damage and cytotoxicity. Parallel experiments were therefore performed in cells incubated with 10 μM L- or D-R8-Alexa488 and propidium iodide (PI), that would only be expected to enter dead or leaky cells. There was no increase in PI labeled cells under these conditions (data not shown) and longer 24 h cell viability assays demonstrated that D and L peptides lacked significant toxicity up to 12.5 μM (Figure 6D).

The majority of studies investigating the uptake mechanisms of CPPs have also utilised peptide concentrations between 0.5 to 10 μM, however the universality of these effects with respects to other types of cells remains to be determined. There is likely to be different threshold concentrations for different cell lines as each will have their unique repertoire of plasma membrane lipids, proteins, and their associated carbohydrates. These may all affect the degree of peptide association with molecules protruding from the plasma membrane and/or with molecules localized within the bilayer itself.

Effects of cholesterol depletion on subcellular distribution of L- and D-R8-Alexa4 As translocation across membranes was occurring at higher concentrations of peptide, we investigated whether this process could be promoted at lower concentrations by perturbing the organisation of the plasma membrane. For this, we depleted plasma membrane cholesterol using a standard method employing the cholesterol sequestering agent methyl-ß-cyclodextrin (MßCD) (26). Cells were pretreated with 5 mM MßCD for 30 min prior to addition of 2 μM L- or D-R8-Alexa488 for 1 h at 37˚C and immediate analysis by fluorescence microscopy. MßCD treated cells had strong diffuse labeling of the cytoplasm and nucleus with very little evidence of vesicular uptake; consistent with our previous experiments, nucleolar labeling was unique to the D-form.

Very different results were obtained when parallel experiments were performed with Alexa488-Tf, and here, cholesterol sequestration completely inhibited vesicular uptake and only the plasma membrane was labeled. MßCD was previously shown to significantly inhibit uptake of TAT peptide (9) and penetratin in a number of cell lines (27), suggesting that uptake is occurring via plasma membrane domains called rafts. These are enriched in cholesterol (28), and MßCD is often used to discriminate between uptake via clathrin coated pits and raft-dependent pathways (29).

Studies in a number of adherent cell lines have however shown that transferrin internalisation is inhibited (40-60%) in MßCD treated cells (30). Thus the widespread use of MßCD and other cholesterol depleting agents should be cautioned unless control experiments with ligands for clathrin mediated uptake and other pathways are also investigated. Our experiments raise the interesting possibility that the organization of the plasma membrane into cholesterol enriched lipid rafts inhibits plasma membrane translocation. They also suggest that the normal site of entry of the peptides, especially at low temperatures, may be the more fluidic regions of the plasma membrane containing less cholesterol.

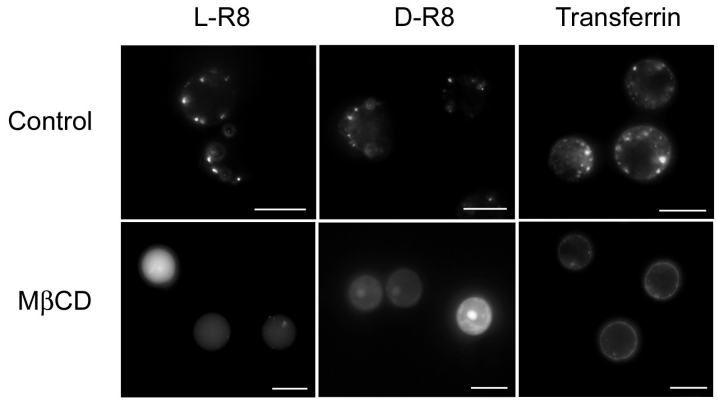

Figure 7. Effect of cholesterol depletion on cellular distribution of R8-Alexa488 peptides and Alexa488-Tf. KG1a cells were pre-incubated in the absence (Control) or presence (MβCD) of 5 mM MβCD for 30 min at 37°C prior to washing and incubation with 2 μM L- or D-R8-Alexa488 or 100 nM Alexa488-Tf for 1 h at 37°C. The cells were then washed and analysed by fluorescent microscopy. Scale bars 10 μm.

At 2 μM concentration, D-R8-Alexa488, unlike L-R8, labeled the nucleolus at all temperatures ≤30˚C, but this was also observed when the peptide concentration was increased 2.5 fold or in plasma membrane cholesterol depleted cells. These are all conditions that showed microscopical evidence for the presence of this peptide in the cytosol, suggesting this is the critical parameter that then allows for sequestration in the nucleolus. At physiological temperatures, proteolysis is likely to contribute much more to L-R8 degradation compared with D-R8 thus the fraction of this peptide that is able migrate to the nucleus and nucleolus is likely to be reduced (8, 31). However we also observe the same differences in localisation when the cells have been pre-cooled to 4˚C and then incubated with the peptides; here protease effects should be significantly diminished. L-R8-Alexa488 is clearly able to translocate to the nucleus at low temperatures, and nuclear, as opposed to nucleolus labeling is often more prominent in L-R8-Alexa488 treated cells (Figure 1). It remains to be seen whether nucleolar sequestration of D-R8 is reducing the extent of the fraction localised to the rest of the nucleus. Nucleolar labeling is a common characteristic of cells that have been incubated with CPPs such as oligoarginine and HIV-TAT and then fixed (7, 32, 33). Our results in unfixed KG1a cells does however support our previous observations of nucleolar labeling of live HeLa cells incubated with the same D-R8 peptide on ice; the extracellular peptide concentration was however appreciably higher at 10 μM (14). An ability to label the nucleolus was also a feature of other CPPs Flu-ß-$(VRR)_4$ and TAT-HA2 (13, 34) suggesting that these also have a propensity to the bind most probably the RNA that is prominent over DNA in these structures.

CONCLUSION

We have analysed in detail the effects of temperature, concentration and peptide chirality on the cellular dynamics of R8 peptide in KG1a cells. Our results suggest that L- and D- forms of the peptides share several similarities such as low temperature translocation but also differences with respect to labeling the nucleolus. Enhancing the fraction of the peptide that localises to the cytosol can be achieved by relatively small increases in peptide concentration or by sequestering plasma membrane cholesterol. These processes seem to be specific for the peptides, as we did not observe any parallel increases in membrane permeability or toxicity. It will now be interesting to investigate whether some of these effects are common to more complex CPPs such as HIV-TAT peptide and penetratin, and also to further determine the capacity of R8 at low temperatures to enhance membrane translocation of associated cargo.

ACKNOWLEDGEMENT

Marjan Fretz is supported by a Marie Curie Host Fellowship for early-stage training in the 6^{th} framework programme of the European Commission. This work was supported in part by Grants-in-Aid for Scientific Research from the Ministry of Education, Culture, Sports, Science and Technology of Japan. Toshihide Takeuchi is grateful for support from the JSPS Research Fellowship for Young Scientists.

REFERENCES

1. S. T. Henriques, M. N. Melo and M. A. Castanho. Cell-penetrating peptides and ant-microbial peptides: how different are they? *Biochem J.* **399:** 1-7 (2006)
2. E. L. Snyder and S. F. Dowdy. Cell-penetrating peptides in drug delivery. *Pharm Res.* **21:** 389-393 (2004)
3. A. H. Joliot and A. Prochiantz. Transduction peptides: from technology to physiology. *Nat Cell Biol.* **6:** 189-196 (2004)
4. S. Deshayes, M. C. Morris, G. Divita and F. Heitz. Cell-penetrating peptides: tools for intracellular delivery of therapeutics. *Cell Mol Life Sci.* **62:** 1839-1849 (2005)
5. K. M. Wagstaff and D. A. Jans. Protein transduction: cell-penetrating peptides and their therapeutic applications. *Curr Med Chem.* **13:** 1371-1387 (2006)
6. M. Lundberg and M. Johansson. Positively charged DNA-binding proteins cause apparent cell membrane translocation. *Biochem Biophys Res Commun.* **291:** 367-71 (2002)
7. J. P. Richard, K. Melikov, E. Vives, C. Ramos, B. Verbeure, M. J. Gait, L. V. Chernomordik and B. Lebleu. Cell-penetrating peptides: A re-evaluation of the mechanism of cellular uptake. *J Biol Chem.* (2002)
8. R. Fischer, K. Kohler, M. Fotin-Mleczek and R. Brock. A stepwise dissection of the intracellular fate of cationic cell-penetrating peptides. *J Biol Chem.* **279:** 12625-12635 (2004)
9. I. M. Kaplan, J. S. Wadia and S. F. Dowdy. Cationic TAT peptide transduction domain enters cells by macropinocytosis. *J Control Release.* **102:** 247-253 (2005)
10. J. P. Richard, K. Melikov, H. Brooks, P. Prevot, B. Lebleu and L. V. Chernomordik. Cellular uptake of unconjugated TAT peptide involves clathrin-dependent endocytosis and heparan sulfate receptors. *J Biol Chem.* **280:** 15300-6 (2005)
11. S. Al-Taei, N. A. Penning, J. C. Simpson, S. Futaki, T. Takeuchi, I. Nakase and A. T. Jones. Intracellular traffic and fate of protein transduction domains HIV-1 TAT and octaarginine, implications for their utilization as drug delivery vectors. *Bioconjug Chem.* **17:** 90-100 (2006)
12. J. R. Maiolo, M. Ferrer and E. A. Ottinger. Effect of cargo molecules on the cellular uptake of arginine-rich cell-penetrating peptides. *Biochem Biophys Acta.* **1712:** 161-72 (2005)
13. G. Tunnemann, R. M. Martin, S. Haupt, C. Patsch, F. Edenhofer and M. C. Cardoso. Cargo-dependent mode of uptake and bioavailability of TAT-containing proteins and peptides in living cells. *Faseb J.* **20:** 1775-84 (2006)
14. I. Nakase, M. Niwa, T. Takeuchi, K. Sonomura, N. Kawabata, Y. Koike, M. Takehashi, S. Tanaka, K. Ueda, J. C. Simpson, A. T. Jones, Y. Sugiura and S. Futaki. Cellular uptake of arginine-rich peptides: roles for macropinocytosis and actin rearrangement. *Mol Ther.* **10:** 1011-22 (2004)
15. P. E. Thoren, D. Persson, P. Isakson, M. Goksor, A. Onfelt and B. Norden. Uptake of analogs of penetratin, Tat(48-60) and oligoarginine in live cells. *Biochem Biophys Res Commun.* **307:** 100-7 (2003)
16. A. Iwasa, H. Akita, I. Khalil, K. Kogure, S. Futaki and H. Harashima. Cellular uptake and subsequent intracellular trafficking of R8-liposomes introduced at low temperature. *Biochem Biophys Acta.* **1758** (2006)
17. S. Afonin, A. Frey, S. Bayerl, D. Fischer, P. Wadhwani, S. Weinkauf and A. S. Ulrich. The cell-penetrating peptide TAT(48-60) induces a non-lamellar phase in DMPC membranes. *Chemphyschem.* **7:** 2134-2142 (2006)
18. C. E. Caesar, E. K. Esbjorner, P. Lincoln and B. Norden. Membrane interactions of cell-penetrating peptides probed by tryptophan fluorescence and dichroism techniques:correlations of structure to cellular uptake. *Biochemistry.* **45:** 7682-7692 (2006)
19. D. Terrone, S. L. Sang, L. Roudaia and J. R. Silvius. Penetratin and related cell-penetrating cationic peptides can translocate across lipid bilayers in the presence of a transbilayer potential. *Biochemistry.* **42** (2003)
20. P. E. Thoren, D. Persson, P. Lincoln and B. Norden. Membrane destabilizing properties of cell-penetrating peptides. *Biophys Chem.* **114:** 169-179 (2005)
21. A. Ziegler, X. L. Blatter, A. Seelig and J. Seelig. Protein transduction domains of HIV-1 and SIV TAT interact with charged lipid vesicles. Binding, mechanism and thermodynamic analysis. *Biochemistry.* **42:** 9185-9194 (2003)
22. T. Mosmann. Rapid colorimetric assay for cellular growth and survival: application of proliferation and cytotoxicity assays. *J Immunol Methods.* **65:** 55-63 (1983)

23. F. R. Maxfield and T. E. McGraw. Endocytic recycling. *Nat Rev Mol Cell Biol.* **5:** 121-132 (2004)
24. E. M. van Dam, T. Ten Broeke, K. Jansen, P. Spijkers and W. Stoorvogel. Endocytosed transferrin receptors recycle via distinct dynamic and phosphatidylinositol 3-kinase-dependent pathways. *J Biol Chem.* **277:** 48876-48883 (2002)
25. D. J. Mitchell, D. T. Kim, L. Steinman, C. G. Fathman and J. B. Rothbard. Polyarginine enters cells more efficiently than other polycationic homopolymers. *J Peptide Res.* **56:** 318-25 (2000)
26. M. Hao, S. Mukherjee, Y. Sun and F. R. Maxfield. Effects of cholesterol depletion and increased lipid unsaturation on the properties of endocytic membranes. *J Biol Chem.* **279:** 14171-14178 (2004)
27. T. Letoha, S. Gaal, C. Somlai, Z. Venkei, H. Glavines, E. Kusz, E. Duda, A. Czajlik, F. Petak and B. Penke. Investigation of penetratin peptides. Part 2. In vitro uptake of penetratin and two of its derivatives. *J Pept Sci.* **11:** 805-811 (2005)
28. E. London. How principles of domain formation in model membranes may explain ambiguities concerning lipid raft formation in cells. *Biochem Biophys Acta.* **1746:** 203-220 (2005)
29. L. Johannes and C. Lamaze. Clathrin-dependent or not: is it still the question? *Traffic.* **3:** 443-451 (2002)
30. S. K. Rodal, G. Skretting, O. Garred, F. Vilhardt, B. Van Deurs and K. Sandvig. Extraction of cholesterol with methyl-beta-cyclodextrin perturbs formation of clathrin-coated endocytic vesicles. *Mol Biol Cell.* **10:** 961-974 (1999)
31. S. T. Gammon, V. M. Villalobos, J. L. Prior, V. Sharma and D. Piwnica-Worms. Quantitative analysis of permeation peptide complexes labeled with Technetium-99m: chiral and sequence-specific effects on net cell uptake. *Bioconjug Chem.* **14:** 368-376 (2003)
32. S. Futaki. Oligoarginine vectors for intracellular delivery: design and cellular uptake mechanisms. *Biopolymers.* **84:** 241-49 (2006)
33. M. Silhol, M. Tyagi, M. Giacca, B. Lebleu and E. Vives. Different mechanisms for cellular internalization of the HIV-1 Tat-derived cell penetrating peptide and recombinant proteins fused to Tat. *Eur J Biochem.* **269:** 494-501 (2002)
34. T. B. Potocky, A. K. Menon and S. H. Gellman. Cytoplasmic and nuclear delivery of a TAT-derived peptide and a beta-peptide after endocytic uptake into HeLa cells. *J Biol Chem.* **278:** 50188-50194 (2003)

4

OVCAR-3 cells internalise TAT-peptide modified liposomes by endocytosis

Marjan M. Fretz, Gerben A. Koning, Enrico Mastrobattista,
Wim Jiskoot and Gert Storm

Published in BBA Biomembranes. 1665: 48-56 (2004)

ABSTRACT

For cytosolic delivery of liposomes containing macromolecular drugs, such as proteins or nucleic acids, it would be beneficial to bypass endocytosis to avoid degradation in the lysosomes. Recent reports pointed to the possibility that coupling of TAT-peptides to the outer surface of liposome particles would enable translocation over the cellular plasma membrane.

Here, we demonstrate that cellular uptake of TAT-liposomes occurs via endocytosis rather than plasma membrane translocation. The coupling of HIV-1 derived TAT-peptide to liposomes enhances their binding to ovarian carcinoma cells. The binding was inhibited by the presence of heparin or dextran sulphate, indicating that cell surface proteoglycans are involved in the binding interaction. Furthermore, living confocal microscopy studies revealed that binding of the TAT-liposomes to the plasma membrane was followed by intracellular uptake in vesicular structures. Staining the endosomes and lysosomes demonstrated that fluorescent liposomal labels are present within the endosomal and lysosomal compartments. Furthermore, incubation at low temperature or addition of a metabolic or an endocytosis inhibitor blocked cellular uptake.

In conclusion, coupling TAT-peptide to the outer surface of liposomes leads to enhanced endocytosis of the liposomes by ovarian carcinoma cells, rather than direct cytosolic delivery by plasma membrane translocation.

INTRODUCTION

Unfavourable physicochemical characteristics of therapeutic macromolecules, like nucleic acids, proteins and peptides, generally limit their application as agents e.g. for cancer therapy. Due to their large molecular weight, hydrophilicity and charged nature, these molecules are inefficient in crossing cellular membranes and therefore in reaching their intracellular target site (1). Therefore, intracellular delivery of these novel biopharmaceuticals rely on delivery systems that allow improved transport across the cell membrane. Currently, attempts are being made to apply targeted liposomes for cytosolic delivery of macromolecules (2-4). However, cytosolic delivery of liposome-encapsulated drugs is often not accomplished as binding of liposomes to the targeted cell surface receptor is followed by endocytic uptake and subsequent lysosomal degradation of the liposomes with their encapsulated contents.

A recently reported approach to avoid endocytosis and to achieve direct cytosolic delivery of poor membrane permeable (macro)molecules is to utilise so-called cell penetrating peptides (CPP) (also referred to as protein transduction domains), which have been described to possess the ability to translocate material across the plasma membrane into the cytoplasm (reviewed in references (5, 6)). These peptides can act as cytosolic delivery vectors for both low and high molecular weight cargoes, like fluorophores (7), proteins (8-10), oligonucleotides (11) and even particulates (12-14).

Torchilin *et al.* were the first to report on cytosolic delivery of liposomes modified with a CPP (the HIV-1 derived TAT peptide) attached directly to the outer liposomal surface or to the terminal ends of PEG-chains present on PEG-coated liposomes (13). The latter PEG-liposomes, also known as sterically stabilized liposomes, are advantageous in vivo because of their prolonged circulation property. The TAT-liposomes were delivered into the cytoplasm via an energy-independent uptake mechanism as concluded from the observations that no significant reduction in cellular uptake occurred when incubated at 4°C instead of 37°C or in the presence of metabolic inhibitors (13). Therefore, translocation into the cytoplasm rather than endocytosis was proposed as cellular uptake mechanism. Similar results on CPP-mediated liposomal translocation were published by Tseng *et al.* (14).

In the meantime, the concept of CPP-mediated plasma membrane translocation was questioned when Lundberg and Johansson showed that cell fixation techniques could induce rigorous artefacts in the cellular distribution of fluorescently labeled CPP (15). In addition, Richard *et al.* reported on characteristic endosomal localization of fluorescently labeled CPP when cell fixation was avoided, as visualised by living cell fluorescence microscopy. Moreover, the cellular uptake kinetics of CPP appeared to be similar to the kinetics of endocytosis and cellular uptake did not occur at 4°C (16). These observations argue for an energy-dependent uptake process and have raised serious doubts about the translocation mechanism of cellular entry.

Here, we have studied the cellular uptake mechanism of TAT-liposomes by living unfixed human ovarian carcinoma cells (OVCAR-3), thus avoiding possible fixation induced artefacts. The results clearly indicate that TAT-mediated uptake of liposomes occurs via endocytosis, rather than via plasma membrane translocation as previously proposed.

EXPERIMENTAL METHODS

Materials

Egg-phosphatidylcholine (EPC) and 1,2-distearoyl-glycero-3-phosphoethanolamine-*N*-[poly(ethylene glycol)2000] (PEG_{2000}-DSPE) were obtained from Lipoid GmbH (Ludwigshafen, Germany). Maleimide-PEG_{2000}-DSPE was obtained from Shearwater Polymers (Huntsville, AL, USA). Cholesterol (CHOL), iodoacetamide, cytochalasin D, heparin, dextran sulphate and FITC-dextran (molecular mass 77 kDa) were from Sigma-Aldrich Co. (St.Louis, MO, USA). 1,1'-dioctadecyl-3,3,3',3'-tetramethylindocarbocyanine, 4-chlorobenzenesulfonate sulfonate salt (DiD) and Lysotracker Red DND-99 were purchased from Molecular Probes Europe BV (Leiden, The Netherlands). Lissamine rhodamine B-labeled glycerophosphoethanolamine (Rho-PE) was obtained from Avanti Polar Lipids Inc. (Alabaster, AL, USA). Titriplex III (EDTA) was obtained from Merck (Darmstadt, Germany). Thiol-acetylated TAT-peptide with the sequence YGRKKRRQRRRK-S-acetylthioacetyl was synthesized by Ansynth BV (Roosendaal, The Netherlands).

Cell culture

The human ovarian carcinoma cell line NIH:OVCAR-3 originates from the laboratory of Dr. Hamilton (National Cancer Institute, Bethesda, MD) (17). OVCAR-3 cells were cultured in Dulbecco's modified Eagle's medium containing 3.7 g/l sodium bicarbonate, 4.5 g/l L-glucose and supplemented with L-glutamine (2 mM), 10% (v/v) foetal calf serum (FCS), penicillin (100 IU/ml), streptomycin (100 µg/ml) and amphotericin B (0.25 µg/ml) at 37°C with 5% CO_2 in humidified air.
All cell-culture related material was obtained from Gibco (Grand Island, NY, USA).

Liposome preparation and characterisation

For the preparation of liposomes, a lipid film was prepared from a mixture of EPC, CHOL, PEG_{2000}-DSPE, maleimide-PEG_{2000}-DSPE (1.85:1:0.09:0.06 molar ratio) in absolute ethanol by solvent evaporation. DiD or Rho-PE (0.1 mol%) was added as lipophilic fluorescent label. Before hydration, the lipid film was flushed with nitrogen for at least 30 minutes. Liposomes were formed by hydration of the lipid film with either HEPES buffered saline (150 mM NaCl, 5 mM HEPES, pH 6.5; HBS) or HBS (pH 6.5) containing 10 mg/ml FITC-dextran. The lipid dispersion was sequentially extruded through polycarbonate membrane filters (Osmonic, Livermore CA, USA) with pore sizes varying from 0.05 µm to 0.65 µm using Lipex high-pressure extrusion equipment (Northern Lipids, Vancouver, Canada).
When hydrated with FITC-dextran-containing solution, non-encapsulated FITC-dextran was separated from the liposomes by size exclusion chromatography using a Sepharose CL-4B column (Amersham Pharmacia Biotech, Uppsala, Sweden).

TAT-peptides were covalently coupled to the maleimide-derivatised PEG-DSPE present in the liposomal bilayer via a sulfhydryl-maleimide coupling reaction as previously described for monoclonal antibodies (18). Briefly, one mg of thiol-acetylated peptide was deacetylated in an aqueous solution containing 0.5 M HEPES, 0.5 M Hydroxylamine-HCl and 0.25 mM EDTA of pH 7.0 for 1 hr at room temperature to obtain free sulfhydryl groups. The deacetylated peptide was added to liposomes (21 μmol total lipid) and the coupling reaction to the maleimide functionalized PEG chains present on the surface of the liposomes, was performed overnight at 4°C. Non-coupled peptide was removed by size exclusion chromatography using a Sepharose CL-4B column. Liposomes lacking the TAT-peptide were used as control.

The phospholipid concentration of the liposome formulations was determined by the colorimetric method of Rouser *et al.* (19). Mean particle size and size distribution were determined by dynamic light scattering with a Malvern 4700 system (Malvern Ltd., Malvern, UK).

Cellular association

OVCAR-3 cells were detached from the culture flask by trypsin/EDTA solution (0.05% (w/v) trypsin and 0.02% (w/v) EDTA in PBS). Cells (1 x 10^5) were incubated for 1 hour at 4°C with different concentrations Rho-PE labeled control liposomes or TAT-liposomes. Cells were washed twice by centrifugation (300 x *g*, 5 min, 4°) and addition of 1 ml PBS (164 mM NaCl, 140 mM Na_2HPO_4, 11 mM NaH_2PO_4; pH 7.4). After centrifugation, the cells were resuspended in 400 μl PBS and analyzed by flow cytometry using a FACSCalibur (Becton&Dickinson, Mountain View, CA, USA).

Fixation induced artifact

OVCAR-3 cells were seeded (2 x 10^4 cells/well) onto 16-well chamber slides and cultured overnight prior to the experiment. Cells were washed with PBS and 150 nmol Rho-PE labeled liposomes (control or TAT-liposomes) in serum-free medium was added. After 1 hour, unbound liposomes were removed and the cells were washed with PBS. The cells were either mounted in PBS and directly visualised by confocal microscopy or fixed with 4% formaldehyde and mounted in FluorSave reagent (Calbiochem, San Diego, CA, USA) before visualisation. Confocal microscopy analysis was performed with a Leica TCS-SP confocal laser scanning microscope equipped with a 488 nm Argon, 568 nm Krypton and 647 nm HeNe laser. Laser power and photomultiplier settings were kept identical for all the samples to be able to compare the results.

Intracellular localisation

OVCAR-3 cells were seeded (2 x 10^4 cells/well) onto 16-well chamber slides and cultured overnight prior to the experiment. Cells were washed with PBS and 150 nmol double fluorescently labeled (DiD as lipophilic bilayer label and FITC-dextran as aqueous marker) control or TAT-liposomes in serum-free medium was added. After 1 hour, the unbound liposomes were removed and the cells were subsequently incubated for either 1 or 23 hours with complete culture medium. Thirty minutes prior to visualisation the cells were incubated with 100 µl Lysotracker Red solution (75 nM in PBS) at 37°C. Cells were washed with PBS, mounted in PBS and covered with coverslip sealed with nail polish. The living cells were directly analyzed with a Leica TCS-SP confocal laser scanning microscope equipped with a 488 nm Argon, 568 nm Krypton and 647 nm HeNe laser. Laser power and photomultiplier settings were kept identical for all the samples to be able to compare the results.

Cellular association in the presence of inhibitors

OVCAR-3 cells were detached by trypsin/EDTA solution and 3 x 10^5 cells/well were added to 6-wells CoStar low-adherence plates (Corning Life Science BV, Schiphol-Rijk, The Netherlands) in a total volume of 5 ml serum-free medium. The experiments were performed at 4°C and 37°C with or without the presence of 1 mM iodoacetamide or 25 µg/ml cytochalasin D. In each well, 450 nmol Rho-PE labeled liposomes (TAT or control liposomes) was added and after incubation of 5 hours, the cells were washed twice by centrifugation (300 x *g*, 5 min, 4°C) and resuspended in PBS. An aliquot of the cell suspension was mounted on glass slides and visualised directly using a Leica TCS-SP confocal laser scanning microscope equipped with 568 nm Krypton laser. Laser power and photomultiplier settings were kept identical for all the samples to be able to compare the results. Cell samples were also analyzed by flow cytometry using a FACSCalibur (Becton&Dickinson, Mountain View, CA, USA).

Cellular association in the presence of heparin and dextran sulphate

OVCAR-3 cells were detached from the culture flask by trypsin/EDTA solution. Cells (1 x 10^5) were incubated for 1 hour at 4°C with 150 nmol Rho-PE labeled TAT-liposomes in the presence of different concentrations heparin or dextran sulphate. Cells were washed twice by centrifugation (300 x *g*, 5 min, 4°) and addition of 1 ml PBS. Cells were resuspended in 400 µl PBS and analysed by flow cytometry using a FACSCalibur (Becton&Dickinson, Mountain View, CA, USA).

RESULTS

Liposome characterisation

Liposomes composed of EPC, CHOL, PEG_{2000}-DSPE and maleimide-PEG_{2000}-DSPE (1.85: 1: 0.09: 0.06 molar ratio) were prepared according to the evaporation/hydration method and the liposomes were reduced in size by extrusion (20). After extrusion the activated TAT-peptide was coupled to the maleimide functionalised PEG-DSPE on the outer liposomal surface as described in Experimental Methods. Type of fluorescent label, mean particle size and size distribution of the used liposomal formulations are given in Table 1. The liposomes investigated had a mean particle size between 135 and 145 nm and a narrow size distribution (PD < 0.1).

Table 1 Characteristics of liposome preparations studied

Liposome Formulation	Lipophilic fluorescent label	Hydrophilic Fluorescent label	Mean particle size (nm)	PD[a]
TAT-liposomes	DiD	FITC-dextran	140	0.09
Control-liposomes	DiD	FITC-dextran	135	0.04
TAT-liposomes	Rho-PE	-	145	0.05
Control-liposomes	Rho-PE	-	140	0.06

[a] Polydispersity: indication of the size distribution of the liposomes; ranges from 0.0 for a monodisperse to 1.0 for an entirely heterodisperse suspension.

Cellular association

OVCAR-3 cells were incubated with different concentrations of Rho-PE labeled TAT-liposomes or control liposomes lacking the TAT-peptide. Figure 1 shows that coupling of the TAT-peptide to the outer surface of the liposomes strongly increased the cellular association of the liposomes with OVCAR-3 cells.

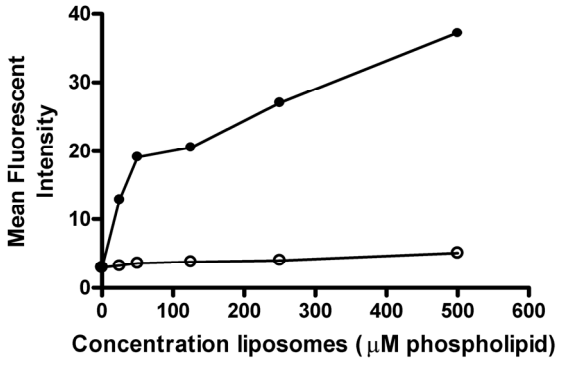

Figure 1. Coupling of TAT-peptide to the outer surface of liposomes increases the cellular association with OVCAR-3 cells. Cells were incubated with different concentrations of Rho-PE labeled control liposomes (○) or TAT-liposomes (●) for 1 hr at 4°C, washed and analysed by flow cytometry. Each point represents the mean fluorescence intensity of 5000 (mean ± SD; n=3). Errors bars are within plot symbols when not visible.

Fixation induced artifact

The influence of fixation techniques on the cellular distribution of fluorescently labeled TAT-liposomes has not been published yet, while it has been demonstrated recently by various research groups that fixation procedures have a major influence on the cellular localization of fluorescently labeled CPP (15, 16, 21). Figure 2 shows confocal microscopy images of living (Figure 2A) and fixed (Figure 2B) OVCAR-3 cells after an 1 hr incubation with Rhodamine-PE labeled TAT-liposomes. After fixation with 4% formaldehyde (Figure 2B) the fluorescence appeared in a diffuse pattern throughout the cytosol. No fluorescence was observed in the nucleus. When living OVCAR-3 cells were directly visualised (Figure 2A), no intracellular localisation was observed but the fluorescent TAT-liposomes were predominantly localised at the plasma membranes of the cells. Control liposomes could not be detected using the same photomultiplier settings (data not shown). These results illustrate that fixation procedures need to be avoided when studying cellular localisation of TAT-liposomes as otherwise misleading results can be obtained.

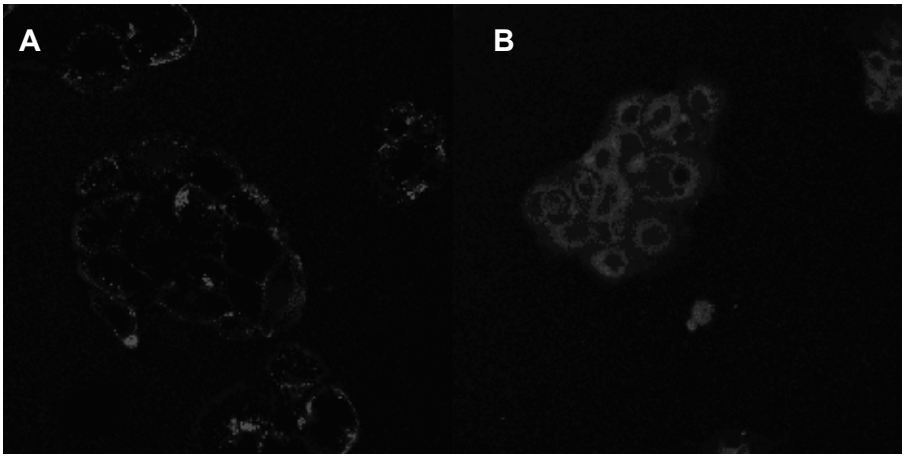

Figure 2. Fixation induced redistribution of liposomal label. OVCAR-3 cells were incubated for 1 hr at 37°C with TAT-liposomes labeled with Rho-PE and either visualised without fixation (A) or after fixation with 4% formaldehyde (B).

Intracellular localisation

Knowing the detrimental effects of fixation on cellular localisation of TAT-liposomes, *living* OVCAR-3 cells were used in all subsequent experiments. Using confocal microscopy, the cellular localisation of double-labeled TAT-liposomes and control liposomes after 1 or 24 hours of incubation was studied.

To examine the liposome integrity during the experiments, both the liposomal bilayer and the aqueous core were fluorescently labeled with DiD and FITC dextran, respectively. Co-localisation of both liposomal labels would be indicative of the presence of intact liposomes.
60

In addition, endosomes and lysosomes were labeled with Lysotracker Red, a compound known to localise primarily in the acidic compartments of cells (22).

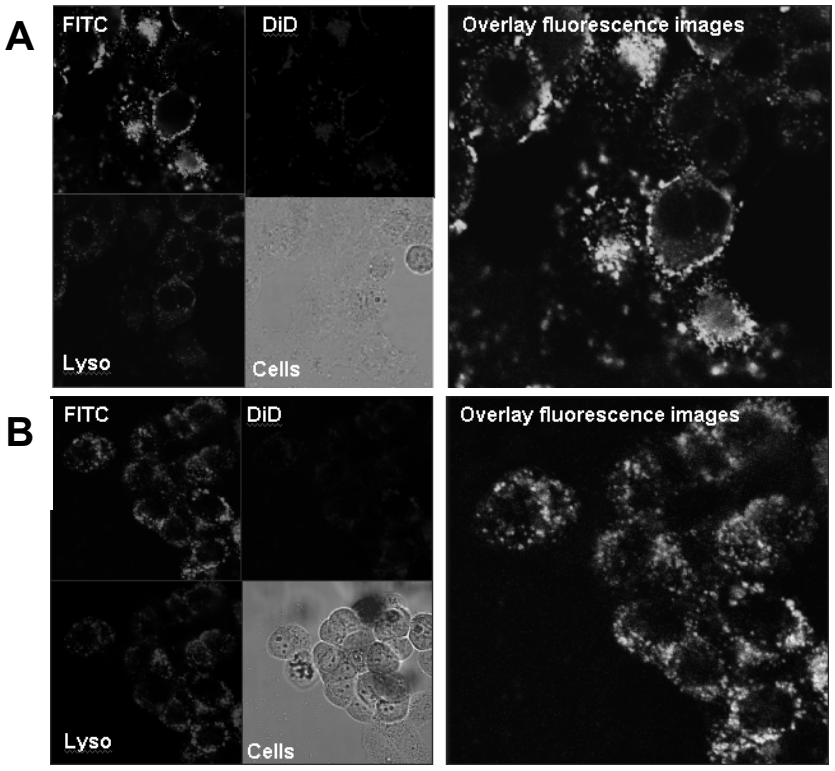

Figure 3. Intracellular localisation of TAT-liposomes. OVCAR-3 cells were incubated with 150 nmol of TAT-liposomes for 1 hr and directly visualised (A) or subsequently incubated for 23 hours with liposome-free medium (B). Endosomes and lysosomes were stained 30 minutes prior to visualisation with Lysotracker Red. In the right panels the different confocal images are electronically merged.

After 1 hour of incubation both liposomal labels were localised at the plasma membrane of the OVCAR-3 cells, which represents cell-bound intact TAT-liposomes (Figure 3A). Endosomes and lysosomes were stained red with Lysotracker Red. An electronically merged image (right panel Figure 3A) shows no evidence of co-localisation of the liposomal labels with Lysotracker Red. However, after 24 hr of incubation, both liposomal labels were present intracellularly in a punctuate pattern (Figure 3B). When these images were electronically merged with the confocal image visualising Lysotracker Red staining, co-localisation of the liposomal labels with the endosomal/lysosomal marker was clearly visible (right panel Figure 3B). From this co-localisation it can be concluded that the

liposomes were present in endocytic vesicles and presumably were taken up by an endocytic process.
No binding or uptake was observed when control liposomes (lacking TAT-peptide) were incubated with OVCAR-3 cells for 1 or 24 hr (data not shown).

Effect of low temperature and inhibitors

A punctuate intracellular distribution of Rho-PE labeled TAT-liposomes was observed when living OVCAR-3 cells in suspension were incubated for 5 hrs at 37°C with TAT-liposomes and directly thereafter visualised using confocal laser scanning microscopy (Figure 4A). When the 5 hr incubation was performed at 4°C, liposome-associated fluorescence was observed only at the plasma membrane of OVCAR-3 cells (Figure 4B). The presence of the metabolic inhibitor iodoacetamide (Figure 4C) or the endocytosis inhibitor cytochalasin D (Figure 4D) in the incubation medium inhibited the uptake of TAT-liposomes at 37°C by OVCAR-3 cells as only membrane-bound fluorescence was detected. Control liposomes were not taken up by OVCAR-3 cells after a 5 hr incubation at 37°C (data not shown).

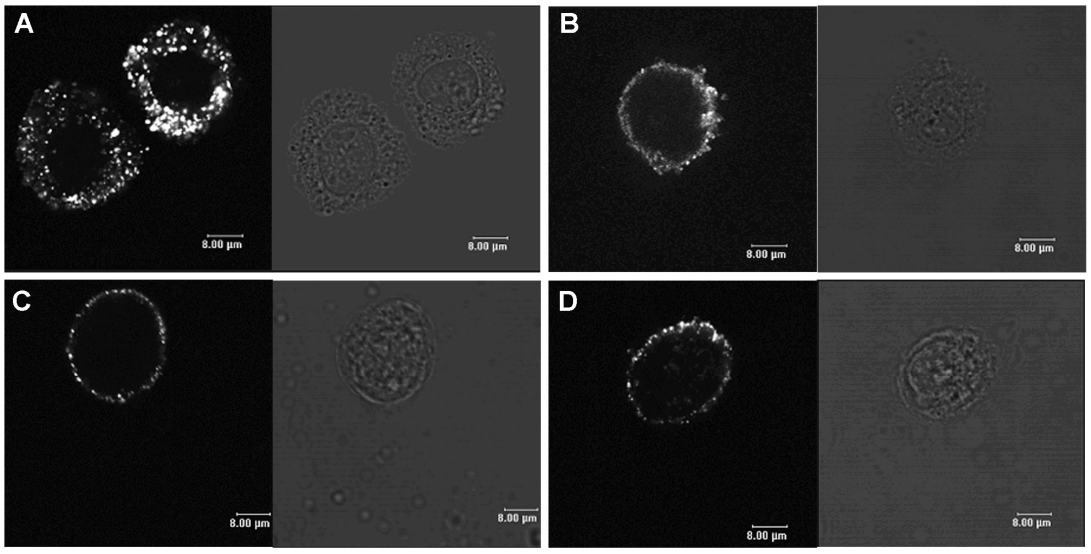

Figure 4. Low temperature and metabolic inhibitors prevent uptake of TAT-liposomes by living OVCAR-3 cells. OVCAR-3 cells were incubated with TAT-liposomes for 5 hours at 37°C (A, C and D) or at 4°C (B). Left panels are confocal images, right panels are phase contrast images. *A,* control, vesicular localisation of TAT-liposomes; *B,* incubation at 4°C, plasma membrane binding of TAT-liposomes; *C,* in the presence of iodoacetamide, plasma membrane binding of TAT-liposomes; *D*, in the presence of cytochalasin D, plasma membrane binding of TAT-liposomes.

To exclude the possibility that cellular uptake of TAT-liposomes in the presence of metabolic or endocytosis inhibitors can not be visualised due to reduced binding of the TAT-liposomes to cells, cellular association in the absence or presence of inhibitor was studied by flow cytometry. Incubations were performed at 4°C which, as demonstrated in Figure 4B, only resulted in binding to the plasma membrane since cellular uptake does not occur at this temperature. Figure 5 shows that plasma membrane binding of TAT-liposomes to OVCAR-3 cells was not reduced due to the presence of iodoacetamide or cytochalasin D in the incubation medium.

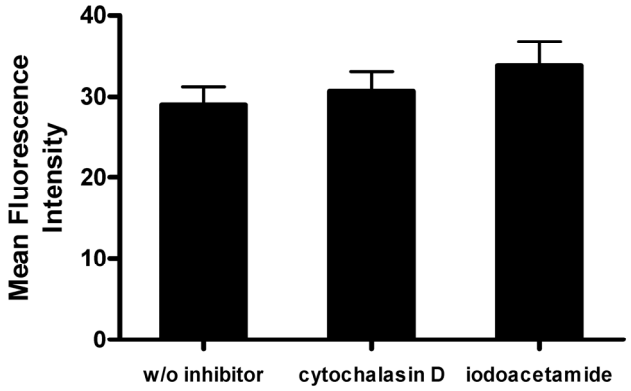

Figure 5 Uptake inhibitors do not influence the binding of TAT-liposomes to OVCAR-3 cells. OVCAR-3 cells were incubated for 1 hr at 4°C with Rho-PE labeled TAT-liposomes, washed and analysed by FACS. Cell-associated fluorescence is depicted as mean fluorescence intensity. Error bars represent the mean ± SD (n=3). Cellular association is not decreased due to the presence of inhibitors.

Effect of polyanions

Recently, cell-surface exposed proteoglycans have shown to play a role in the binding of the TAT-peptide to the cellular surface (23). In addition, several studies have shown that the TAT-peptide interacts with numerous soluble polyanions, like heparin, heparan sulphate and pentosan sulphate (24-26). The presence of those polyanions reduces the cellular uptake of the TAT-peptide.

The effect of two of these polyanions, heparin and dextran sulphate, present in the incubation medium, on the binding of TAT-liposomes to OVCAR-3 cells is shown in Figure 6. As no significant cellular uptake occurs at 4°C (shown in Figure 4B), plasma membrane binding can be studied at this temperature.

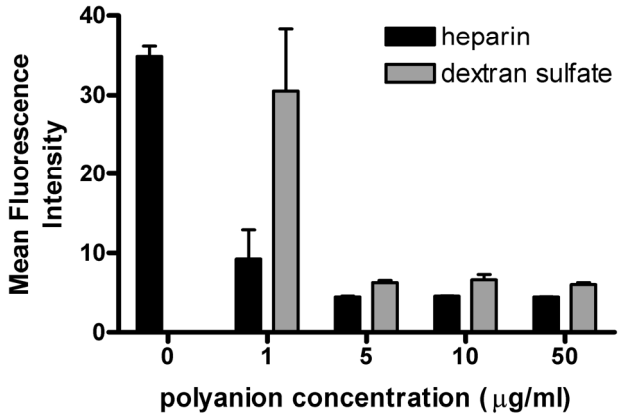

Figure 6 Heparin and dextran sulphate reduce cellular association of TAT-liposomes to OVCAR-3 cells. OVCAR-3 cells were incubated for 1 hr at 4°C with Rho-PE labeled TAT-liposomes in the presence of different concentrations heparin or dextran sulphate. Cells were washed twice and analyzed by FACS for cell-associated fluorescence which is depicted as mean fluorescence intensity. Error bars represent the mean ± SD (n=3) and are within plot symbol when not visible.

Both heparin and dextran sulphate reduced the binding of TAT-liposomes to OVCAR-3 cells in a concentration dependent fashion (Figure 6), heparin being somewhat more effective than dextran sulphate. These results indicate that glycosaminoglycans present on the cell surface are involved in the binding of TAT-liposomes to the plasma membrane of OVCAR-3 cells.

DISCUSSION

Direct cytosolic delivery of liposomal macromolecular drugs, rather than uptake via endocytosis would be advantageous as degradation of encapsulated macromolecules in the lysosomal compartments is prevented. It was recently reported that direct cytosolic delivery of liposomes could be realised by coupling the TAT-peptide to the outer surface of the liposomes (13, 14). Translocation over the plasma membrane was suggested as uptake mechanism for TAT-liposomes as the uptake mechanism was considered to be time-, receptor- and energy-independent (13, 14). However, the results presented herein demonstrate that endocytosis rather than plasma membrane translocation is the underlying mechanism of cellular uptake of TAT-liposomes.

Coupling the TAT-peptide to the outer surface of liposomes strongly increases the binding of liposomes to OVCAR-3 cells (Figure 1). It has been observed by others that the TAT-protein can enter a wide range of different cell types and that soluble heparin inhibits the biological activity of TAT-protein (24-26). The latter observation raised the hypothesis that cell surface proteoglycans are involved in the uptake mechanism (23), which was supported by the finding that soluble heparin and dextran sulphate could inhibit binding of TAT-peptide to cells (23). Moreover, TAT-peptide is unable to bind to cells genetically defective in the biosynthesis of fully sulphated heparan sulphate proteoglycans (23). Figure 6 shows that the presence of heparin or dextran sulphate almost completely reduces the degree of binding of TAT-liposomes to OVCAR-3 cells to the level of control liposomes, lacking the TAT-peptide. This indicates that cell surface proteoglycans are involved in the binding of TAT-liposomes to cells as was also suggested for TAT-peptides coupled to a small fluorescent cargo (23).

When living OVCAR-3 cells were visualised after a 1-hour of incubation with double labeled TAT-liposomes, binding of intact TAT-liposomes to the plasma membrane of the cells was observed. After 24 hours of incubation, both fluorescent labels co-localised with Lysotracker Red, a marker for endosomal and lysosomal compartments. This indicates that TAT-liposomes are taken up in an intact form by an endocytic pathway rather than via plasma membrane translocation. For fluorescently labeled CPP it has already been discussed by various researchers that the cellular uptake occurs by endocytosis (16, 27-30). Endocytosis as the route of uptake for TAT-liposomes is further supported by the data shown in Figure 4. At 4°C or in the presence of the metabolic inhibitor iodoacetamide or the endocytosis inhibitor cytochalasin D only membrane binding and no uptake of TAT-liposomes was observed, in contrast to incubation at 37° where liposomes are present intracellularly in vesicles.

The difference in results presented here and previously reported for the cellular uptake of TAT-liposomes (13, 14) is likely explained by artifacts produced during fixation, which was avoided in these studies.

We clearly show that fixation of TAT-liposome incubated cells caused a redistribution of liposomal label across the plasma membrane and a corresponding misinterpretation of microscopy data (Figure 3). These results are in line with other reports indicating that fixation procedures can result in redistribution of fluorescently labeled CPP in cells (15, 16). In conclusion, TAT-peptide mediated uptake of liposomes occurs via endocytosis rather than membrane translocation. This implies that TAT-liposomes do not have an advantageous mechanism of cell entry over other targeted drug delivery systems and that encapsulated drugs are still exposed to the degrading environment in the lysosomes. Nevertheless, extent of endocytic uptake is enhanced using TAT-peptides covalently coupled to liposomes, which may be intrinsically beneficial. In particular in combination with endosomal escape promoters, such a virus derived fusogenic peptides, which may further enhance cytosolic delivery of encapsulated macromolecules. Similar concepts are described in literature for endosomal escape of immunoliposomal drugs (4) and of TAT-fusion proteins (31).

REFERENCES

1. B. Lebleu. Delivering information-rich drugs--prospects and challenges. *Trends Biotechnol.* **14:** 109-10 (1996)
2. M. H. Vingerhoeds, P. A. Steerenberg, J. J. Hendriks, L. C. Dekker, Q. G. Van Hoesel, D. J. Crommelin and G. Storm. Immunoliposome-mediated targeting of doxorubicin to human ovarian carcinoma in vitro and in vivo. *Br J Cancer.* **74:** 1023-9 (1996)
3. M. H. Vingerhoeds, P. A. Steerenberg, J. J. Hendriks, D. J. Crommelin and G. Storm. Targeted delivery of diphtheria toxin via immunoliposomes: efficient antitumor activity in the presence of inactivating anti-diphtheria toxin antibodies. *FEBS Lett.* **395:** 245-50 (1996)
4. E. Mastrobattista, G. A. Koning, L. Van Bloois, A. C. Filipe, W. Jiskoot and G. Storm. Functional Characterization of an Endosome-disruptive Peptide and Its Application in Cytosolic Delivery of Immunoliposome-entrapped Proteins. *J Biol Chem.* **277:** 27135-43 (2002)
5. A. Prochiantz. Messenger proteins: homeoproteins, TAT and others. *Curr Opin Cell Biol.* **12:** 400-6 (2000)
6. M. Lindgren, M. Hallbrink, A. Prochiantz and U. Langel. Cell-penetrating peptides. *Trends Pharmacol Sci.* **21:** 99-103 (2000)
7. E. Vives, P. Brodin and B. Lebleu. A truncated HIV-1 Tat protein basic domain rapidly translocates through the plasma membrane and accumulates in the cell nucleus. *J Biol Chem.* **272:** 16010-7 (1997)
8. H. Nagahara, A. M. Vocero-Akbani, E. L. Snyder, A. Ho, D. G. Latham, N. A. Lissy, M. Becker-Hapak, S. A. Ezhevsky and S. F. Dowdy. Transduction of full-length TAT fusion proteins into mammalian cells: TAT-p27Kip1 induces cell migration. *Nat Med.* **4:** 1449-52 (1998)
9. S. R. Schwarze, A. Ho, A. Vocero-Akbani and S. F. Dowdy. In vivo protein transduction: delivery of a biologically active protein into the mouse. *Science.* **285:** 1569-72 (1999)
10. S. Fawell, J. Seery, Y. Daikh, C. Moore, L. L. Chen, B. Pepinsky and J. Barsoum. Tat-mediated delivery of heterologous proteins into cells. *Proc Natl Acad Sci U S A.* **91:** 664-8 (1994)
11. A. Astriab-Fisher, D. Sergueev, M. Fisher, B. R. Shaw and R. L. Juliano. Conjugates of antisense oligonucleotides with the Tat and antennapedia cell-penetrating peptides: effects on cellular uptake, binding to target sequences, and biologic actions. *Pharm Res.* **19:** 744-54 (2002)
12. M. Lewin, N. Carlesso, C. H. Tung, X. W. Tang, D. Cory, D. T. Scadden and R. Weissleder. Tat peptide-derivatized magnetic nanoparticles allow in vivo tracking and recovery of progenitor cells. *Nat Biotechnol.* **18:** 410-4 (2000)
13. V. P. Torchilin, R. Rammohan, V. Weissig and T. S. Levchenko. TAT peptide on the surface of liposomes affords their efficient intracellular delivery even at low temperature and in the presence of metabolic inhibitors. *Proc Natl Acad Sci U S A.* **98:** 8786-91 (2001)
14. Y. L. Tseng, J. J. Liu and R. L. Hong. Translocation of liposomes into cancer cells by cell-penetrating peptides penetratin and tat: a kinetic and efficacy study. *Mol Pharmacol.* **62:** 864-72 (2002)
15. M. Lundberg and M. Johansson. Positively charged DNA-binding proteins cause apparent cell membrane translocation. *Biochem Biophys Res Commun.* **291:** 367-71 (2002)
16. J. P. Richard, K. Melikov, E. Vives, C. Ramos, B. Verbeure, M. J. Gait, L. V. Chernomordik and B. Lebleu. Cell-penetrating peptides: A re-evaluation of the mechanism of cellular uptake. *J Biol Chem.* (2002)
17. T. C. Hamilton, R. C. Young, W. M. McKoy, K. R. Grotzinger, J. A. Green, E. W. Chu, J. Whang-Peng, A. M. Rogan, W. R. Green and R. F. Ozols. Characterization of a human ovarian carcinoma cell line (NIH:OVCAR-3) with androgen and estrogen receptors. *Cancer Res.* **43:** 5379-89 (1983)
18. G. A. Koning, H. W. Morselt, M. J. Velinova, J. Donga, A. Gorter, T. M. Allen, S. Zalipsky, J. A. Kamps and G. L. Scherphof. Selective transfer of a lipophilic prodrug of 5-fluorodeoxyuridine from immunoliposomes to colon cancer cells. *Biochim Biophys Acta.* **1420:** 153-67 (1999)
19. G. Rouser, S. Fkeischer and A. Yamamoto. Two dimensional then layer chromatographic separation of polar lipids and determination of phospholipids by phosphorus analysis of spots. *Lipids.* **5:** 494-6 (1970)
20. F. Olson, C. A. Hunt, F. C. Szoka, W. J. Vail and D. Papahadjopoulos. Preparation of liposomes of defined size distribution by extrusion through polycarbonate membranes. *Biochim Biophys Acta.* **557:** 9-23 (1979)
21. M. Lundberg, S. Wikstrom and M. Johansson. Cell surface adherence and endocytosis of protein transduction domains. *Mol Ther.* **8:** 143-50 (2003)

22. R. D. Palmiter, T. B. Cole and S. D. Findley. ZnT-2, a mammalian protein that confers resistance to zinc by facilitating vesicular sequestration. *Embo J.* **15:** 1784-91 (1996)
23. M. Tyagi, M. Rusnati, M. Presta and M. Giacca. Internalization of HIV-1 tat requires cell surface heparan sulfate proteoglycans. *J Biol Chem.* **276:** 3254-61 (2001)
24. M. Rusnati, D. Coltrini, P. Oreste, G. Zoppetti, A. Albini, D. Noonan, F. d'Adda di Fagagna, M. Giacca and M. Presta. Interaction of HIV-1 Tat protein with heparin. Role of the backbone structure, sulfation, and size. *J Biol Chem.* **272:** 11313-20 (1997)
25. M. Rusnati, G. Tulipano, D. Spillmann, E. Tanghetti, P. Oreste, G. Zoppetti, M. Giacca and M. Presta. Multiple interactions of HIV-I Tat protein with size-defined heparin oligosaccharides. *J Biol Chem.* **274:** 28198-205 (1999)
26. M. Rusnati, G. Tulipano, C. Urbinati, E. Tanghetti, R. Giuliani, M. Giacca, M. Ciomei, A. Corallini and M. Presta. The basic domain in HIV-1 Tat protein as a target for polysulfonated heparin-mimicking extracellular Tat antagonists. *J Biol Chem.* **273:** 16027-37 (1998)
27. S. D. Kramer and H. Wunderli-Allenspach. No entry for TAT(44-57) into liposomes and intact MDCK cells: novel approach to study membrane permeation of cell-penetrating peptides. *Biochim Biophys Acta.* **1609:** 161-9 (2003)
28. G. Drin, S. Cottin, E. Blanc, A. R. Rees and J. Temsamani. Studies on the internalisation mechanism of cationic cell-penetrating peptides. *J Biol Chem.* (2003)
29. S. Console, C. Marty, C. Garcia-Echeverria, R. Schwendener and K. Ballmer-Hofer. Antennapedia and HIV TAT 'protein transduction domains' promote endocytosis of high Mr cargo upon binding to cell surface glycosaminoglycans. *J Biol Chem.* (2003)
30. A. Fittipaldi, A. Ferrari, M. Zoppe, C. Arcangeli, V. Pellegrini, F. Beltram and M. Giacca. Cell membrane lipid rafts mediate caveolar endocytosis of HIV-1 Tat fusion proteins. *J Biol Chem.* **278:** 34141-9 (2003)
31. J. S. Wadia, R. V. Stan and S. F. Dowdy. Transducible TAT-HA fusogenic peptide enhances escape of TAT-fusion proteins after lipid raft macropinocytosis. *Nat Med.* **10:** 310-315 (2004)

5

Effects of Na+/H+ exchanger inhibitors on subcellular localisation of endocytic organelles and intracellular dynamics of protein transduction domains HIV-TAT peptide and octa-arginine

Marjan M. Fretz, Jing Jin, Robin Conibere, Neal A. Penning, Saly Al-Taei,
Gert Storm, Shiroh Futaki, Toshihide Takeuchi,
Ikuhiko Nakase and Arwyn T. Jones

.

Published in Journal of Controlled Release.116:247-254 (2006)

ABSTRACT

Protein transduction domains such as those derived from the HIV protein TAT have great potential as vectors for delivery of therapeutic entities such as genes and proteins into cells. Extensive studies have shown that a major fraction of the most studied variants enter cells via an endocytic mechanism. However, controversy surrounds the exact uptake mechanism and whether a specific pathway is utilised. Studies showing inhibition of uptake of protein transduction domains in the presence of ion-transport inhibitors such as amiloride and its more potent analogue 5-(*N*-ethyl-*N*-isopropyl) amiloride (EIPA) suggest a link between peptide internalisation and macropinocytosis. In this study, using immunolabeling of early and late components of the endocytic pathway, we show that treatment of cells with EIPA and to a lesser extent amiloride, affects the morphology and subcellular location of early, late endosomes and lysosomes. Enlarged early and late endocytic structures were observed in EIPA-treated cells, and these organelles accumulated in a perinuclear region. Results from experiments investigating the effects of EIPA on distribution of fluorescent octaarginine were in agreement with the immunolocalisation studies. Treatment of the $CD34^+$ leukaemia cell line KG1a with EIPA in the presence of fluorescent conjugates of HIV-TAT peptide and octaarginine showed distinct vesicular staining in agreement with untreated cells but EIPA treated cells were additionally characterised by increased localisation of the peptides in the cytosol. At levels previously shown to inhibit uptake of HIV-TAT peptide and octaarginine in other cell lines, EIPA was without major effect on uptake of both peptides in KG1a cells.

INTRODUCTION

An ability to characterise the mechanism of uptake and intracellular traffic of macromolecular entities designed for drug delivery through endocytic pathways is fundamental to realisation of their true potential as candidate therapies (1, 2). This knowledge aids in the understanding of the processes of interaction between macromolecules and cells at the plasma membrane, and then, how membrane traffic orchestrates delivery to one of several intracellular stations such as endosomes and lysosomes or back to the cell surface via the recycling pathway. The term endocytosis, however, is used to describe several different uptake mechanisms that flow into highly complex and poorly understood networks of membrane vesicles and tubules (3). Uptake can be mediated via a number of different pathways utilising clathrin-dependent and independent routes and caveolae. Difficulties in assigning distinct uptake mechanism for specific molecules arises in part due to a lack of pharmacological inhibitors that specifically inhibit a single pathway leaving delivery through other avenues unperturbed. Increasingly, in cell biology studies, cells characterised by having molecular defects in specific endocytic proteins such as dynamin and components of clathrin-coated vesicles are being utilised for characterisation of mechanisms of uptake (4). These cell lines are also more recently gaining prominence in drug delivery research (5). Interpretation of data using these models is still, however, complex as there is significant overlap between uptake pathways with respect to the proteins that regulate their execution.

Protein transduction domains (PTD) - often referred to as cell penetrating peptides - such as those derived from the HIV-TAT protein have been extensively studied in drug delivery research on account of their abilities to deliver themselves and associated cargo through biological barriers such as the plasma and nuclear membrane (6-9). An ability to control delivery of a therapeutic entity via its association with one of these peptides would be an important addition to the increasing demand for systems to deliver therapeutic entities to specific subcellular stations in a controlled manner. Despite widespread research and numerous publications, there remains a great deal of controversy as to how these molecules translocate biological barriers as evidence exists for energy-independent and -dependent mechanisms such as endocytosis (9).

Macropinocytosis is a term commonly used to describe membrane ruffling that most often occurs in response to growth factor stimulation with resulting extension of extended external domains of the plasma membrane to engulf large volumes of extracellular fluid (10-12). Macropinocytosis is also involved in antigen uptake and presentation by, for example, dendritic cells and is also utilised for entry of a number of pathogens. Material ingested by macropinocytosis is eventually invaginated as macropinosomes; these contain fluid phase material whose uptake into the cell is enhanced by this process. In epidermal growth factor-stimulated cells the accompanying increased fluid phase uptake was found to be inhibited by the ion-exchange inhibitor amiloride, however, uptake of transferrin and the growth factor

via clathrin-coated uptake was unaffected (13). In a separate study, an enhanced fluid phase uptake, driven by adenovirus-induced macropinocytosis was inhibited by 5-(*N*-ethyl-*N*-isopropyl) amiloride (EIPA), a more potent analogue of amiloride (14). Consequently, these agents are regularly utilised as specific inhibitors of macropinocytosis. Amiloride and EIPA also strongly inhibited receptor-mediated uptake of albumin in renal proximal tubule-derived epithelial cells (15-17). As this process occurs most probably in a clathrin-dependent manner, it suggests that these agents, directly or indirectly, affect a multitude of endocytic processes.

More recently, amiloride and EIPA were shown to exert an inhibitory effect on the uptake of PTD such as HIV-TAT peptide raising the possibility of a link between macropinocytosis and uptake of PTDs (5, 18, 19). In support of this are data showing attenuating effects of PTDs on tumour necrosis factor receptor signaling via enhancing endocytic downregulation of the receptors at the plasma membrane (20). However there is also evidence suggesting that a fraction (50-90%) of HIV-TAT and R8 peptides uptake occurs independently of inhibition by these ion-transport inhibitors (18, 21) and that peptide length and/or charge may be a determining factor. Studies have also shown that cytosolic delivery of oligoarginine and uptake of a PTD-immunogenic antigen chimera was unaffected by amiloride treatment (22, 23).

To gain a better understanding of the effects of these inhibitors on PTD dynamics in cells and ascertain their usefulness as inhibitors of macropinocytosis, we initially assessed the effects of EIPA and amiloride on the distribution of early and late endocytic components on the endocytic pathway. We report that EIPA mediates a number of effects on the endocytic pathway in HeLa cells, and toxicity in non-adherent $CD34^+$ KG1a leukaemia cells. We extended these findings to show altered subcellular distribution of fluorescent conjugates of HIV-TAT peptide and octaarginine in the two cell lines incubated in the presence of EIPA.

EXPERIMENTAL METHODS

Materials

Hoechst 33342, propidium iodide (PI), amiloride, HEPES and 5-(*N*-ethyl-*N*-isopropyl) amiloride (EIPA) were from Sigma; the inhibitors were dissolved in dimethyl sulphoxide (DMSO) to a 50 mM stock, aliquoted and stored at –20˚C until use. Mouse antibodies recognising EEA1 were from BD Transduction laboratories (Oxford, UK), mouse anti-LampII antibodies (H4A4) were from DSHB (Iowa, USA); they were used at dilutions of 1:400 and 1:250 respectively. Secondary antibodies for immunofluorescence microscopy were from Invitrogen (Paisley, UK).

All peptides used in this study were synthesised using Fmoc solid-phase strategy and characterised by HPLC and matrix assisted laser desorption ionization time-of-flight mass spectrometry as previously described (18, 21). Alexa488-TAT and –R8 and Texas-red (TxR)-R8 were synthesised and purified as previously described (21). The peptides were dissolved to 1 mM stocks in 10 mM phosphate buffered saline, pH 7.4 (PBS) and stored at – 80˚C.

Cell culture

Cells were maintained at 37˚C in a humidified 5% CO_2 incubator. KG1a leukaemia cells were maintained at a confluency of 0.5 – 2 x 10^6 in RPMI 1640 media supplemented with 10% foetal calf serum (FCS), 100 IU/mL penicillin and 100 μg/mL streptomycin. HeLa cells were maintained in DMEM supplemented with 10% FCS, 100 IU/mL penicillin and 100 μg/mL streptomycin. All cell culture reagents were from Invitrogen.

Fluorescence microscopy

Epifluorescence microscopy was performed on a Leica DMIRB inverted fluorescent microscope as previously described (21) and confocal microscopy was performed using an Olympus Fluoview 1000 confocal laser scanning microscope on an inverted IX 81 frame. Images were collected using 488, 568 nm dichroic mirrors and spectral channels 1 and 2 on the confocal microscope.

Live cell imaging of fluorescent peptides in HeLa and KG1a cells

HeLa cells (2 x 10^5) were allowed to adhere on glass bottomed 35 mm culture dishes (MatTek Corporation, Ashland, USA) for 18-24 hours. The cells were then pre-incubated at 37˚C for 30 min in complete medium containing the 50 μM EIPA or DMSO diluent. TxR-R8 peptides were then added directly to the pre-incubation medium and the cells were further incubated for 1 or 2 hours. The cells were then washed 3 times in PBS and imaged by fluorescent microscopy in clear RPMI 1640 media containing 25 mM HEPES pH 7.4.

KG1a cells (5 x 10^5) were resuspended in complete media containing 0 - 100 μM EIPA for 30 min prior to addition of TxR-R8 or Alexa488-TAT. The cells were incubated for a further 1 h at 37˚C, washed 3 times in PBS and analysed as previously described in RPMI 1640 media containing 25 mM HEPES pH 7.4 (21).

Immunostaining

HeLa Cells (2 x 10^5) were plated on glass coverslips in 35 mm wells and incubated for 18-24 hours. The medium was replaced with fresh medium containing the designated concentrations of EIPA or amiloride or an equivalent volume of DMSO diluent. The cells were incubated for periods between 60 - 150 min prior to washing 3 times in PBS and fixing for 20 min in 3% (w/v) paraformaldehyde (PFA) in PBS. The cells were then labeled with antibodies against Early Endosome Antigen 1 (EEA1) or lysosome associated membrane protein (Lamp) II as previously described (24). Briefly, free aldehyde groups were quenched with 50 mM NH_4Cl for 10 min and cells were then permeabilised in 0.2 % (w/v) Triton-X100 in PBS. The cells were incubated with the primary antibodies for 30 min and, after washing, were labeled with Alexa594 goat anti-mouse antibodies (1:400). The cells were washed and incubated for 10 min in the presence of 2.5 μg/ml Hoechst 33342 prior to further washing in PBS, inverted into mounting oil on cover slides and analysed by fluorescent microscopy.

Cell viability studies

KG1a cells (5 x 10^5) were centrifuged for 5 min at 1000 x *g* and resuspended in 0.5 ml complete medium and incubated with 0 – 200 μM EIPA at 37˚C for 15 min. Unlabeled R8 or TAT was added to a final concentration of 3 μM and the cells were further incubated for 1 hour. The cells were centrifuged and washed 3 times in ice-cold PBS, resuspended in 200 μl ice-cold PBS and propidium iodide was added to a final concentration of 5 μg/ml. The cells were incubated for 5 min prior to flow cytometry analysis using the FL2 detector of a Beckton Dickinson FACScalibur cytometer.

Quantification of peptide uptake in cells

For each experiment, 5 x 10^5 cells were centrifuged for 2 min at 1500 x *g* and resuspended in complete medium containing 0, 25 or 50 μM EIPA. The cells were pre-incubated with the drug for 30 min at 37°C prior to centrifugation and resuspension in complete medium (with or without EIPA) containing 1 μM Alexa488-R8 peptide and incubated for a further 1 h at 37°C. Cells were then washed 3 times in PBS and incubated at 37˚C for 5 min in 0.25 mg/ml trypsin prior to addition of excess ice cold PBS followed by a further 3 washes in PBS containing 14 μg/ml heparin. The final cell pellet was resuspended in 200 μl PBS and fluorescence was quantified by flow cytometry. Fluorescence of 10,000 live cells was acquired. Alternatively and to measure total cell-associated peptide both the trypsin

incubation and heparin wash step were omitted after peptide incubation, and the cells were washed 3 times in PBS prior to analysis by flow cytometry.

RESULTS

The original identification of amiloride as an inhibitor of growth factor induced fluid phase uptake has resulted in its more recent use as a specific inhibitor of macropinocytosis. In view of the ability of this drug and its more potent analogue EIPA to inhibit uptake of PTDs and albumin, we initially investigated whether treatment of cells with these drugs affected the subcellular distribution of components of the endocytic pathway. For this, HeLa cells were incubated in the absence or presence of either 50 μM EIPA or amiloride for either 1 or 2.5 hr prior to fixing and labeling with antibodies recognising proteins associated with either early endosomes or late endosomes and lysosomes. Time of incubation and concentration of drugs utilised in this study were consistent with other studies investigating uptake of PTD and/or effects of ion-exchange inhibition on endocytosis. EEA1 is localised to the cytosol and early endosomes, is required for endosome-endosome fusion and is commonly assigned as a marker of early endosomes and more recently macropinosomes (24-26). In HeLa cells, EEA1 labeling was as expected, prominent in disperse vesicular structures (Figure 1A) and treatment for 1 h with 50 μM EIPA resulted in the appearance of swollen EEA1 positive structures. With increasing time in the presence of the drug these tended to accumulate in a perinuclear region (Figure 1B-C). LampII is a transmembrane membrane glycoprotein enriched in late endosomes and lysosomes and is a common marker for these structures (27, 28). In untreated cells, the protein was predominantly localised to a perinuclear region and on more peripheral vesicles emanating towards the plasma membrane (Figure 1F). After 1 h and especially 2.5 h in the presence of 50 μM EIPA, LampII was localised to enlarged structures that, like EEA1, accumulated in the perinuclear region (Figure 1G-H).

After 2.5 h EIPA treatment, the more peripheral LampII vesicles almost completely disappeared. Treatment of HeLa cells with 50 μM amiloride also resulted in a similar relocation of both EEA1 and LampII structures but the effects were much less obvious (Figure 1D-J). Cells incubated with EIPA for 2.5 hours had a tendency to dislodge from coverslips during the immunolabeling process; the same was not observed in amiloride treated cells (data not shown).

Experiments were then performed to investigate whether these effects were apparent in EIPA-treated HeLa cells that were then allowed to internalise TxR-R8. Cells were pre-incubated with or without EIPA for 30 min and then further incubated for 1 or 2 hours in the presence of TxR-R8; in EIPA treated cells the drug was therefore present during the pre-incubation and peptide incubation steps. The distribution of the peptides in live-cells was then analysed by fluorescent microscopy. Figure 2 shows the typical dispersed labeling of the peptides in HeLa-cell vesicles that we have previously characterised as being endosomes and lysosomes (18, 21). EIPA treated cells tended to accumulate the peptide in a perinuclear region and longer co-incubations with the drug and peptide resulted in the appearance of larger perinuclear structures.

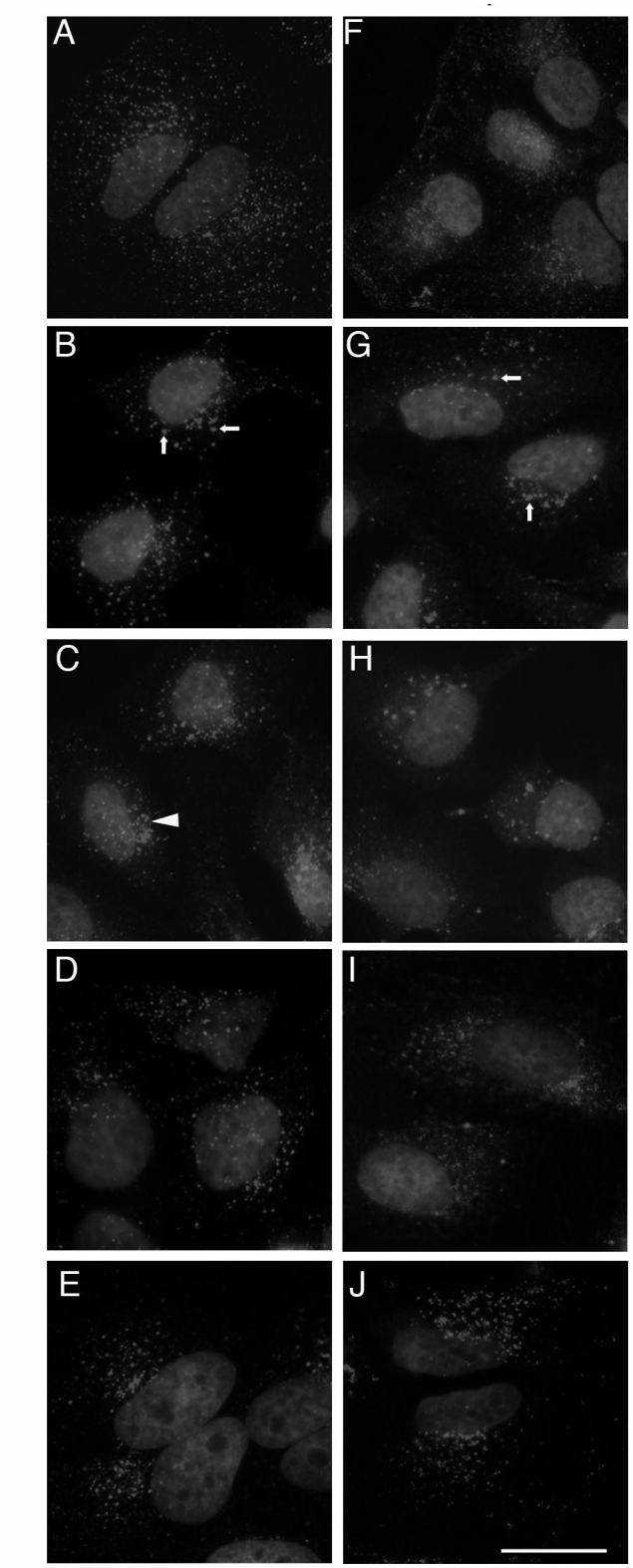

Figure 1. Effects of EIPA and amiloride on subcellular distribution of early and late organelles of endocytic pathways. HeLa cells were incubated in the presence of DMSO diluent (A and F), 50 μM EIPA (B-C and G-H) or 50 μM amiloride (D-E and I-J) for 1 (B, D, G and I) or 2.5 hours (C, E, H and J). The cells were then fixed, labeled with antibodies against EEA1 or LampII and then Alexa594 conjugated secondary anti-mouse antibodies and analysed by fluorescence microscopy. The nuclei in A-J were labeled with Hoechst 33342. Arrows show enlarged EEA1 and LampII vesicles in EIPA treated cells. Arrowheads show accumulation of vesicles in a perinuclear region. Scale bar 20 μm.

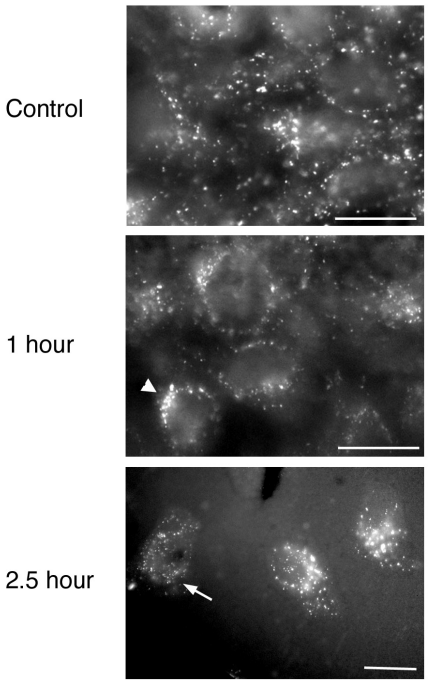

Figure 2. Subcellular distribution of TxR-R8 in EIPA-treated HeLa cells. HeLa cells were pre-incubated in the absence (control) or presence of 50 μM EIPA for 30 min prior to adding TxR-R8 to a final concentration of 1 μM and incubating for a further 1 or 2 hours The cells were then washed and analysed by fluorescent microscopy. Arrow shows an EIPA – treated cell with normal distribution of vesicles, arrowhead shows peptide accumulation in the perinuclear region. Scale bars 20 μm.

There was some heterogeneity with respect to the distribution pattern as a few EIPA-treated cells (Figure 2, shown by the arrow) had relatively normal distribution of peptide. These were, however, much less commonly observed with the longer incubations. Thus the effects of EIPA on peptide localisation in live cells, mirrored the effects of the drug on the distribution of proteins localised to the endocytic pathway.

Our results in HeLa cells prompted further experiments in a $CD34^+$ acute myeloid leukaemia cell line that we have utilised as a model for intracellular dynamics of R8 and HIV-TAT peptide (21). We had previously commented on our inability to study the effects of EIPA in this and another leukaemia cells line and hypothesised that it may be due to toxicity issues. To further investigate this, cells were pre-treated with 0 - 100 μM EIPA prior to addition of TxR-R8 or Alexa488-TAT followed by live cell confocal microscopy. Control cells were characterised by having peptide-labeled vesicles (Figure 3), that we had previously identified as being endosomes and lysosomes (21).

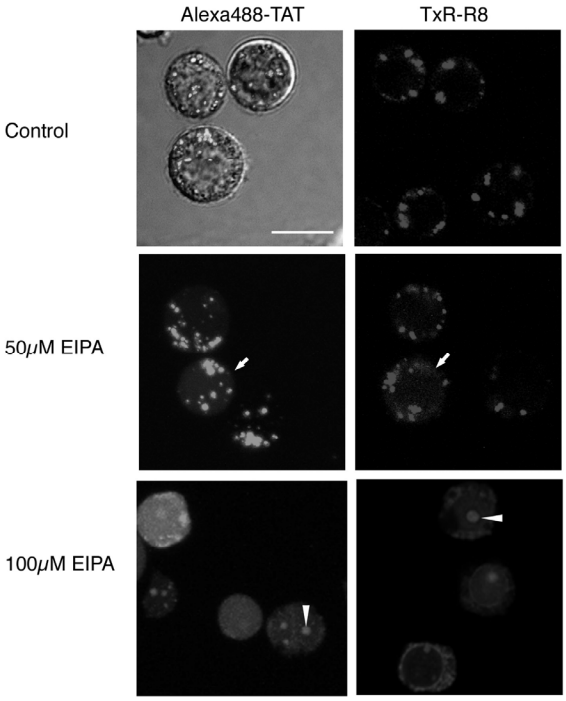

Figure 3. Subcellular distribution of Alexa488-TAT and TxR-R8 in EIPA-treated KG1a cells. KG1a cells were preincubated in the absence (control) or in the presence of 50 or 100 μM EIPA for 30 minutes prior to addition of 3 μM Alexa488-TAT or 1 μM TxR-R8. After 1 h the cells were washed and imaged by live cell confocal microscopy. All images are Z-stacked images from 15-20 sections of ~ 0.5 μm. Top left shows an overlay of peptide distribution against a phase image of the cells. Arrows show cells with cytosolic fluorescence, arrowhead shows peptide labeled nucleolus. Scale bars 10μm.

The phase/fluorescence overlay image shows that the peptide is located in distinct vesicles that are distributed throughout the cell. Sectioning through the z-axis to generate these z-stacked images revealed the peptide was inside the cell but not located in the nucleus; this occupies ~ 70 % of the cell volume. In a number of cells pre-incubated with 50 μM EIPA we observed, together with the typical vesicular labeling, weak diffuse cytosolic labeling. Increasing the EIPA concentration to 100 μM resulted in the appearance of cells that were highly fluorescent, and the peptide labeled the cytosol, nucleus and nucleolus. We also observed that cells in this population showed signs of morphological aberrations suggesting that EIPA at this level was toxic.

The apparent toxicity associated with incubating these cells in EIPA was therefore quantified and additional experiments were performed to assess whether any cell damage was occurring at lower than 100 μM. Additionally we investigated whether EIPA and peptides at concentrations used for microscopy studies were synergistic with respects to promoting cell damage. For this, cells were incubated with or without EIPA in the presence or absence of 3 μM unlabeled R8 or TAT peptide and cell integrity was then assessed by incubation the cells with propidium iodide.

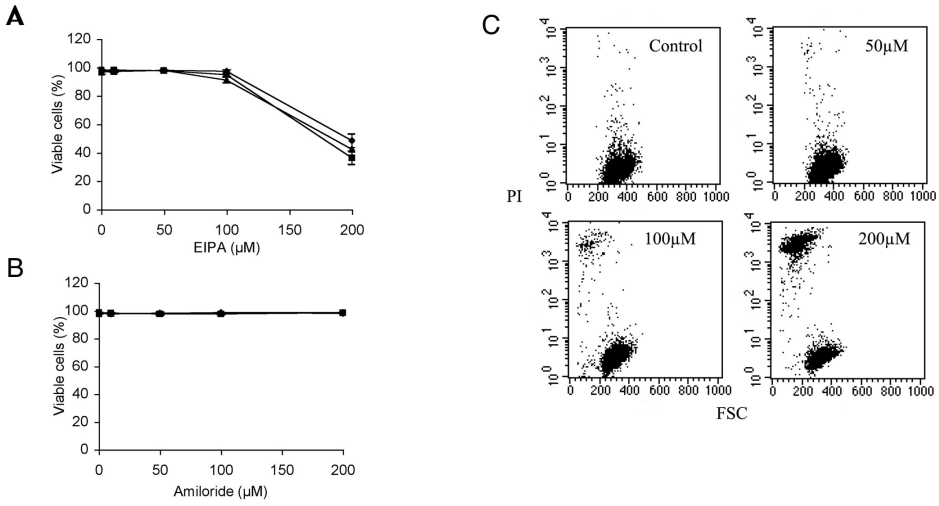

Figure 4. Cell viability of KG1a cells incubated in the presence of EIPA. KG1a cells were pre-incubated with 0-200 μM EIPA (A) or amiloride (B) for 15 min prior to addition of unlabeled R8 (3 μM), HIV-TAT (3 μM) peptide or PBS control. The cells were further incubated for 1 h before addition of PI. Data, expressed as mean and standard error of the mean, were generated from a single representative experiment performed in triplicate. Cell viability is expressed as the percentage of PI negative cells ♦ control, ■ R8, ▲ TAT. (C) Representative dot-plot of cells incubated in 0, 50, 100 and 200 μM EIPA in the absence of peptide.

Figure 4A shows that 0 - 50 μM EIPA in the presence or absence of peptide was without major effects on cell viability. At 100 μM EIPA, evidence of cytotoxicity was apparent and this was most clearly seen on the flow cytometry dotplots (Figure 4C) that revealed a population of PI positive cells that were absent in the control and 50 μM plots. These effects were only marginally enhanced by the presence of the peptides. From repeated experiments, the percentage of PI positive cells after treatment with 100 μM EIPA ranged from 5 - 25 %. At 200 μM, EIPA caused 40 - 50% cell death and analysis of the flow cytometry dotplots clearly showed that two populations of cells were present (Figure 4C). Identical experiments performed with amiloride rather than EIPA, showed no evidence of toxicity up to 200 μM (Figure 4B). In view of the fact that the cells, with and without 3 μM R8 and TAT peptides, were impermeable to PI at 50 μM EIPA, we assessed up to this concentration whether treatment of cells with this drug had any effects on peptide uptake. As EIPA could conceivably affect uptake and surface binding of peptides, we performed 1 h Alexa488-R8 uptake experiments in cells pre-incubated for 30 min with 25 or 50 μM EIPA. Following incubation with the peptide, the cells were either immediately analysed by flow cytometry or further incubated in trypsin and heparin; conditions that have previously been shown to

reduce surface labeling (5, 29). In this cell line trypsinisation and heparin treatment only marginally reduced total cell fluorescence (Figure 5), equally there was only a small reduction (< 20%) in total cell-associated and internal fluorescence in cells incubated with 0 - 50 µM EIPA.

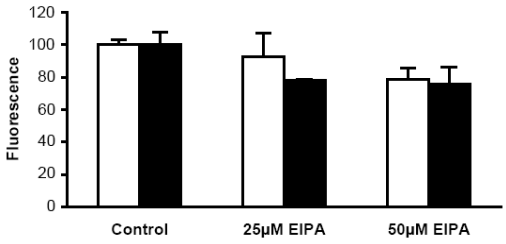

Figure 5. Quantification of cell-associated and internalized Alexa488-R8 in EIPA treated KG1a cells. KG1a cells were pre-incubated for 30 min in the presence of 0, 25 or 50 µM EIPA prior to incubation with 1 µM Alexa488-R8 for 1 h. Results are expressed as a percentage of the fluorescence in cell incubated with the peptides in the absence of drug. Open columns: fluorescence was quantified directly after peptide incubations and washing in PBS; filled columns: fluorescence was quantified after trypsinisation and heparin washes. Data show means and standard error of the mean from a single representative experiment performed in triplicate.

DISCUSSION

Analysis of the interaction of PTDs such as HIV-TAT and octaarginine with cells has received intense scrutiny. This includes aspects relating to their contact with the plasma membrane, their mechanism of internalisation and, for endocytic capture, their downstream fate. Currently there is more controversy than consensus surrounding all these issues. It is still disputed as to the exact importance of endocytosis for PTD activity, as the possibility still exists that the important cytosolic fraction arrives at this location via direct translocation through the plasma membrane. We have previously reported on the downstream traffic of HIV-TAT peptide and R8 in both cells that were utilised in this study and a major fraction of the peptide that was internalised to vesicles was, within 1 hour, delivered to lysosomes; however the uptake mechanism was not investigated (21). The possibility that macropinocytosis may be a general mechanism of entry for these peptides is gaining acceptance based on the fact that a number of studies have shown that incubating cells in the presence of amiloride and amiloride analogues inhibits peptide uptake. Rational for performing these experiments are based on findings that amiloride inhibited growth factor induced uptake of the fluid-phase marker horseradish peroxidase. However a number of issues, including our current data, suggest that caution should be given to interpretation of data from experiments performed with these drugs. The first is the fact that these agents have a significant number of other cellular effects beyond the remit of inhibition of Na^+ channels, Na^+/H^+ antiporter isoforms and Na^+/Ca^{2+} exchange (30, 31). Noted cellular effects of these drugs include loss of the ability to regulate cell volume, decreasing cytosolic pH and collapsing pH gradients in acidic vesicles (15). All are likely to have significant effects on a number of endocytic processes.

This view is supported by findings that both amiloride and EIPA are potent inhibitors of clathrin coated vesicle mediated uptake of albumin in kidney cells. The IC_{50} of the inhibition of albumin uptake by EIPA of 20 μM was approximately 10-fold lower than that for amiloride and we also show that the effects of 50 μM amiloride on subcellular redistribution of endocytic organelles is less extensive than that seen with an equivalent concentration of EIPA. In HeLa cells we have previously reported a 30% inhibition of R8 uptake by 100 μM EIPA however in Namalwa cells, uptake at 10 μM EIPA was inhibited by 60% without any inhibition in the uptake of the fluid-phase marker dye FM4-64 (5). Conversely, in the erythroleukaemia cell line K562, we observed less than 20% inhibition with 10 μM EIPA and now report that up to 50 μM EIPA is without significant effect on peptide uptake in another leukaemic cell line. Studies have also shown that whereas 100 μM EIPA rapidly inhibited 80% of albumin uptake it was without effect on the uptake of the fluid phase marker dextran (15).

Our previous analysis of HIV-TAT and R8 in leukaemia cells revealed that there is very little plasma membrane labeling in comparison with adherent cells (21). Profiling the three-dimensions of cells as shown in this study clearly shows the peptide to be almost

exclusively in cytosolic vesicles. In cells incubated with 50 μM EIPA, however, we also observed that a significant amount of the peptide was located in the cytosol and as the concentration was increased to 100 μM the nucleus and nucleolus were also labeled. Both R8 and HIV-TAT conjugated to different fluorescent probes were equally sensitive to this effect. Further analysis showed that the cells in the presence of 100 - 200 μM EIPA became leaky to propidium iodide but this was not due to the presence of peptides, and a significant proportion showed clear morphological deformations. Previous studies demonstrated that the intracellular pH of KG1a cells was reduced from 7.5 to 7.0 after a two hour incubation with 1 mM 5-(N,N-hexamethylene)-amiloride, and after 5 hours of treatment >70% of the cells were apoptotic (32). It remains to be determined whether our effects seen at 50 μM EIPA is due to leakage through a plasma membrane that may be deformed, or translocation from the clearly identified endocytic vesicles. Of interest is recent data showing that treatment of HeLa cells with 100 μM amiloride, inhibited oligoarginine ($YG(R)_9$) uptake by 40% but had no effect on the ability of this molecule to reach the cytosol (23). In all, these studies strongly point to the fact that the action of EIPA and possibly amiloride is highly cell-type dependent and that great care must be taken to refute any possibility that any effects are not simply due to collapse of pH gradients and membrane leakage. We also observed some loss of EIPA activity upon storage (personal communication A.T. Jones and S. Futaki) and this may also contribute to the lack of agreement regarding the effects of this drug on peptide uptake.

In view of the fact that EIPA affects a number of endocytic processes we also investigated the effects of EIPA and amiloride on the integrity of the endocytic pathway in HeLa cells. Incubation of these cells with 50 μM EIPA had clear and consistent effects on the morphology and subcellular distribution and of both early and the late components of the endocytic pathway, with the later being the most affected. Amiloride had less pronounced effects and this may be attributed to the fact that it is less potent compared with EIPA at inhibiting most Na^+/H^+ antiporter isoforms (< 100 fold) and the Na^+/Ca^+ exchanger (< 8.5 fold) (30, 31). Previous studies showed that macrophage lysosomes were rapidly dispersed after treatment with 1 mM amiloride and the localisation of these organelles was extremely sensitive to cytoplasmic pH (33). It remains to be seen what effects amiloride and especially EIPA at these lower concentrations would have in macrophages and other cell lines but suggests that the effects we observed were not due to, and dominant over the effects of cytosolic acidification. Concentrations used here and elsewhere to assess peptide uptake are still extremely high relative to that required to inhibit the Na^+/H^+ antiporter (30), however, the general nature of the effects on endocytic vesicles was similar for both drugs, suggesting both were acting via a common mechanism(s). EIPA was shown to have significant effects on cell morphology via, in part, collapse of actin stress fibres and redistribution of the actin cytoskeleton (34). As endocytic organelles traverse along the cytoskeleton it is highly probable that their distribution would be susceptible to agents that disrupt this organisation.

These lipophilic, weak base drugs could also accumulate in acidic vesicles and increase vesicle pH (15, 30), a process known to disrupt endocytic processes including traffic from early to late endosomes (35). The swollen peptide-labeled structures may therefore be early rather than late-endosomes as EIPA would hinder traffic from EEA1 positive early to LampII structures. As these agents affect so many cellular processes it is extremely difficult to assign the observed phenotypes to a single mechanism.

CONCLUSIONS

The study of macropinocytosis in a number of cell types is hampered by there being a paucity of information on the requirements for specific proteins to execute its function and also by the lack of specific macropinocytosis probes. The use of amiloride and analogues undoubtedly provides useful information with respect to the dynamics of PTD in cells but if utilised alone they will not fully characterise the process or processes that govern their internalisation or that of other macromolecules.

ACKNOWLEDGEMENTS

The authors would like to thank Andy Hill from Olympus for assistance with confocal microscopy. Jing Jin is supported by the Leukaemia Research Fund (Grant No 04075), Marjan Fetz is supported by a Marie Curie Host Fellowship for early-stage training in the 6th framework programme of the European Commission.

REFERENCES

1. A. T. Jones, M. Gumbleton and R. Duncan. Understanding endocytic pathways and intracellular trafficking: a prerequisite for effective design of advanced drug delivery systems. *Adv Drug Deliv Rev.* **55:** 1353-1357 (2003)
2. P. Watson, A. T. Jones and D. J. Stephens. Intracellular trafficking pathways and drug delivery: fluorescence imaging of living and fixed cells. *Adv Drug Deliv Rev.* **57:** 43-61 (2005)
3. S. D. Conner and S. L. Schmid. Regulated portals of entry into the cell. *Nature.* **422:** 37-44 (2003)
4. F. Huang, A. Khvorova, W. Marshall and A. Sorkin. Analysis of clathrin-mediated endocytosis of epidermal growth factor receptor by RNA interference. *J Biol Chem.* **279:** 16657-16661 (2004)
5. J. S. Wadia, R. V. Stan and S. F. Dowdy. Transducible TAT-HA fusogenic peptide enhances escape of TAT-fusion proteins after lipid raft macropinocytosis. *Nat Med.* **10:** 310-315 (2004)
6. A. H. Joliot and A. Prochiantz. Transduction peptides: from technology to physiology. *Nat Cell Biol.* **6:** 189-196 (2004)
7. E. L. Snyder and S. F. Dowdy. Cell-penetrating peptides in drug delivery. *Pharm Res.* **21:** 389-393 (2004)
8. S. Deshayes, M. C. Morris, G. Divita and F. Heitz. Cell-penetrating peptides: tools for intracellular delivery of therapeutics. *Cell Mol Life Sci.* **62:** 1839-1849 (2005)
9. R. Fischer, M. Fotin-Mleczek, H. Hufnagel and R. Brock. Break on through to the other side - biophysics and cell biology shed light on cell-penetrating peptides. *ChemBioChem.* **6:** 2126-2142 (2005)
10. M. Maniak (2001) *Macropinocytosis* (Oxford University Press, Oxford).
11. M. Amyere, M. Mettlen, P. Van der Smissen, A. Platek, B. Payrastre, A. Veithen and P. J. Courtoy. Origin, originality, functions, subversions and molecular signalling of macropinocytosis. *Int J Med Microbiol.* **291:** 487-494 (2002)
12. L. Johannes and C. Lamaze. Clathrin-dependent or not: is it still the question? *Traffic.* **3:** 443-451 (2002)
13. M. A. West, M. S. Bretscher and C. Watts. Distinct endocytic pathways in epidermal growth factor-stimulated human carcinoma A431 cells. *J Cell Biol.* **109:** 2731-2739 (1989)
14. O. Meier, K. Boucke, S. V. Hammer, S. Keller, R. P. Stidwill, S. Hemmi and U. F. Greber. Adenovirus triggers macropinocytosis and endosomal leakage together with its clathrin-mediated uptake. *J Cell Biol.* **158:** 1119-1131 (2002)
15. M. Gekle, K. Drumm, S. Mildenberger, R. Freudinger, B. Gassner and S. Silbernagl. Inhibition of Na+-H+ exchange impairs receptor-mediated albumin endocytosis in renal proximal tubule-derived epithelial cells from opossum. *J Physiol.* **520:** 709-721 (1999)
16. M. Gekle, R. Freudinger and S. Mildenberger. Inhibition of Na+-H+ exchanger-3 interferes with apical receptor-mediated endocytosis via vesicle fusion. *J Physiol.* **531:** 619-629 (2001)
17. K. Drumm, E. Lee, S. Stanners, B. Gassner, M. Gekle, P. Poronnik and C. Pollock. Albumin and glucose effects on cell growth parameters, albumin uptake and Na+/H+-exchanger isoform 3 in OK cells. *Cell Physiol Biochem.* **13:** 199-206 (2003)
18. I. Nakase, M. Niwa, T. Takeuchi, K. Sonomura, N. Kawabata, Y. Koike, M. Takehashi, S. Tanaka, K. Ueda, J. C. Simpson, A. T. Jones, Y. Sugiura and S. Futaki. Cellular uptake of arginine-rich peptides: roles for macropinocytosis and actin rearrangement. *Mol Ther.* **10:** 1011-22 (2004)
19. I. M. Kaplan, J. S. Wadia and S. F. Dowdy. Cationic TAT peptide transduction domain enters cells by macropinocytosis. *J Control Release.* **102:** 247-253 (2005)
20. M. Fotin-Mleczek, S. Welte, O. Mader, F. Duchardt, R. Fischer, H. Hufnagel, P. Scheurich and R. Brock. Cationic cell-penetrating peptides interfere with TNF signalling by induction od TNF receptor internalization. *J Cell Sci.* **118:** 3339-33351 (2005)
21. S. Al-Taei, N. A. Penning, J. C. Simpson, S. Futaki, T. Takeuchi, I. Nakase and A. T. Jones. Intracellular traffic and fate of protein transduction domains HIV-1 TAT and octaarginine, implications for their utilization as drug delivery vectors. *Bioconjug Chem.* **17:** 90-100 (2006)
22. R. B. Batchu, A. M. Moreno, S. M. Szmania, G. Bennett, G. C. Spagnoli, S. Ponnazhagan, B. Barlogie, G. Tricot and F. van Rhee. Protein transduction of dendritic cells for NY-ESO-1-based immunotherapy of myeloma. *Cancer Res.* **65:** 10041-10049 (2005)
23. J. L. Zaro, T. E. Rajapaska, C. T. Okamoto and W. C. Shen. Membrane transduction of oligoarginine in HeLa cells is not mediated by macropinocytosis. *Mol Pharm.* **3:** 181-186 (2006)

24. J. C. Simpson, G. Griffiths, M. Wesseling-Resnick, J. A. Fransen, H. Bennett and A. T. Jones. A role for the small GTPase Rab21 in the early endocytic pathway. *J Cell Sci.* **117:** 6297-6311 (2004)
25. I. G. Mills, A. T. Jones and M. J. Clague. Involvement of the endosomal autoantigen EEA1 in homotypic fusion of early endosomes. *Curr Biol.* **8:** 881-884 (1998)
26. M. Hamasaki, N. Araki and T. Hatae. Association of early endosomal autoantigen 1 with macropincytosis in EGF-stimulated A431 cells. *Anat Rec A Discov Mol Cell Evol Biol.* **277:** 298-306 (2004)
27. E. L. Eskelinen, A. L. Illert, Y. Tanaka, G. Schwarzmann, J. Blanz, K. Von Figura and P. Saftig. Role of LAMP-2 in lysosome biogenesis and autophagy. *Mol Biol Cell.* **13:** 3355-3368 (2002)
28. E. L. Eskelinen, Y. Tanaka and P. Saftig. At the acidic edge: emerging functions for lysosomal membrane proteins. *Trends Cell Biol.* **13:** 137-145 (2003)
29. J. P. Richard, K. Melikov, H. Brooks, P. Prevot, B. Lebleu and L. V. Chernomordik. Cellular uptake of unconjugated TAT peptide involves clathrin-dependent endocytosis and heparan sulfate receptors. *J Biol Chem.* **280:** 15300-6 (2005)
30. T. R. Kleyman and E. J. Cragoe Jr. Amiloride and its analogs as tools in the study of ion transport. *J Membr Biol.* **105:** 1-21 (1988)
31. B. Masereel, L. Pochet and D. Laeckmann. An overview of inhibitors of Na+/H+ exchanger. *Eur J Med Chem.* **38:** 547-554 (2003)
32. I. N. Rich, D. Worthington-White, O. A. Garden and P. Musk. Apoptosis of leukemic cells accompanies reduction in intracellular pH after targeted inhibition of the Na+/H+ exchanger. *Blood.* **95:** 1427-34 (2000)
33. J. Heuser. Changes in lysosome shape and distribution correlated to cytoplasmic pH. *J Cell Biol.* **108:** 855-864 (1989)
34. A. Lagana, J. Vadnais, P. U. Le, T. N. Nguyen, R. Laprade, I. R. Nabi and J. Noel. Regulation of the formation of tumor cell pseudopodia by the Na+/H+ exchanger NHE1. *J Cell Sci.* **113:** 3649-3662 (2000)
35. M. J. Clague, S. Urbe, F. Aniento and J. Gruenberg. Vacuolar ATPase activity is required for endosomal carrier vesicle formation. *J Biol Chem.* **269:** 21-24 (1994)

6

Cytosolic delivery of liposomally targeted proteins induced by photochemical internalisation

Marjan M. Fretz, Anders Høgset, Gerben A. Koning,
Wim Jiskoot and Gert Storm

Accepted for publication in Pharmaceutical Research

ABSTRACT

Purpose The application of therapeutic proteins is often hampered by limited cell entrance and lysosomal degradation, as intracellular targets are not reached. By encapsulation of proteins into targeted liposomes, cellular uptake via endocytosis can be enhanced. To prevent subsequent lysosomal degradation and promote endosomal escape, photochemical internalisation (PCI) was studied here as a tool to enhance endosomal escape. PCI makes use of photosensitising agents which localize in endocytic vesicles, inducing endosomal release upon light exposure.

Methods The cytotoxic protein saporin was encapsulated in different types of targeted liposomes. Human ovarian carcinoma cells were incubated with the photosensitiser TPPS2a and liposomes. To achieve photochemical internalisation, the cells were illuminated for various time periods. Cell viability was used as read-out. Illumination time and amount of encapsulated proteins were varied to investigate the influence of these parameters.

Results The cytotoxic effect of liposomally targeted saporin was enhanced by applying PCI, likely due to enhanced endosomal escape. The cytotoxic effect was dependent on the amount of encapsulated saporin and the illumination time.

Conclusion PCI is a promising technique for promoting cytosolic delivery of liposomally targeted saporin. PCI may also be applicable to other liposomally targeted therapeutic proteins with intracellular targets.

INTRODUCTION

An increasing number of biomolecules, like proteins and nucleic acids, are being developed for therapeutic use. However, intracellular delivery of such macromolecules to their target sites present in the cytosol or nucleus is often inefficient. Their hydrophilic and charged nature together with their high molecular weight, make cell membrane passage difficult. Furthermore, these molecules often have poor pharmacokinetic and biodistribution properties and are highly susceptible to degradation by extra- and intracellular enzymes. Therefore, delivery systems, like liposomes, are required to improve the therapeutic efficacy of labile macromolecular drugs. Liposomes can improve pharmacokinetics, provide protection from degradation, mediate targeting to the pathological site and facilitate uptake by the target cells (1, 2). However, although pharmacokinetics, tissue distribution, and cellular uptake can be improved using (targeted) liposomes, the liposomal drug usually ends up in the endo- and lysosomes, where both the liposome particles as well as the encapsulated macromolecules are subject to degradation (3, 4).

Therefore, endosomal escape of liposome-encapsulated macromolecules is a vital issue in drug delivery research. In the liposome field, various approaches are being investigated to realise endosomal escape of liposomal contents. One approach makes use of lipids with pH-dependent membrane-destabilising properties. Upon acidification, as occurring in the endosomal/lysosomal compartment where the targeted liposomes end up after internalisation by target cells, these lipids undergo a phase transition and when incorporated in the liposomal membrane, they promote fusion with and/or destabilisation of the endosomal membrane. The most commonly used lipid in this context is dioleoyl phosphatidyl ethanolamine (DOPE) in combination with acidic lipids such as cholesteryl hemisuccinate (CHEMS), oleic acid (OA), *N*-palmitoyl homocysteine (PHC) and dipalmitoyl succinyl glycerol (DSPG). This approach is adequately reviewed in reference (5). Lee and co-workers reported on the successful cytosolic delivery of liposomal contents by co-encapsulation of the pore forming protein listeriolysin O (LLO) in pH-sensitive liposomes. This delivery system mimics the intracellular invasion strategy of the pathogen *Listeria monocytogenes* which uses LLO to escape from the endosomes (6-8). Co-encapsulation of a fusogenic peptide derived from the influenza virus haemagglutinin resulted in efficient cytosolic delivery of liposomal diphtheria toxin A-chain as reported by Mastrobattista *et al*. (9). Kakuda *et al.* demonstrated that the insertion of cholesterol derivatised GALA-peptide into the liposomal bilayer also stimulated release of liposomal contents into the cytosol (10).

Recently a new technique, referred to as photochemical internalisation (PCI) has been reported to be useful for the promotion of endosomal escape of macromolecules or particulate systems (reviewed in (11)). The technique is based on the specific localisation of a photosensitiser in endosomal membranes. Photosensitisers with an amphiphilic nature will, when added to cells, localise in the plasma membranes and, upon endocytosis,

accumulate primarily in endosomal membranes. Including a photosensitiser free incubation period in the experimental PCI protocol will ascertain localisation of the photosensitiser predominantly in the endosomal membranes. Upon illumination, highly reactive singlet oxygen species are formed which damage the endosomal membranes and make it permeable for endocytosed material. Upon illumination release of lysosomal enzymes into the cytosol was observed without extensive cell death (12).

The plant toxins gelonin and saporin, members of the type I ribosome-inactivating protein family, lack specific domains for cell entrance and if they are taken up via endocytosis, they will be degraded within the endosomal/lysosomal pathway. However, if they are delivered into the cytoplasm, their potent inhibitory effect on the cellular protein synthesis results in severe cytotoxicity (13). Therefore, these macromolecules are useful for demonstrating the occurrence of endosomal escape.

The recently introduced technique PCI was applied for the cytosolic delivery of saporin via liposomes. Saporin was encapsulated into different types of liposomes, designed to deliver the toxin into EGF-receptor positive human ovarian cancer cells. To stimulate cellular uptake, positively charged and EGF-receptor targeted liposomes were employed. As cytotoxic activity of liposomal saporin was only observed in combination with PCI, it is demonstrated here for the first time that the combination of the use of targeted liposomes with PCI is a valuable approach for the cytosolic delivery of liposome-entrapped proteins.

EXPERIMENTAL METHODS

Materials

Egg-phosphatidylcholine (EPC) and 1,2-distearoyl-glycero-3-phosphoethanolamine-*N*-[poly(ethylene glycol)2000] (PEG_{2000}-DSPE) were obtained from Lipoid GmbH (Ludwigshafen, Germany). Maleimide-PEG_{2000}-DSPE (Mal-PEG-DSPE) was obtained from Shearwater Polymers (Huntsville, AL, USA). 1,2-dioleoyl-3-trimethylammonium-propane chloride salt (DOTAP) was purchased from Avanti Polar Lipids (Alabaster, AL, USA). Cholesterol (CHOL), S-acetylthioglycolic acid N-hydroxysuccinimide ester (SATA), XTT sodium salt and saporin were purchased from Sigma-Aldrich Co. (St. Louis, MO, USA). Titriplex III (EDTA) was obtained from Merck (Darmstadt, Germany). Hepes was purchased from Acros (Geel, Belgium). Hydroxylamine hydrochloride was from ICN Biomedicals (Aurora, OH, USA). ^{125}I was purchased from Amersham Biosciences (Diegem, Belgium).

1,1'-dioctadecyl-3,3,3',3'-tetramethylindocarbocyanine, 4-chlorobenzenesulfonate sulfonate salt (DiD) was obtained from Molecular Probes Europe BV (Leiden, The Netherlands). Murine monoclonal antibody mAb425 of isotype IgG2b, directed against the human epidermal growth factor receptor (EGFR) was kindly donated by Merck KGaA (Darmstadt, Germany). Irrelevant isotype matched murine monoclonal antibody directed against the influenza virus HA (clone 12CA5) was kindly donated by Dr. E. Boot (Immunology Division, Department of Infectious Diseases and Immunology, Utrecht University, Utrecht, The Netherlands).

The photosensitiser LumiTrans^{TM} (tetraphenylporphine disulfonate, $TPPS_{2a}$) was a generous gift from PCI Biotech (Oslo, Norway).

Cell culture

The human ovarian carcinoma cell line NIH:OVCAR-3 was obtained from the ATCC (Manassas, USA). The cells were cultured in Dulbecco's modified Eagle's medium containing 3.7 g/l sodium bicarbonate, 4.5 g/l L-glucose and supplemented with L-glutamine (2 mM), 10% (v/v) foetal calf serum (FCS), penicillin (100 IU/ml), streptomycin (100 μg/ml) and amphotericin B (0.25 μg/ml) at 37°C with 5% CO_2 in humidified air. All cell-culture related material was obtained from Gibco (Grand Island, NY, USA).

Liposome preparation and characterisation

The solvent evaporation/hydration method was used to prepare liposomes. Briefly, EPC, CHOL, PEG_{2000}-DSPE and maleimide-PEG_{2000}-DSPE (molar ratio1.85:1.00:0.09:0.06) or EPC, CHOL and DOTAP (molar ratio 4:1:1) were dissolved in chloroform/methanol (2:1 v/v). For FACS analysis, 0.1 mol% DiD was added as fluorescent marker. After evaporation of the solvent, the lipid film was hydrated with a solution of 0.5 mg/ml or 0.1 mg/ml saporin

in Hepes buffered saline (HBS; 10 mM Hepes, 137 mM NaCl, pH 7.4). The liposomes were sized to 150 nm by extrusion using a Lipex high pressure extruder (Northern Lipids, Vancouver, Canada). Non-encapsulated saporin was removed by size exclusion chromatography using Sepharose CL-4B (Amersham Pharmacia Biotech, Uppsala, Sweden). The monoclonal antibody mAb425 and the irrelevant isotype antibody were modified with SATA to introduce sulfhydryl groups randomly as described previously (14). In short, an 8-fold molar excess of SATA dissolved in DMF was added to the antibody solution (1/10 of volume) and incubated for 45 minutes at room temperature. The non-coupled SATA was removed using Vivaspin columns (MWCO 50,000 Da, Vivascience, Hannover, Germany). The sample was centrifuged three times for 15 minutes at 5,500 rpm at 4°C and washed with HBS pH 7.4.
Before coupling of the antibody to the maleimide-derivatised PEG-DSPE present on the liposome surface, the SATA-group was activated using a hydroxylamine solution (0.5 M Hepes, 0.5 M hydroxylamine HCl and 0.25 mM EDTA; pH 7.0) for 1 hour at room temperature. Coupling of the antibody to the maleimide-PEG-DSPE present on the liposomal surface occurred overnight at 4°C. Non-coupled antibody was removed by size exclusion chromatography using Separose CL-4B.
The liposomes were characterised with respect to size using dynamic light scattering, phospholipid content according to Rouser (15) and amount of saporin encapsulated using ^{125}I determination.

Labeling of saporin with ^{125}I

Saporin was labeled with ^{125}I using Iodobeads (Pierce, Rockford, IL, USA). 5 MBq of a ^{125}I-solution in 0.01 M NaOH (370 MBq/100 µl) was diluted in 200 µl HBS pH 7.0 and incubated with two Iodobeads for 5 minutes at room temperature. Subsequently, 1 ml of a saporin solution (1 mg/ml in water) was added and incubated for an additional 20 minutes at room temperature. Next, saporin and unbound ^{125}I were separated on a PD-10 column (Amersham Pharmacia Biotech) using HBS pH 7.0 as an eluent. Specific activity was determined by measuring activity on a Wallac 1480 “Wizard 3” sodium iodide counter and by detecting the UV absorbance at 280 nm using a Shimadzu UV-1601 spectrophotometer. The specific activity was 1.6 MBq/mg protein.

Binding studies

OVCAR-3 cells were detached from the culture flask by trypsin/EDTA solution (0.05% (w/v) trypsin and 0.02% (w/v) EDTA in PBS). Cells, (100,000) were incubated for 1 hour with fluorescently labeled liposomes at 4°C. Cells were washed twice by centrifugation (300 x *g*, 5 min, 4°C). Flow cytometry analysis was performed using a FACScalibur (Beckton&Dickinson, Mountain View, CA, USA) and data were analysed using WinMDI 2.8 software, which was kindly provided by Joseph Trutter.

Cellular uptake of liposomal saporin

OVCAR-3 cells were seeded (10^5 cells/well) in 6-well plates and cultured overnight prior to the experiment. The cells were incubated for 18 hrs with saporin-liposomes (50 nmol liposomal lipid). After three washing steps using PBS, the cells were subsequently chased for 4 hours with liposome free medium. After washing, the cells were lysed with a 1% Triton X-100 solution (w/v in water) and frozen to -20°C. The thawed cell lysate was used for analysis on the Wallac sodium iodide counter.

Efficacy studies

OVCAR-3 cells (5 x 10^3 cells/well) were seeded into 96-well plates and cultured overnight prior to the experiment. Culture medium was removed and fresh culture medium was added containing either liposomes, photosensitiser or both. The photosensitiser was always added at a final concentration of 0.5 µg/ml, while the liposome concentration varied. After 18 hours, liposomes and/or photosensitiser were removed and the cells were incubated for 4 hr with fresh culture medium before 75 sec of illumination with the LumiSource (Osram 18W/67 with light intensity 7mW/cm^2, PCI Biotech, Oslo, Norway). Cells were incubated for another 48 hrs before the cell viability was measured using the XTT assay as previously described (16).

Effect of illumination time

OVCAR-3 cells were incubated with 0.1 µM saporin-liposomes and 0.5 µg/ml photosensitiser for 18 hrs and subsequently for 4 hrs with complete culture medium. The cells were illuminated for 45, 75 or 120 sec. Cell viability was assessed with the XTT assay 48 hrs after illumination.

Contribution of PDT to cell death

OVCAR-3 cells were incubated with 0.1 µM saporin-liposomes and 0.5 µg/ml photosensitiser for 18 hrs and subsequently for 4 hrs with complete culture medium. The cells were illuminated for 45, 75 or 120 sec. Cell viability was assessed with the XTT assay 48 hrs after illumination. The contribution of photodynamic therapy (PDT) effects to cell death was calculated with the following formulas:

$$Total\ Cell\ Viability\ (TCV) = \left(\frac{Absorbance(treated\ with\ liposomes,\ photosensitiser\ and\ light)}{Absorbance(non-treated)} \right) \times 100\%$$

$$Cell\ Viability\ after\ PDT\ (CVPDT) = \left(\frac{Absorbance(treated\ with\ photosensitiser\ and\ light)}{Absorbance(non-treated)} \right) \times 100\%$$

Cell death PDT = 100 – CVPDT
Cell death PCI = 100 – Cell death PDT – TCV
Total cell death = Cell death PDT + Cell death PCI = 100 – TCV

$$Contribution\ of\ PDT\ to\ cell\ death = \left(\frac{Cell\ death\ PDT}{Total\ Cell\ death} \right) \times 100\%$$

$$Contribution\ of\ PCI\ to\ cell\ death = \left(\frac{Cell\ death\ PCI}{Total\ cell\ death} \right) \times 100\%$$

RESULTS AND DISCUSSION

Liposome characteristics

The following liposome types were used to deliver saporin into human ovarian carcinoma cells (OVCAR-3): 1. Cationic liposomes (DOTAP-L) were prepared by incorporation of the positively charged lipid DOTAP (17 mol% of total lipid) into EPC/CHOL liposomes. The cationic nature of these liposomes mediates a strong affinity for negatively charged cell membranes (17). 2. Epidermal growth factor receptor (EGFR) targeted PEG-liposomes (EGFR-L) were prepared to target to the EGFR by coupling an anti-EGFR antibody to the distal end of the PEG-chains. The EGFR is overexpressed in several tumour cell lines and is an internalising receptor, which makes it an attractive target for drug delivery (18). As already shown by former studies in our laboratory, EGFR-L can be used to specifically target OVCAR-3 cells (9). 3. PEG-liposomes (PEG-L) without an antibody attached were used as a control. Due to the PEG-layer surrounding these liposomes, the cellular association and uptake by OVCAR-3 cells is low as shown previously (9, 19).

All liposome types used had a particles size between 140 and 160 nm and a polydispersity index <0.2, which indicates a narrow size distribution. As quantified by ^{125}I-saporin determination, the encapsulated amount of saporin varied between 0.3 and 0.9 µg/µmol lipid which correspond to an encapsulation efficiency varying between 3.0 and 5.4%. The fluorescent bilayer marker DiD was incorporated (0.1 mol%) in case of experiments designed to monitor the cellular binding of the liposomes.

Cellular binding and uptake of saporin-liposomes

The binding of the different liposome types to OVCAR-3 cells was investigated by flow cytometry using the fluorescent bilayer marker DiD (Figure 1A). The highest level of cellular association was observed in case of the positively charged DOTAP-L. Electrostatic interaction between the positively charged DOTAP-L and negatively charged cell membranes results in a strong binding. The use of targeted EGFR-L resulted in a 20-60 fold increased fluorescence signal compared to non-targeted PEG-L. This indicates that the EGFR-targeted liposomes do interact with the EGF-receptor expressed on the OVCAR-3 cells and that targeting the EGF-receptor may be useful for increasing the delivery of liposomal proteins. The coupling of an irrelevant isotype match antibody to liposomes results in a degree of cell binding of the liposomes which is comparable to that of non-targeted PEG-liposomes. Furthermore, competition by adding excess of free antibody could partially reduce cell binding of the EGFR-L (results not shown). Additionally, we measured the amount of cellular saporin after incubation at 37°C using ^{125}I-labeled saporin. OVCAR-3 cells were incubated with DOTAP-L, EGFR-L or PEG-L, all containing ^{125}I-labeled saporin and the results shown in Figure 1B correspond to the cell-binding data in Figure 1A. The extent of liposome-mediated delivery of saporin to the cells decreased in the following

order: DOTAP-L > EGFR-L > PEG-L. It is known that (targeted) liposomes can be taken up by endocytosis, which in this case most probably results in the degradation of the liposomal saporin in the lysosomes (20). To 'rescue' saporin from degradation, we included PCI in the treatment to achieve endosomal release of the liposomal saporin.

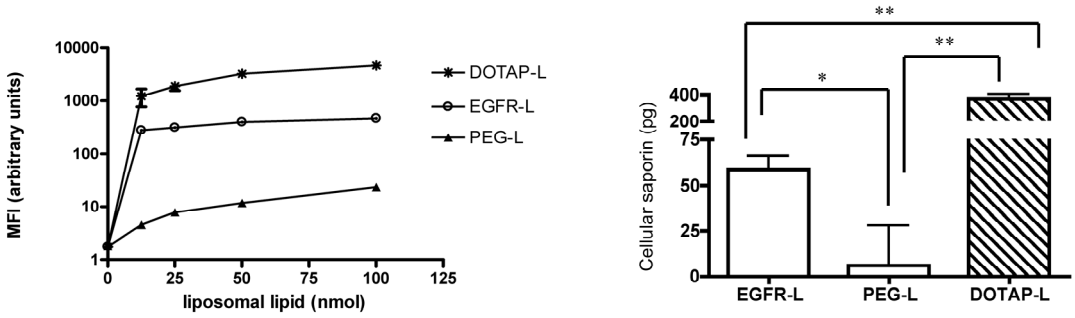

Figure 1. Cellular binding and uptake of different liposome types containing saporin. (A) Binding of different types of saporin-liposomes to OVCAR-3 cells. Fluorescently labelled liposomes were incubated for 1 hr at 4°C with OVCAR-3 cells, washed and analysed by flow cytometry. Data represents mean ± SD (n=3). Error bars are within plot symbol when not visible. Statistical analysis was performed using a F-test. All curves are significantly different ($P < 0.0001$). (B) Cellular ^{125}I-saporin after 18 hr incubation with liposomal ^{125}I-saporin followed by 4 hr chase period with liposome free medium. Data represent mean ± SD (n=3). Statistical analysis was performed using a one-way ANOVA ($P < 0.0001$) followed by Newman-Keuls post-hoc multiple comparison test (* $P < 0.05$ and ** $P < 0.001$).

Efficacy studies

Recent studies have shown that the PCI technique is capable to induce selective release of material from the endosomes into the cytoplasm. Selbo *at al.* demonstrated that the use of PCI enhanced the potency of the plant toxin gelonin in inhibiting cellular protein synthesis by a factor of 300 (21). In addition, the low-molecular weight drug bleomycin (22), antigenic peptides (23), immunotoxins (24, 25), peptide nucleic acids (26) and even colloidal carriers for gene delivery (27-29) have been successfully delivered into the cytosol via PCI. These agents generally are not able to reach their intracellular target site efficiently, due to lack of capability to pass cellular membranes and/or the occurrence of degradation within endocytic vesicles. The endosomal release of liposomal drugs enabled by PCI has not been demonstrated yet. As liposomes have a prominent place in the arsenal of advanced drug delivery systems developed over the years, it is important to evaluate whether PCI can be employed to further improve the efficacy of liposomal drug formulations.

To investigate whether the PCI technique is able to enhance the cytosolic delivery of liposomal proteins in vitro, OVCAR-3 cells were incubated with different types of saporin-

liposomes and/or the photosensitiser $TPPS_{2a}$ and subsequently illuminated to activate the photosensitiser. Since the ribosome-inactivating protein saporin will only have cytotoxic properties when delivered in its active form into the cytosol, cell viability was chosen as read-out (13).

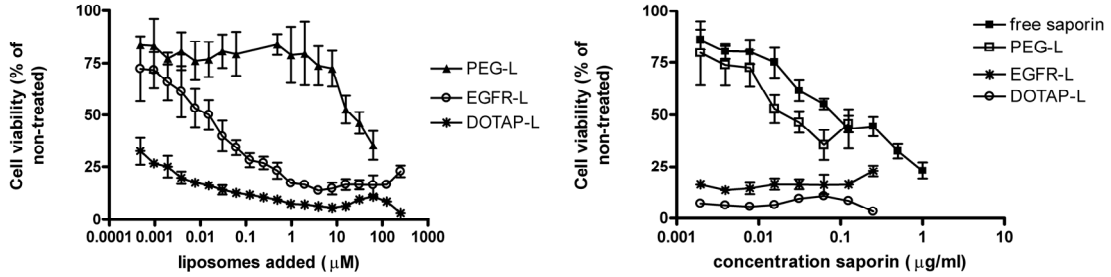

Figure 2. Effect of PCI on cytotoxicity after exposure to liposomal saporin (A). Comparison of liposomal saporin with free saporin in combination with PCI (B). OVCAR-3 cells were incubated for 18 hrs with liposomes and photosensitiser, subsequently washed away and incubation was continued for 4 hrs before the onset of 75 sec of illumination. 48 hrs after illumination, the cell viability was assessed with the XTT assay. Data represent mean ± SD (n=4). Error bars are within plot symbols when not visible. Statistical analysis was performed on Figure 2A using an F-test. Curves are significantly different ($P < 0.0001$).

Figure 2A shows the cell viability of OVCAR-3 cells after incubation with the different types of liposomes and photosensitiser, followed by illumination. Both DOTAP-L as well as EGFR-L strongly decreased cell viability compared to PEG-L, with DOTAP-L being superior over EGFR-L. Even at the lowest concentration added (0.5×10^{-3} μM liposomes) only 30% of the cells survived the treatment with saporin-containing DOTAP-L in combination with PCI, compared to 75% survival when EGFR-L are used at this concentration. Saporin in PEG-L was cytotoxic only at concentrations higher than 10 μM, which is at a level of 4 orders of magnitude higher than for EGFR-L and 5 orders of magnitude higher than for DOTAP-L. When the cytotoxic effect of saporin-liposomes in combination with PCI is compared with that of free saporin combined with PCI (Figure 2B), it is obvious that both DOTAP-L and EGFR-L are by far more cytotoxic due to the enhanced cytosolic delivery of saporin. Combination of PCI with free saporin was comparable to that of saporin-containing PEG-L combined with PCI, indicating limited cytosolic delivery of saporin yielding sub-threshold levels for cytotoxicity.

To demonstrate that the use of PCI is essential for cytosolic delivery of saporin, different control experiments were carried out. Figure 3A demonstrates that only the combination of saporin-liposomes (DOTAP-L) with both photosensitiser and illumination (PCI) has cytotoxic properties. Empty DOTAP-L, i.e. devoid of saporin, were examined and did not

show any cytotoxicity in combination with PCI. In addition, when saporin-containing DOTAP-L were used in combination with only photosensitiser or only illumination or neither of those, no decrease in cell viability was seen (data not shown in case of saporin-containing liposomes in combination with illumination, but without photosensitiser).

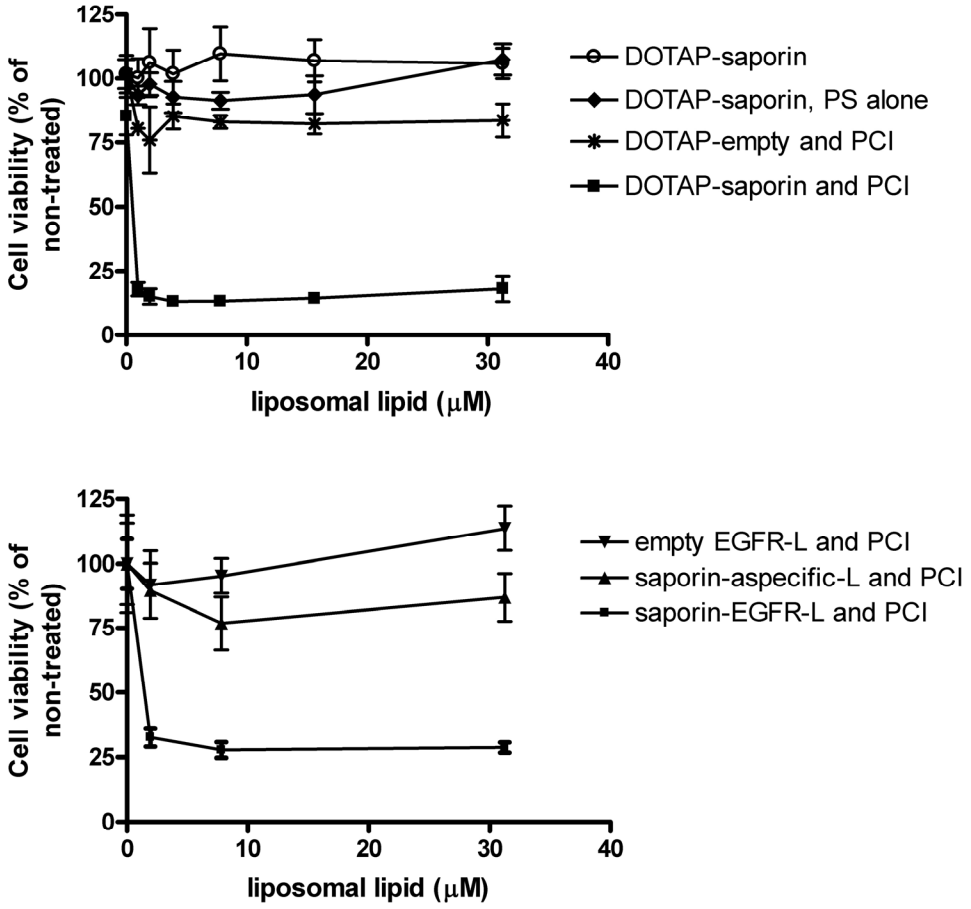

Figure 3. Cytotoxicity after different control treatments. (A) OVCAR-3 cells were incubated with saporin-containing (○, ♦, ■) or empty (✳) DOTAP-L in the presence (♦, ✳, ■) or absence (○) of photosensitiser for 18 hrs, subsequently washed away and incubation was continued for 4 hr before 75 sec illumination (✳, ■). Cell viability was assessed 48 hr after illumination with the XTT assay. (B) OVCAR-3 cells were incubated with saporin-containing (▼, ●) or empty (■) immunoliposomes and photosensitiser for 18 hr, subsequently washed and incubation was continued for 4 hr before 75 sec illumination. Cell viability was assessed 48 hr after illumination with the XTT assay. The liposomes contained either an antibody targeting the EGFR (■,▼) or an aspecific antibody (●). Data represents mean ± SD (n=4). Error bars are within plot symbols when not visible.

Analogous control experiments using of saporin-containing EGFR-L showed similar results (data not shown).

Figure 3B shows that saporin-liposomes with an irrelevant isotype control antibody in combination with PCI did not decrease the cell viability. This result demonstrates that the active targeting of the liposomes using an anti-EGF-receptor antibody is an essential requirement for these liposomes to deliver saporin to the cytosol in combination with PCI. In addition, empty EGFR-L in combination with PCI did not cause any cytotoxicity indicating that the cytotoxicity of saporin containing EGFR-L with PCI is not caused by an EGF-receptor mediated cell death cascade.

Effect of illumination time

As illumination time may play a critical role, its effect on the cytotoxic properties of saporin-liposomes in combination with PCI was assessed. The effect of the illumination time on cytotoxicity is shown in Figure 4. A general trend can be observed: the longer the illumination time, the stronger the cytotoxic effect. This observation corresponds to observations done by others using PCI in combination with the plant toxin gelonin (21, 23). Routinely, we used 75 sec as illumination time in our experiments.

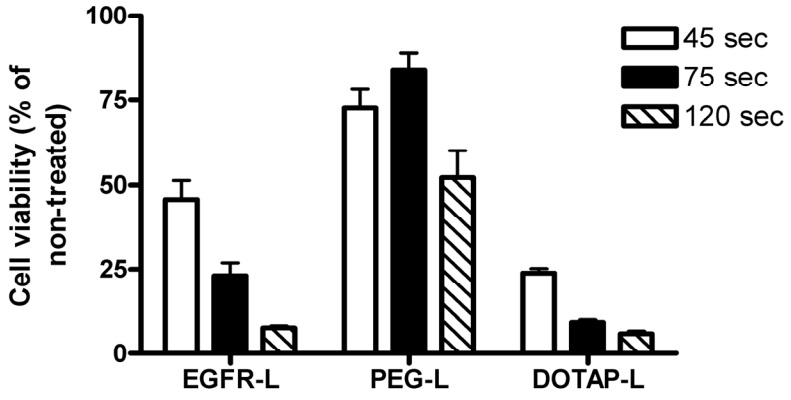

Figure 4. Effect of illumination time on cytotoxicity after treatment with saporin-liposomes with PCI. OVCAR-3 cells were incubated with 0.1 μM saporin-containing liposomes and 0.5 μg/ml photosensitiser for 18 hrs, subsequently washed away and incubation was continued for 4 hrs before the onset of illumination (45, 75 or 120 sec). 48 hrs after illumination, the cell viability was assessed with the XTT assay. Data represents mean ± SD (n=4). Statistical analysis was performed using an F-test. Data is significantly different ($P < 0.05$).

Contribution of PDT to cytotoxicity

Photodynamic therapy (PDT) is a treatment that uses photosensitising agents to kill tumour cells. Like in PCI, reactive oxygen species are generated upon illumination of the photosensitiser which damage cellular organelles like mitochondria with cell death as an end result. Besides damage to tumour cells, tumour associated vasculature can be damaged. Furthermore, an immune response against tumour cells can be induced leading to indirect tumour cell death (30, 31). To address the question to which extent cell death is caused by the photosensitiser and illumination alone (i.e., a PDT effect) and to which extent by the release of saporin from the endosomes induced by the photosensitiser and illumination (i.e., PCI), the relative contribution of a PDT effect on the observed cytotoxicity was studied (Figure 5).

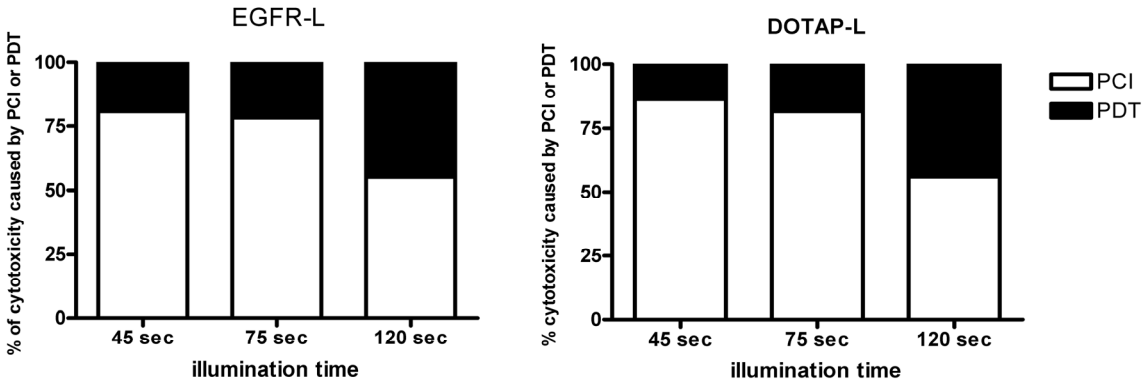

Figure 5. Relative contribution of PDT and PCI to cytotoxicity. OVCAR-3 cells were incubated with 0.1 µM saporin-containing liposomes and 0.5 µg/ml photosensitiser for 18 hr, subsequently washed away and incubation was continued for 4 hr before the onset of illumination (45, 75 or 120 sec). 48 hr after illumination, the cell viability was assessed with the XTT assay. PDT effect was calculated as percentage cytotoxicity caused by photosensitiser and illumination treatment alone. The cytotoxicity caused by PCI was calculated by subtraction the PDT attribution from the total cytotoxicity. Data represents mean ± SD (n=4)

The graphs show that the PDT effect is approximately 20% for the shorter illumination times (45 or 75 sec). On prolonged illumination (120 sec) the PDT contribution to cell death is increased to almost 50%.

The total cell viability decreases upon longer incubation (Figure 4), which is mainly caused by the more pronounced PDT effect at longer illumination times. Thus, efficient PCI is already achieved at the shorter illumination times, without considerable PDT effect. Upon prolonged illumination, PDT effects become more prominent. Obviously, the occurrence of an additional PDT effect in cancer treatment is beneficial as it will strengthen the PCI-mediated anti-tumour effect.

Effect of amount of encapsulated saporin

To investigate whether the amount of encapsulated protein in the liposomes influences the PCI-promoted cytotoxicity, liposomes were prepared containing different amounts of saporin. The results presented in Figure 6 indeed show that liposomes prepared by hydrating the lipid film either in 0.1 or 0.5 mg/ml saporin, do differ substantially in cytotoxic effect when combined with PCI up to a liposomal lipid concentration of 0.5 μM. Above this concentration similar cytotoxicity was observed.

The estimated EC50 values are 0.11 and 0.005 μM for the low and high saporin-containing liposomes, respectively. These results indicate that both the amount of encapsulated toxin and liposomal lipid dose are important determinants of PCI-promoted cytotoxicity.

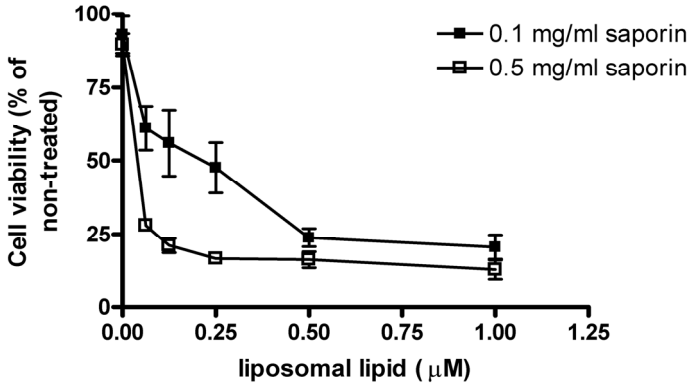

Figure 6. Effect of encapsulated amount of saporin. OVCAR-3 cells were incubated with DOTAP-L, which were prepared with a hydration medium containing 0.1 (■) or 0.5 (□) mg/ml saporin in the presence of photosensitiser for 18 hrs, washed away and incubation continued for 4hrs before the onset of the 75 sec illumination. Cell viability was assessed 48 hrs after illumination. Data represent mean ± SD (n=4). Error bars are within plot symbols when not visible. Statistical analysis was performed using an F-test. Curved are significantly different ($P < 0.01$).

CONCLUSION

In conclusion, this study demonstrates that PCI is a useful tool to enhance the cytosolic delivery of liposomally encapsulated proteins. By encapsulating saporin in positively charged liposomes (DOTAP-L) or EGFR-targeted PEG-liposomes (EGFR-L), the cytosolic delivery of saporin to OVCAR-3 cells and resulting cytotoxicity was strongly enhanced. The use of targeted liposomes (targeting mediated by cationic charge or targeting ligand) appears essential, as the cytotoxicity of saporin in non-targeted PEG-L was not enhanced when compared to free saporin in combination with PCI. Increasing the illumination time decreases the cell viability, which is probably caused by an additional cytotoxic PDT effect. We conclude that PCI is a promising technique for promoting cytosolic delivery of liposomally targeted proteins. In addition to proteins, also other macromolecules like nucleic acids are expected to benefit from this liposomal intracellular targeting approach. Fortunately, although this paper is based on in vitro experimentation, the translation to the in vivo situation is considerable favoured by the recent developments in fibre optics and laser technology which have made it possible to illuminate many sites in the human body.

ACKNOWLEDGEMENTS

The authors would like to thank the Norwegian Research Foundation for financial support. Dr. Raymond M. Schiffelers is kindly acknowledged for his help with the statistical analysis of the data.

REFERENCES

1. A. A. Gabizon, H. Shmeeda and S. Zalipsky. Pros and cons of the liposome platform in cancer drug targeting. *J Liposome Res.* **16:** 175-183 (2006)
2. J. M. Metselaar, E. Mastrobattista and G. Storm. Liposomes for intravenous drug targeting: design and applications. *Mini Rev Med Chem.* **2:** 319-329 (2002)
3. R. M. Straubinger, K. Hong, D. S. Friend and D. Papahadjopoulos. Endocytosis of liposomes and intracellular fate of encapsulated molecules: encounter with a low pH compartment after internalisation in coated vesicles. *Cell.* **32:** 1069-1079 (1983)
4. J. Huwyler, J. Yang and W. M. Pardridge. Receptor mediated delivery of daunomycin using immunoliposomes: pharmacokinetics and tissue distribution in rats. *J Phamacol Exp Ther.* **282:** 1541-1546 (1997)
5. S. Simoes, J. N. Moreira, C. Fonseca, N. Duzgunes and M. C. de Lima. On the formulation of pH-sensitive liposomes with long circulation times. *Adv Drug Deliv Rev.* **56:** 947-65 (2004)
6. C. J. Provoda, E. M. Stier and K. D. Lee. Tumor cell killing enabled by listeriolysin O-liposome-mediated delivery of the protein toxin gelonin. *J Biol Chem.* (2003)
7. M. Mandal and K. D. Lee. Listeriolysin O-liposome-mediated cytosolic delivery of macromolecule antigen in vivo: enhancement of antigen-specific cytotoxic T lymphocyte frequency, activity, and tumor protection. *Biochim Biophys Acta.* **1563:** 7-17 (2002)
8. E. M. Stier, M. Mandal and K. D. Lee. Differential cytosolic delivery and presentation of antigen by listeriolysin O-liposomes to macrophages and dendritic cells. *Mol Pharm.* **2:** 74-82 (2005)
9. E. Mastrobattista, G. A. Koning, L. Van Bloois, A. C. Filipe, W. Jiskoot and G. Storm. Functional Characterization of an Endosome-disruptive Peptide and Its Application in Cytosolic Delivery of Immunoliposome-entrapped Proteins. *J Biol Chem.* **277:** 27135-43 (2002)
10. T. Kakudo, S. Chaki, S. Futaki, I. Nakase, K. Akaji, T. Kawakami, K. Maruyama, H. Kamiya and H. Harashima. Transferrin-modified liposomes equipped with a pH-sensitive fusogenic peptide: an artificial viral-like delivery system. *Biochemistry.* **43:** 5618-28 (2004)
11. A. Hogset, L. Prasmickaite, P. K. Selbo, M. Hellum, B. O. Engesaeter, A. Bonsted and K. Berg. Photochemical internalisation in drug and gene delivery. *Adv Drug Deliv Rev.* **56:** 95-115 (2004)
12. K. Berg and J. Moan. Lysosomes as photochemical target. *Int J Cancer.* **59:** 814-822 (1994)
13. F. Stirpe. Ribosome-inactivating proteins. *Toxicon.* **44:** 371-83 (2004)
14. G. A. Koning, H. W. Morselt, M. J. Velinova, J. Donga, A. Gorter, T. M. Allen, S. Zalipsky, J. A. Kamps and G. L. Scherphof. Selective transfer of a lipophilic prodrug of 5-fluorodeoxyuridine from immunoliposomes to colon cancer cells. *Biochim Biophys Acta.* **1420:** 153-67 (1999)
15. G. Rouser, S. Fkeischer and A. Yamamoto. Two dimensional then layer chromatographic separation of polar lipids and determination of phospholipids by phosphorus analysis of spots. *Lipids.* **5:** 494-6 (1970)
16. D. A. Scudiero, R. H. Shoemaker, K. D. Paull, A. Monks, S. Tierney, T. H. Nofziger, M. J. Currens, D. Seniff and M. R. Boyd. Evaluation of a soluble tetrazolium/formazan assay for cell growth and drug sensitivity in culture using human and other tumor cell lines. *Cancer Res.* **48:** 4827-33 (1988)
17. C. Arigita, L. Bevaart, L. A. Everse, G. A. Koning, W. E. Hennink, J. C. Van de Winkel, M. J. Van Vught, G. F. Kersten and W. Jiskoot. Liposomal meningococcal B vaccination: role of dendritic cell targeting in development of a protective immune response. *Infect Immun.* **71:** 5210-5218 (2003)
18. D. E. Davies and S. G. Chamberlin. Targeting the epidermal growth factor receptor for therapy of carcinomas. *Biochem Pharmacol.* **55:** 1101-1110 (1996)
19. M. M. Fretz, G. A. Koning, E. Mastrobattista, W. Jiskoot and G. Storm. OVCAR-3 cells internalize TAT-peptide modified liposomes by endocytosis. *Biochim Biophys Acta.* **1665:** 48-56 (2004)
20. E. Mastrobattista, G. A. Koning and G. Storm. Immunoliposomes for the targeted delivery of antitumor drugs. *Adv Drug Deliv Rev.* **40:** 103-127 (1999)
21. P. K. Selbo, K. Sandvig, V. Kirveliene and K. Berg. Release of gelonin from endosomes and lysosomes to cytosol by photochemical internalisation. *Biochim Biophys Acta.* **1475:** 307-13 (2000)
22. K. Berg, A. Dietze, O. Kaalhus and A. Hogset. Site-specific drug delivery by photochemical internalisation enhances the antitumor effect of bleomycin. *Clin Cancer Res.* **11:** 8476-85 (2005)
23. K. Berg, P. K. Selbo, L. Prasmickaite, T. E. Tjelle, K. Sandvig, J. Moan, G. Gaudernack, O. Fodstad, S. Kjolsrud, H. Anholt, G. H. Rodal, S. K. Rodal and A. Hogset. Photochemical internalisation: a novel technology for delivery of macromolecules into cytosol. *Cancer Res.* **59:** 1180-3 (1999)

24. P. K. Selbo, G. Sivam, O. Fodstad, K. Sandvig and K. Berg. Photochemical internalisation increases the cytotoxic effect of the immunotoxin MOC31-gelonin. *Int J Cancer.* **87:** 853-9 (2000)
25. A. Weyergang, P. K. Selbo and K. Berg. Photochemically stimulated drug delivery increases the cytotoxicity and specificity of EGF-saporin. *J Control Release.* **111:** 165-173 (2006)
26. M. Folini, K. Berg, E. Millo, R. Villa, L. Prasmickaite, M. G. Daidone, U. Benatti and N. Zaffaroni. Photochemical internalisation of a peptide nucleic acid targeting the catalytic subunit of human telomerase. *Cancer Res.* **63:** 3490-4 (2003)
27. L. Prasmickaite, A. Hogset, V. M. Olsen, O. Kaalhus, S. O. Mikalsen and K. Berg. Photochemically enhanced gene transfection increases the cytotoxicity of the herpes simplex virus thymidine kinase gene combined with ganciclovir. *Cancer Gene Ther.* **11:** 514-23 (2004)
28. A. Hogset, L. Prasmickaite, M. Hellum, B. O. Engesaeter, V. M. Olsen, T. E. Tjelle, C. J. Wheeler and K. Berg. Photochemical transfection: a technology for efficient light-directed gene delivery. *Somat Cell Mol Genet.* **27:** 97-113 (2002)
29. B. O. Engesaeter, A. Bonsted, K. Berg, A. Hogset, O. Engebraten, O. Fodstad, D. T. Curiel and G. M. Maelandsmo. PCI-enhanced adenoviral transduction employs the known uptake mechanism of adenoviral particles. *Cancer Gene Ther.* **12:** 439-48 (2005)
30. S. B. Brown, E. A. Brown and I. Walker. The present and future role of photodynamic therapy in cancer treatment. *The lancet oncology.* **5:** 497-508 (2004)
31. D. E. J. G. J. Dolmans, F. D and R. K. Jain. Photodynamic therapy for cancer. *Nat Rev Cancer.* **3:** 380-387 (2003)

7

Targeted liposomes for boron neutron capture therapy (BNCT): importance of target receptor density

Marjan M. Fretz, Gerard C. Krijger, Ula Woroniecka, Sander A. Nievaart, Wim Jiskoot, Raymond Moss,Gerben A. Koning and Gert Storm

Manuscript in preparation

ABSTRACT

Targeted liposomes are promising candidates as drug delivery vehicles for Boron Neutron Capture Therapy (BNCT). Their capacity to encapsulate high amounts of boron-compounds is a major advantage, since the effectiveness of BNCT is dependent on the tumour-specific delivery of a relatively large number of Boron-10 atoms. The epidermal growth factor receptor (EGFR) is an attractive target receptor, since many tumours overexpress this receptor. This study investigates EGFR-targeted liposomes containing a hydrophilic boronated compound for BNCT. These EGFR-targeted liposomes were compared to non-targeted PEG-L using two tumour cell lines, A431 and OVCAR-3. The results demonstrate that OVCAR-3 cells, which showed only a low level of EGFR expression, do not or hardly bind EGFR-targeted liposomes. Differences in binding and uptake of targeted versus non-targeted liposomes were much more pronounced when A431 cells were used, which was in good agreement with the relatively high level of EGFR expression in case of A431 cells. Accordingly, the BNCT effect mediated by EGFR-L proved to be only slightly better than PEG-L in case of OVCAR-3 cells, while the EGFR-L were clearly superior over PEG-L in case of A431 cells. Apparently, the degree of EGFR expression is a major success factor for the use of EGFR-targeted liposomes for BNCT.

INTRODUCTION

Boron neutron capture therapy (BNCT) is based on the delivery of the stable isotope Boron-10 to tumour cells and the production of local radioactivity upon irradiation with a thermal neutron beam. The nuclear reaction is as follows:

$$^{10}B + \text{neutron} \longrightarrow {}^{4}He\ (\alpha\text{-particle}) + {}^{7}Li + 2.31\ MeV$$

Both the resulting α-particles and the Li nuclei are high linear energy transfer (LET) particles contributing to the cytotoxic effect. LET particles have a short range of radiation (approximately 10 μm), which limits the radiation damage to those cells that contain Boron-10. By selective targeting of the boron compounds to the tumour cells, damage to surrounding tissue will be limited. For more information on BNCT, the reader is referred to (1, 2).

The major challenge for successful BNCT-based therapy lies in the relatively large amount of Boron-10 which needs to be delivered to tumour cells, namely over 15 μg/g tumour tissue (3). Therefore, the tumour selective delivery of boron compounds using a tumour-targeted vehicle is an attractive concept. Several strategies are being explored. Covalent coupling of boron-containing molecules to macromolecular vehicles, like antibodies, dendrimers and dextrans, is addressed in the literature (reviewed in (4)). The use of tumour-targeted liposomes as delivery vehicle for BNCT is also a good option.

Liposomes are vesicles composed of a phospholipid bilayer surrounding an aqueous core. High quantities of hydrophilic compounds can be encapsulated in the aqueous compartment, which is an appealing property for BNCT. Liposomes can be coated with hydrophilic polymers like poly(ethylene)glycol (PEG), which gives them long-circulating properties (5). A long circulation time favours tumour accumulation, enabled by the so-called EPR (enhanced permeability and retention) effect. Tumour vasculature is often 'leaky' and nanoparticles like liposomes can extravasate from the bloodstream into tumour tissue provided that they circulate for a prolonged period of time (passive targeting) (6). In addition to this passive targeting effect, coupling of targeting moieties, like antibodies and other receptor ligands to the surface of liposomes may improve the selective targeting to tumour cells and promote tumour cell uptake. Because of these properties, liposomes have been studied as BNCT delivery vehicles and promising results have been reported (7-12).

The epidermal growth factor receptor (EGFR) is overexpressed on a variety of tumours cells and is generally considered as a rational target for drug delivery (13, 14). The EGFR has already been studied as target for boron-containing liposomes (9, 10, 15) and boronated dendrimer-EGF bioconjugates (16-18), but value for BNCT has only been demonstrated at the level of targeting and not at the level of therapeutic efficacy.

Although the expression of the EGFR is enhanced in many tumours, the absolute expression levels between different tumour cell types may differ considerably. In this study, we

compared two different tumour cell lines (OVCAR-3 and A431) expressing the EGFR to a different extent and studied the binding, uptake, cellular retention and intracellular distribution of boron-loaded EGFR-targeted and PEG-liposomes. Furthermore, we compared the two cells lines with regard to their response to BNCT using boron-loaded EGFR-targeted liposomes.

EXPERIMENTAL METHODS

Materials

Dipalmitoylphosphatidylcholine (DPPC) and 1,2-distearoyl-glycero-3-phosphoethanolamine-*N*-[poly(ethylene glycol)2000] (PEG_{2000}-DSPE) were obtained from Lipoid GmbH (Ludwigshafen, Germany). Maleimide-PEG_{2000}-DSPE was obtained from Shearwater Polymers (Huntsville, AL, USA). Cholesterol (CHOL) and *N*-succinimidyl-*S*-acetylthioacetate (SATA) were from Sigma-Aldrich Co. (St.Louis, MO, USA). Lissamine rhodamine B-labeled glycerophosphoethanolamine (Rho-PE) was purchased from Avanti Lipids Inc. (Alabaster, AL, USA). Murine mAb425 of isotype IgG2b directed against the human epidermal growth factor receptor (EGFR) was kindly donated by Merck KgA (Darmstadt, Germany). Dodecahydrododecaborate sodium salt ($Na_2[B_{12}H_{12}]$, Boron-10 enriched; abbreviated as DHDB) was supplied by Katchem (Prague, Czech Republic). EGF-Alexa488 and Texas Red-1,2-dihexadecanoyl-*sn*-glycero-3-phosphoethanolamine, triethylammonium salt (TxR-PE) was purchased from Molecular Probes Europe BV (Leiden, The Netherlands).
All other reagents were commercially available reagents of at least analytical grade.

Liposome preparation and characterisation

For the preparation of liposomes, a lipid film was prepared from a mixture of DPPC, CHOL, PEG_{2000}-DSPE, maleimide-PEG_{2000}-DSPE (1.85:1:0.09:0.06 molar ratio) in absolute ethanol by solvent evaporation. The fluorescent labels Rho-PE or TxR-PE were incorporated in the lipid bilayer at 0.1 mol% for confocal microscopy and flow cytometry analysis, respectively. Before hydration, the lipid film was flushed with nitrogen for at least 30 minutes. Liposomes (50 μmol) were formed by hydration of the lipid film with 1ml of a solution containing 30 mg/ml DHDB in HEPES buffer (10 mM, pH 7.5). The lipid dispersion was sequentially extruded through polycarbonate membrane filters (Osmonic, Livermore CA, USA) with pore sizes varying from 0.05 μm to 0.65 μm using Lipex high-pressure extrusion equipment (Northern Lipids, Vancouver, Canada). The non-encapsulated DHDB was removed by ultracentrifugation (1 hr, 60,000 rpm, 4°C) and the liposome pellet was resuspended in HEPES buffered saline (HBS; 10 mM HEPES, 137 mM NaCl, pH 6.5).
For liposomes targeting the EGF-receptor, the monoclonal antibody mAb425 was coupled to the maleimide groups at the distal end of PEG essentially as described by Koning *et al*. (19). Briefly, free sulfhydryl groups were introduced in the antibody by modifying the mAb425 with an 8-fold molar excess of SATA for 45 minutes. Unconjugated SATA was removed by centrifugation (5500 rpm, 15 minutes, 4°C) using a Vivaspin concentrator (MWCO 30,000 Da) (Depex, Houten, The Netherlands). Directly before conjugation to the liposomes, the SATA groups were deacetylated to obtain free sulfhydryl groups by adding a hydroxylamine solution (0.5 M HEPES, 0.5 M hydroxylamine-HCl and 0.25 mM EDTA of

pH 7.0). One micromole of liposomes was incubated with 30 μg of antibody overnight at 4°C. Gel permeation chromatography using Sepharose CL-4B (Amersham Pharmacia Biotech, Uppsala, Sweden) was used to separate non-coupled antibody from the liposomes.
The phospholipid concentration of the liposome formulations was determined by the colorimetric method of Rouser *et al.* (20). Mean particle size and size distribution were determined by dynamic light scattering with a Malvern 4700 system (Malvern Ltd., Malvern, UK). The amount of encapsulated boron was determined by inductively coupled plasma-optical emission spectroscopy (ICP-OES) using a Perkin-Elmer 4300 Dual View ICP-OES spectrometer. Before analysis, liposome samples were diluted up to 1000 fold in water containing 1 % (w/v) Triton X-100.

Cell culture

The human ovarian carcinoma cell line NIH:OVCAR-3 and the human epidermoid carcinoma cell line A431 were obtained from the ATCC (Manassas, USA). The cells were cultured in complete media which consists of Dulbecco's modified Eagle's medium containing 3.7 g/l sodium bicarbonate, 4.5 g/l L-glucose and supplemented with L-glutamine (2 mM), penicillin (100 IU/ml), streptomycin (100 μg/ml) and amphotericin B (0.25 μg/ml). For the culturing of OVCAR-3 cells the medium was supplemented with 10% heat-inactivated foetal calf serum (FCS) whereas for A431 7.5% FCS was used. Culture conditions were 37°C with 5% CO_2 in humidified air. All cell-culture related materials were obtained from Gibco (Grand Island, NY, USA).

Flow cytometry analysis

For flow cytometry analysis, 10^5 OVCAR-3 or A431 cells in a volume of 500 μl were incubated with complete media containing EGF-Alexa488, final concentrations varying from 5 to 1000 ng/ml or with complete media containing fluorescently labeled liposomes (PEG-L or EGFR-L) with final concentrations varying from 25 to 500 nmol/ml total lipid. After 1 hr incubation at 4°C, cells were washed 3 times with PBS by centrifugation and resuspended in 300 μl PBS. Flow cytometry analysis was done by a FACScalibur (Beckton&Dickinson, Mountain View, CA, USA) and data were analysed using WinMDI 2.8 software, which was kindly provided by Joseph Trutter.

Cell-associated liposomal boron

OVCAR-3 and A431 cells were seeded (2 x 10^5 cells/well) into a 6-well plate in compete media and grown until 80% confluency. DHDB-containing liposomes, both PEG-L and EGFR-L were added at various concentrations in complete media and after 1 hr incubation at 4°C, the cells were washed 2 times with ice-cold PBS. To lyse the cells a 1% (w/v) Triton X-100 solution in water was added and the cell lysates were frozen at -20°C until analysis.

The cell lysate was analysed for boron content using ICP-OES and total protein content using a Pierce BCA protein assay (Pierce, Rockford, IL, USA).

Cellular uptake and retention of liposomal boron

OVCAR-3 and A431 cells were seeded (2 x 10^5 cells/well) into a 6-well plate in complete media and grown until 80% confluency. For uptake studies, cells were incubated with PEG-L and EGFR-L containing in total 15 μg Boron-10 in complete media for different times at 37°C. For retention studies, cells were incubated with PEG-L and EGFR-L containing in total 15 μg Boron-10 in complete media for 4 hr, cells were washed and subsequently incubated for various times in complete culture media at 37°C. Cell lysis before analysis by ICP-OES was identical to the procedure described in the previous section.

Intracellular localisation of boron-containing liposomes

OVCAR-3 and A431 cells were seeded (1 x 10^4 cells/well) onto 16-well chamber slides in complete media and cultured overnight. The cells were incubated with 500 μM Rho-PE labeled PEG-L or EGFR-L containing DHDB in complete media for 24 hrs. Cells were washed twice with PBS, fixed with 4% paraformaldehyde and mounted with FluorSave (CalbioChem, San Diego, CA, USA). The samples were visualised with a Leica TCS-SP confocal laser scanning microscope. Laser power and settings for detection were kept identical to ensure appropriate comparison of the results.

In vitro BNCT efficacy

OVCAR-3 and A431 cells were seeded (5 x 10^3 cells/well) into 96-wells plates in complete media and cultured overnight. The cells were incubated with different concentrations of DHDB-containing PEG-L or EGFR-L for 24 hrs. To prevent scattering of the thermal neutrons, autoclaved reversed osmosis water was added in the space between the wells. The cells were transported on ice in HEPES (final concentration 10 mM) buffered complete culture media to the High Flux Reactor in Petten (The Netherlands) and irradiated for 1 hr with 1 x 10^9 epithermal (neutron energy 0.025 - 1 eV) neutrons/cm^2/sec at room temperature. After transportation on ice, the cell culture medium was replaced and the cells were subsequently cultured for 48 hrs before the cell viability was assessed by using the XTT assay (21).

RESULTS

Liposome characteristics

As already described before by Krijger *et al.*, we were able to efficiently encapsulate the hydrophilic Boron-10 enriched compound dodecahydrododecaborate (DHDB) into PEG-liposomes. These liposomes are stable for over two weeks time with respect to size and encapsulated boron (22). The liposomes were sized to 100-120 nm and had a low polydispersity index (≤ 0.25), which is a measure for the size distribution and varies from 0 (absolutely monodisperse) to 1 (extremely polydisperse). We were able to encapsulate up to 30 µg boron per µmol lipid as determined with ICP-OES, which corresponds to an encapsulation efficiency of about 5%. This is in good agreement with the expected aqueous volume present within this type of liposomes.

Flow cytometry

It is well known that the epidermal growth factor receptor (EGFR) is upregulated on the surface of certain tumour cell types. Using flow cytometry, the extent of binding of the natural ligand EGF labeled with the fluorochrome Alexa488 to both OVCAR-3 and A431 cells was measured. Figure 1A shows that after incubation for 1 hr at 4°C the binding of EGF-Alexa488 to OVCAR-3 cells was much lower when compared to A431 cells. The difference in degree of binding varies from a factor 15 to 65 depending on the concentration EGF added to the cells. This implies a strong difference in receptor expression level and confirmed western blot data (Sabrina Oliveira, Utrecht University, personal communication).

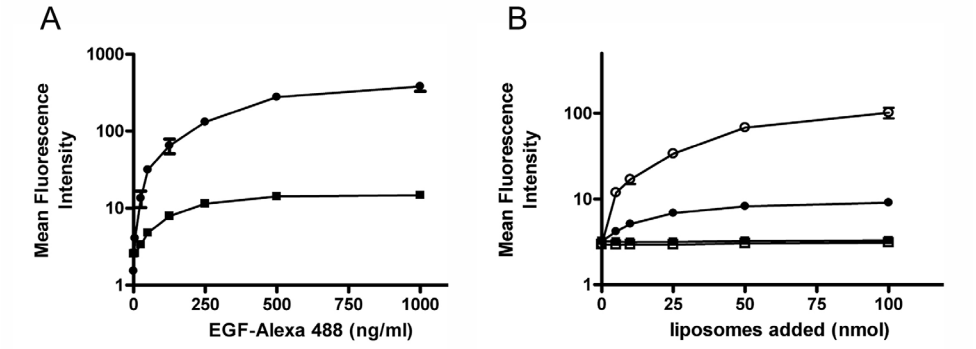

Figure 1. Binding of EGF-Alexa488 (A) or liposomes (B) to OVCAR-3 and A431 cells. (A) Different concentrations of EGF-Alexa488 were incubated with OVCAR-3 (■) or A431 (●) cells for 1 hr at 4ºC. The cells were washed and analyzed with flow cytometry. (B) Different concentrations of fluorescently labelled EGFR-L (● and ○) or PEG-L (■ and □) were incubated with OVCAR-3 cells (closed symbols) or A431 cells (closed symbols). Data represent mean ± SD (n=3). Error bars are within plot symbols when not visible.

The degree of cell binding of fluorescently labeled PEG-liposomes (PEG-L) and EGFR-targeted liposomes (EGFR-L) to both cell types was investigated. Different amounts of PEG-L and EGFR-L were incubated with both cell types for 1 hr at 4°C. As shown in Figure 1B, the extent of binding of the targeted, but not of the untargeted liposomes differs between the cell lines. The EGFR-L bound more extensively to A431 cells than to OVCAR-3 cells, which is in line with the EGF binding results seen in Figure 1A. PEG-L did not show significant interaction with either cell line, confirming that binding is mediated by specific interaction between the anti-EGFR antibody and the EGFR. Specific binding of EGFR-L to OVCAR-3 cells has been shown in previous studies of our group (23).

Cell-associated liposomal boron

To investigate the extent of cellular binding of the two types of liposomes with respect to the amount of boron associated with the cells, OVCAR-3 and A431 cells were incubated for 1 hr at 4°C with both boron-loaded liposome types. After washing, the cells were lysed using a detergent and the amount of boron was measured and expressed relative to the cellular protein content (Figure 2).

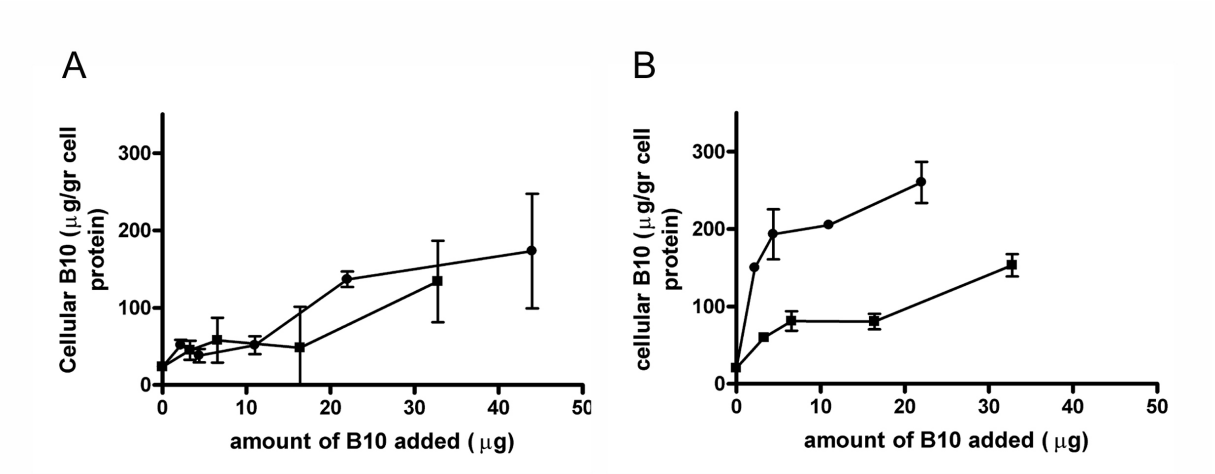

Figure 2. Liposomal boron: Cellular association at 4°C. OVCAR-3 (A) or A431 (B) cells were incubated with different concentrations of boron-loaded EGFR-L (●) or PEG-L (■) for 1 hr at 4ºC. The cells were washed, lysed and cellular boron and protein content were determined. Data represent mean ± SD (n=3). Error bars are within plot symbols when not visible.

Despite the difference in cell binding (Figure 1B), no significant difference in the amount of OVCAR-3 cell-bound boron between PEG-L and EGFR-L incubations could be seen (Figure 2A). The amount of cell-associated boron increased for both PEG-L and EGFR-L to a similar extent with increasing amounts of added liposomal boron. This is in opposite to the results found with A431 cells; here the cell-bound boron was significantly higher when the cells were incubated with EGFR-L compared to PEG-L (Figure 2B). When cells, either OVCAR-3 or A431 are incubated with free DHDB, no binding (or uptake) of boron could be detected compared to non-treated cells (data not shown).

Cellular uptake and retention of liposomal boron

OVCAR-3 and A431 cells were incubated for varying times with 15 µg boron/ml encapsulated in PEG-L and EGFR-L at 37°C. For successful BNCT over 15 µg Boron-10/g tumour is necessary. This requirement is met by both PEG-L and EGFR-L in both cell lines (Figure 3), clearly illustrating the value of liposomal delivery of boron to tumour cells.

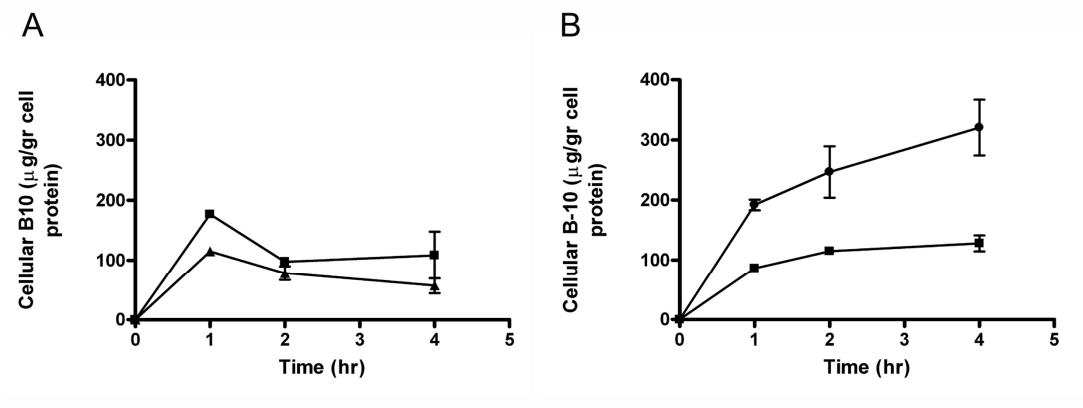

Figure 3. Liposomal boron: Cellular association at 37°C. OVCAR-3 (A) or A431 (B) cells were incubated with boron-loaded EGFR-L (●) or PEG-L (■) for varying times at 37ºC. The cells were washed, lysed and cellular boron and protein content were determined. Data represent mean ± SD (n=3). Error bars are within plot symbols when not visible.

However, no apparent difference over time was observed between EGFR-L and PEG-L in case of OVCAR-3 cells (Figure 3A). These results are opposite to those obtained with A431 cells, where EGFR-L are taken up to a much larger extent: using EGFR-L up to 2.5 times more boron is present in the A431 cells compared to A431 incubated with PEG-L (Figure 3B).

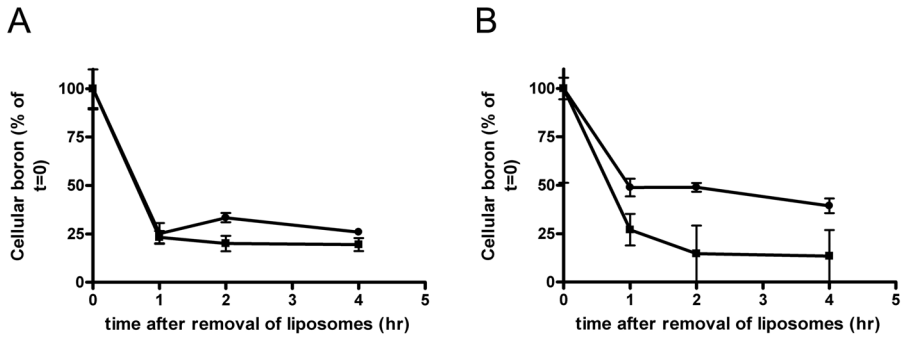

Figure 4. Liposomal boron: Cellular retention. OVCAR-3 (A) and A431 (B) cells were incubated with boron-loaded EGFR-L (●) or PEG-L (■) for 4 hr at 37ºC. The cells were subsequent incubated for various times in liposome-free complete culture medium. The cells were washed, lysed and cellular boron and protein content were determined. Data represent mean ± SD (n=3). Error bars are within plot symbols when not visible.

The cellular retention of liposomal boron was measured by incubating the cells for 4 hr with liposomes, followed by incubation of the treated cells in liposome-free media for various times. As shown in Figure 4, already 1 hr after the removal of the liposomes, 50% or more of the initially cellular boron did not remain cell-associated. In case of OVCAR-3 cells, the rate and extent of cellular loss of boron was similar for both EGFR-L and PEG-L, while A431 cells retain boron to a higher extent when exposed to EGFR-L.

Intracellular distribution of boron-containing liposomes

For effective BNCT, the intracellular localisation of the boron atoms is important. The therapeutic efficacy increases when the boron atoms are present in close proximity of the nucleus (24). With confocal laser scanning microscopy, the subcellular distribution of the fluorescently labeled liposomes within the two cell types was visualised (Figure 5 A-D). Both PEG-L and EGFR-L, showed a vesicular intracellular distribution pattern with accumulation of the liposomes in the perinuclear region. With the photomultiplier settings (detection level) used here, no fluorescence was detectable in non-treated cells (data not shown). The intensity of the fluorescence seen in OVCAR-3 cells with both PEG-L and EGFR-L was similar (Figure 5 A and B), whereas in the case of A431 cells the fluorescence signal was much higher for the cells incubated with EGFR-L (Figure 5C) compared to PEG-L (Figure 5D). The vesicular labeling pattern points to presence of the liposomes in endosomes and lysosomes. Endocytic uptake of liposomes is already reported and generally accepted as main cellular uptake mechanism for both targeted and non-targeted liposomes (25, 26).

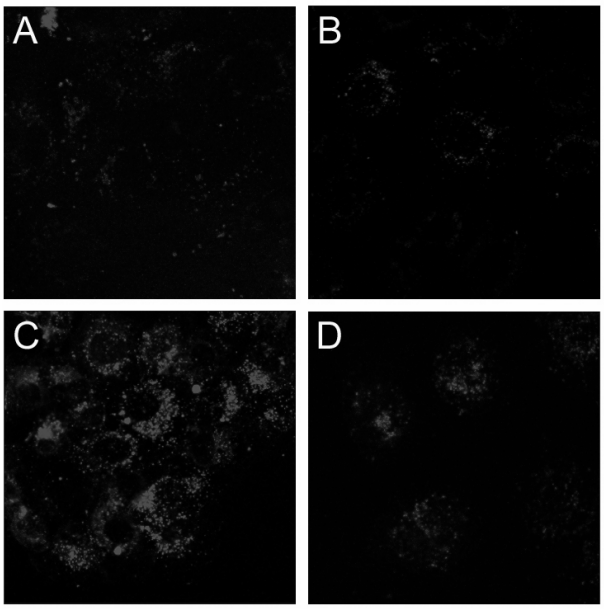

Figure 5. Intracellular distribution of liposomes. OVCAR-3 (A and B) or A431 (C and D) were incubated with fluorescently labeled EGFR-L (A and C) and PEG-L (B and D) for 24 hr at 37ºC. The cells were washed, fixed and analysed with confocal microscopy.

In vitro efficacy of BNCT

To demonstrate the possible tumour cell-killing effect of liposomal Boron-10, OVCAR-3 and A431 cells were incubated with different concentrations of boron- containing PEG-L and EGFR-L and radiated with thermal neutrons to form the cytotoxic α-particles. The cytotoxic effect was measured 48 hr after the radiation process by assessing the cell viability (Figure 6).

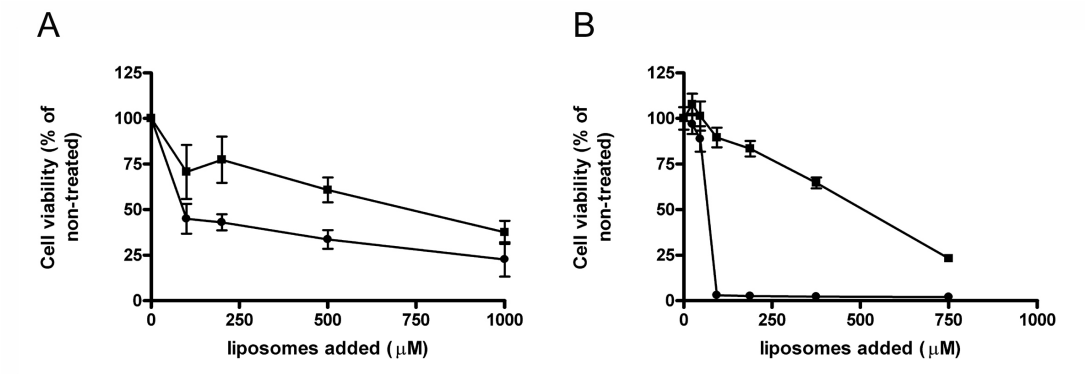

Figure 6. Cell viability after BNCT with liposomes. OVCAR-3 (A) or A431 (B) cells were incubated with boron-loaded EGFR-L (●) or PEG-L (■) for 24 hr and subsequently treated with 1 hr of neutron radiation. The cell viability was assessed 48 hr after irradiation with XTT assay. Data represent mean ± SD (n=3). Error bars are within plot symbols when not visible

With both cell types, EGFR-L were more cytotoxic than PEG-L. However, the superiority of EGFR-L over PEG-L was by far much stronger in case of A431 cells, which is in line with the increased cellular delivery and retention of boron in this case.

DISCUSSION

Since the EGFR is overexpressed by many tumour cell types, the EGFR has been exploited previously to target drugs and delivery vehicles to tumour cells (13, 14). EGFR-targeted conjugates have been synthesised and evaluated for BNCT (9, 10, 15-18, 27, 28). Preparation of conjugates between boron and EGF or anti-EGFR-antibodies have been described (27, 28). The disadvantage of this approach is that only a small number of boron molecules can be attached, as with higher amounts coupled the specificity of the targeting ligand is lost (29). Drug delivery vehicles that are able to carry relatively large numbers of boron atoms are therefore favourable. Boronated dendrimers and liposomes targeted to the EGFR have been described (9, 10, 15-18). Although targeting to EGFR-expressing cells has been achieved, the effects of the level of receptor expression on the degree of targeting and BNCT mediated cytotoxicity have not been addressed so far. This issue is important, as the absolute level of EGFR expression will vary between different tumour types and even within one tumour the expression can be heterogeneous (30).

In this chapter, the effect of targeting liposomes to the EGFR for BNCT was compared using two human carcinoma cell lines, human epidermoid carcinoma A431 and human ovarian carcinoma OVCAR-3. Both cell lines are considered EGFR-positive (31, 32), but no comparison has been made between the two cell lines with respect to the level of EGFR expression. Using flow cytometry, a minor but significant increase in binding was observed when OVCAR-3 cells were incubated with EGFR-L compared with the binding of PEG-L to OVCAR-3 cells. The binding of PEG-L to A431 cells was comparable to that of OVCAR-3 cells, but EGFR-L were bound to a much higher extent (Figure 1B). Taking into account that the EGF-Alexa488 was also bound to a higher extent to A431 cells than to OVCAR-3 cells (Figure 1A), the differences in binding of EGFR-L between both cells lines is likely to be explained by the differences in receptor level expression. Remarkably, when OVCAR-3 cell-associated boron was measured, both binding and uptake of the liposomes were not significantly enhanced in case of EGFR-L compared to PEG-L (Figure 2A and 3A). Using A431 cells, which express high levels of EGFR, a substantial increase in both binding and cellular uptake of EGFR-L compared to PEG-L was seen (Figure 2B and 3B).

The cellular retention of liposome encapsulated boron was poor also in the case of A431 cells, but A431 cells clearly retained EGFR-L delivered boron to a higher extent than PEG-L delivered boron. Nevertheless, the poor cellular retention of liposomally delivered boron is a concern for further in vivo application.

To measure therapeutic efficacy, in this study the cytotoxicity after BNCT. No considerable differences between EGFR-L and PEG-L could be seen with OVCAR-3 cells, whereas in A431 the EGFR-L were significantly more effective than PEG-L. The literature also reports on absence of improved efficacy of targeted liposomal formulations related to low EGFR expression levels. Mamot *et al.* showed that EGFR-targeted liposomes mediate uptake and efficient delivery of the encapsulated doxorubicin resulting in cytotoxic effects towards

EGFR-overexpressing cells. In contrast, with cells lacking the expression of EGFR, uptake and cytotoxic effects were comparable to control liposomes devoid of the EGFR-targeting ligand (33). In addition, both in vitro and in vivo data reported by Park and colleagues confirmed the importance of the receptor expression level for the efficacy of a targeted liposome type. They showed that MCF-7 breast cancer cells, which have a relatively low or basal level of expression of the HER2-receptor (~10^4 receptor/cell), do not internalise HER2-targeted immunoliposomes more efficiently than liposomes lacking the targeting ligand. Also, HER-2 targeted liposomal doxorubicin was equally effective in delaying in vivo MCF-7 of tumour growth as control liposomes. This is in contrast to several other cell and xenograft models, which express the HER2 receptor to a larger extent (≥10^5 receptors/cell) and where significant improvement in tumour growth delay was seen when doxorubicin was encapsulated in HER2-targeted liposomes compared to liposomal doxorubicin without targeting ligand. These results point to a minimal threshold of HER2 density to attain therapeutic efficacy (26, 34), which supports our 'threshold hypothesis'.
Recently, liposomes targeting the transferrin receptor, transferrin-PEG-liposomes (Tf-liposomes), were used to target mercaptoundecahydrododecaborate (BSH) to tumour cells in vitro and in vivo. The in vitro targeting effect of Tf-liposomes compared to non-targeted liposomes comprised an approximate 5-fold increase in binding and uptake of boron by tumour cells. In vivo studies showed that significant difference in boron concentration in tumour cells was observed between targeted and non-targeted liposomes, but only at 72 hours after i.v. administration of the BSH-containing liposomes. When the tumours were irradiated with neutrons 72 hr after liposome administration, both PEG-liposomes and Tf-liposomes showed similar tumour-killing capacity, suggesting that the targeting effect was not strong enough to enhance the BNCT mediated cytotoxicity (8).

CONCLUSION

In this study, the use of EGFR-targeted liposomes for BNCT was evaluated in vitro using two tumour cell lines. The two cell types differed significantly regarding the level of EGFR expression. It is demonstrated here that successful BNCT with targeted liposomes is dependent on the target receptor expression level and that a certain threshold expression level is required to achieve successful BNCT.

REFERENCES

1. A. H. Soloway, W. Tjarks, B. A. Barnum, F. G. Rong, R. F. Barth, I. M. Codogni and J. G. Wilson. The Chemistry of Neutron Capture Therapy. *Chem Rev.* **98:** 1515-1562 (1998)
2. R. F. Barth, J. A. Coderre, M. G. Vicente and T. E. Blue. Boron neutron capture therapy of cancer: current status and future prospects. *Clin Cancer Res.* **11:** 3987-4002 (2005)
3. R. F. Barth, A. H. Soloway, R. G. Fairchild and R. M. Brugger. Boron neutron capture therapy for cancer. Realities and prospects. *Cancer.* **70:** 2995-3007 (1992)
4. G. Wu, R. F. Barth, W. Yang, R. J. Lee, W. Tjarks, M. V. Backer and J. M. Backer. Boron containing macromolecules and nanovehicles as delivery agents for neutron capture therapy. *Anticancer Agents Med Chem.* **6:** 167-84 (2006)
5. M. C. Woodle and D. D. Lasic. Sterically stabilized liposomes. *Biochem Biophys Acta.* **1132:** 171-99 (1992)
6. H. Maeda, J. Wu, T. Sawa, Y. Matsumura and K. Hori. Tumor vascular permeability and EPR effect in macromolecular therapeutics: a review. *J Control Release.* **65:** 271-84 (2000)
7. J. Carlsson, E. B. Kullberg, J. Capala, S. Sjoberg, K. Edwards and L. Gedda. Ligand liposomes and boron neutron capture therapy. *J Neurooncol.* **62:** 47-59 (2003)
8. K. Maruyama, O. Ishida, S. Kasaoka, T. Takizawa, N. Utoguchi, A. Shinohara, M. Chiba, H. Kobayashi, M. Eriguchi and H. Yanagie. Intracellular targeting of sodium mercaptoundecahydrododecaborate (BSH) to solid tumors by transferrin-PEG liposomes, for boron neutron-capture therapy (BNCT). *J Control Release.* **98:** 195-207 (2004)
9. E. B. Kullberg, M. Nestor and L. Gedda. Tumor-cell targeted epiderimal growth factor liposomes loaded with boronated acridine: uptake and processing. *Pharm Res.* **20:** 229-36 (2003)
10. E. B. Kullberg, Q. Wei, J. Capala, V. Giusti, P. U. Malmstrom and L. Gedda. EGF-receptor targeted liposomes with boronated acridine: Growth inhibition of cultured glioma cells after neutron irradiation. *Int J Radiat Biol.* **81:** 621-9 (2005)
11. H. Yanagie, H. Kobayashi, Y. Takeda, I. Yoshizaki, Y. Nonaka, S. Naka, A. Nojiri, H. Shinnkawa, Y. Furuya, H. Niwa, K. Ariki, H. Yasuhara and M. Eriguchi. Inhibition of growth of human breast cancer cells in culture by neutron capture using liposomes containing 10B. *Biomed Pharmacother.* **56:** 93-9 (2002)
12. H. Yanagie, K. Maruyama, T. Takizawa, O. Ishida, K. Ogura, T. Matsumoto, Y. Sakurai, T. Kobayashi, A. Shinohara, J. Rant, J. Skvarc, R. Ilic, G. Kuhne, M. Chiba, Y. Furuya, H. Sugiyama, T. Hisa, K. Ono, H. Kobayashi and M. Eriguchi. Application of boron-entrapped stealth liposomes to inhibition of growth of tumour cells in the in vivo boron neutron-capture therapy model. *Biomed Pharmacother.* (2005)
13. S. Oliveira, P. M. Van Bergen en Henegouwen, G. Storm and R. M. Schiffelers. Molecular biology of epidermal growth factor receptor inhibition for cancer therapy. *Expert Opin Biol Ther.* **6:** 498-543 (2006)
14. J. Mendelsohn. Targeting the epidermal growth factor receptor for cancer therapy. *J Clin Oncol.* **20:** 1S-13S (2002)
15. E. B. Kullberg, N. Bergstrand, J. Carlsson, K. Edwards, M. Johnsson, S. Sjoberg and L. Gedda. Development of EGF-conjugated liposomes for targeted delivery of boronated DNA-binding agents. *Bioconjug Chem.* **13:** 737-43 (2002)
16. W. Yang, R. F. Barth, G. Wu, A. K. Bandyopadhyaya, B. T. Thirumamagal, W. Tjarks, P. J. Binns, K. Riley, H. Patel, J. A. Coderre, M. J. Ciesielski and R. A. Fenstermaker. Boronated epidermal growth factor as a delivery agent for neutron capture therapy of EGF receptor positive gliomas. *Appl Radiat Isot.* **61:** 981-5 (2004)
17. G. Wu, R. F. Barth, W. Yang, M. Chatterjee, W. Tjarks, M. J. Ciesielski and R. A. Fenstermaker. Site-specific conjugation of boron-containing dendrimers to anti-EGF receptor monoclonal antibody cetuximab (IMC-C225) and its evaluation as a potential delivery agent for neutron capture therapy. *Bioconjug Chem.* **15:** 185-94 (2004)
18. R. F. Barth, W. Yang, D. M. Adams, J. H. Rotaru, S. Shukla, M. Sekido, W. Tjarks, R. A. Fenstermaker, M. Ciesielski, M. M. Nawrocky and J. A. Coderre. Molecular targeting of the epidermal growth factor receptor for neutron capture therapy of gliomas. *Cancer Res.* **62:** 3159-66 (2002)

19. G. A. Koning, H. W. Morselt, A. Gorter, T. M. Allen, S. Zalipsky, G. L. Scherphof and J. A. Kamps. Interaction of differently designed immunoliposomes with colon cancer cells and Kupffer cells. An in vitro comparison. *Pharm Res.* **20:** 1249-57 (2003)
20. G. Rouser, S. Fkeischer and A. Yamamoto. Two dimensional then layer chromatographic separation of polar lipids and determination of phospholipids by phosphorus analysis of spots. *Lipids.* **5:** 494-6 (1970)
21. D. A. Scudiero, R. H. Shoemaker, K. D. Paull, A. Monks, S. Tierney, T. H. Nofziger, M. J. Currens, D. Seniff and M. R. Boyd. Evaluation of a soluble tetrazolium/formazan assay for cell growth and drug sensitivity in culture using human and other tumor cell lines. *Cancer Res.* **48:** 4827-33 (1988)
22. G. C. Krijger, M. M. Fretz, U. D. Woroniecka, O. M. Steinebach, W. Jiskoot, G. Storm and G. A. Koning. Tumor cell and tumor vasculature targeted liposomes for neutron capture therapy. *Radiochim Acta.* **93:** 589-593 (2005)
23. E. Mastrobattista, G. A. Koning, L. Van Bloois, A. C. Filipe, W. Jiskoot and G. Storm. Functional Characterization of an Endosome-disruptive Peptide and Its Application in Cytosolic Delivery of Immunoliposome-entrapped Proteins. *J Biol Chem.* **277:** 27135-43 (2002)
24. D. Gabel, S. Foster and R. G. Fairchild. The Monte Carlo simulation of the biological effect og the 10B(n, alpha)7Li reaction in cells and its implication for boron neutron capture therapy. *Radiat Res.* **111:** 14-25 (1987)
25. R. M. Straubinger, K. Hong, D. S. Friend and D. Papahadjopoulos. Endocytosis of liposomes and intracellular fate of encapsulated molecules: encounter with a low pH compartment after internalization in coated vesicles. *Cell.* **32:** 1069-1079 (1983)
26. D. B. Kirpotin, J. W. Park, K. Hong, S. Zalipsky, W. Li, P. Carter, C. C. Benz and D. Papahadjopoulos. Sterically stabilized anti-HER2 immunoliposomes: design and targeting to human breast cancer cell in vitro. *Biochemistry.* **36:** 66-75 (1997)
27. J. Capala, R. F. Barth, M. Bendayan, M. Lauzon, D. M. Adams, A. H. Soloway, R. A. Fenstermaker and J. Carlsson. Boronated epidermal growth factor as a potential targeting agent for boron neutron capture therapy of brain tumors. *Bioconjug Chem.* **7:** 7-15 (1996)
28. N. Carlsson, L. Gedda, C. Gronvik, T. Hartman, A. Lindstrom, P. Lindstrom, H. Lundqvist, A. Lovqvist, J. Malmqvist and P. Olsson. Strategy for boron neutron capture therapy against tumor cells with overexpression of the epidermal growth factor receptor. *Int J Radiat Biol Phys.* **30:** 105-115 (1994)
29. S. C. Mehta and D. R. Lu. Targeted drug delivery for boron neutron capture therapy. *Pharm Res.* **13:** 344-51 (1996)
30. D. S. Salomon, R. Brandt, F. Ciardiello and N. Normanno. Epidermal growth factor-related peptides and their receptor in human malignancies. *Crit Rev Oncol Hematol.* **19:** 183-232 (1995)
31. E. Mastrobattista. Comparison of immunoliposomes targeting to three different receptors expressed by human ovarian carcinoma (OVCAR-3) cells. *Dissertation thesis.* (2001)
32. P. Nagy, D. J. Arndt-Jovin and T. Jovin. Small interfering RNAs suppress the expression of endogenous and GFP-fused epidermal growth factor receptor (erbB1) and induce apoptosis in erbB1-overexpressing cells. *Exp Cell Res.* **285:** 39-49 (2003)
33. C. Mamot, D. C. Drummond, U. Greiser, K. Hong, D. B. Kirpotin, J. D. Marks and J. W. Park. Epidermal growth factor receptor (EGFR)-targeted immunoliposomes mediate specific and efficient drug delivery to EGFR- and EGFRvIII-overexpressing tumor cells. *Cancer Res.* **63:** 3154-3161 (2003)
34. J. W. Park, K. Hong, D. B. Kirpotin, G. Colbern, R. Shalaby, J. Baselga, Y. Shao, U. B. Nielsen, J. D. Marks, D. Moore, D. Papahadjopoulos and C. C. Benz. Anti-HER2 immunoliposomes: enhanced efficacy attributtable to targeted delivery. *Clin Cancer Res.* **8:** 1172-1181 (2002)
35. M. M. Fretz, A. Hogset, G. A. Koning, W. Jiskoot and G. Storm. Cytosolic delivery of liposomally targeted proteins induced by photochemical internalization. *Pharm Res Accepted for publication.*

8

Summarising discussion

INTRODUCTION

Biotechnological advances increased the number of novel macromolecular drugs and new drug targets. The latter are mostly found intracellular. Unfortunately, most of the new macromolecular drugs rely on drug delivery tools for their intracellular delivery because their unfavourable physicochemical properties hamper them to cross cellular barriers such as the plasma and endosomal membranes. Therefore, they are unable to reach their intracellular target.

This thesis aims to improve intracellular drug delivery by applying targeted liposome systems. Two different approaches to improve delivery of (targeted) liposomal contents into the cytoplasm were evaluated. In addition, the use of targeted liposomes for intracellular delivery of boron-containing compounds to improve boron neutron capture therapy (BNCT) was assessed.

Chapter 1 dealt with a general overview of the recent literature and the aims and outline of the thesis. **Chapter 2** briefly discussed three different strategies utilised by our laboratory to achieve cytosolic delivery of liposomal proteins.

I. CELL-PENETRATING PEPTIDES TO IMPROVE INTRACELLULAR DRUG DELIVERY

The discovery of the ability of cell-penetrating peptides (CPP) to translocate over cellular membranes in an energy-, time- and specificity- independent fashion caused excitement in the drug delivery field. Circumvention of endocytosis by direct translocation over the plasma membrane into the cytosol of cells would be highly beneficial for labile macromolecules like proteins and nucleic acids, because it avoids their degradation in the endocytic pathway. Upon conjugation, several cargos ranging from fluorophores to proteins and to even nanoparticles, were reported to be translocated over the plasma membrane, adequately reviewed in (1). However, recently this direct translocation mechanism was questioned, since studies in living cells have shown that the translocation could be attributed to artifacts caused by fixation methods (2, 3). From then on most studies on CPP where done with live cells and indicated that endocytosis can also play an important, if not primary, role in the cellular uptake of these CPP (3). Nevertheless, there is still the strong convincement that direct translocation also occurs (4-6), leaving the uptake mechanism of CPP a controversial subject.

In **chapter 3**, the cellular association and intracellular distribution of the CPP octaarginine (R8), composed of either L- or D-arginine, at different temperatures was investigated in leukaemia $CD34^+$ KG1a cells. At temperatures below 19°C, fluorescent conjugates of both peptides were diffusely distributed throughout the whole cell; D-R8 also strongly labels the nucleolus, whereas this labeling was absent in cells incubated with L-R8. At 37°C both peptides were primarily localised in endocytic vesicles. Between these temperatures, both

octaarginine peptides were localised in both cytosol (and for D-R8 nucleolar labeling) and endocytic vesicles, suggesting that the cells internalise the peptides via two distinct mechanisms. Vesicular labeling characteristic for incubation at 37°C was changed to diffuse labeling in cells incubated with the cholesterol sequestering agent methyl-β-cyclodextrin, suggesting a role for plasma membrane cholesterol. Relatively small increases in peptide concentration could also change the vesicular labeling at 37°C to labeling of the cytoplasm, nucleus and in case of D-R8 the nucleolus. We therefore speculated that these peptides are taken up by two different uptake mechanisms. The relative importance of each mechanism is determined by factors like plasma membrane cholesterol, peptide concentration and temperature.

Recently, two studies presented evidence that the cellular uptake mechanism is dependent on the type and size of the cargo conjugated to the CPP (7, 8). Upon conjugation of small peptides or fluorophores to the CPP translocation seems to occur, whereas endocytosis becomes more prominent when larger units like proteins or quantum dots are attached (7). It has been reported that also liposomes with their surface modified with CPP can be translocated over the plasma membrane into the cytoplasm. However, these studies were carried out with fixed cells (9, 10). In **chapter 4,** flow cytometry and *live* cell imaging were used to investigate the cellular uptake mechanism of TAT-peptide modified liposomes. The TAT-peptide is one of the most studied CPP and is derived from the HIV-1 TAT-protein. The peptide contains a large number of lysines and arginines, giving it a strong positive charge at physiological pH (11). TAT-peptide modification strongly enhanced the binding and internalisation of the liposomes compared to control liposomes lacking TAT. After 1 hr incubation of human ovarian carcinoma cells (OVCAR-3) with TAT-liposomes, the liposomes were predominantly present at the plasma membrane, while after 24 hrs incubation, the liposomes were present in vesicular structures within the cytoplasm and co-localised with an endo- and lysosomal marker. Furthermore, on incubation at low temperature (4°C) or in the presence of iodoacetamide (metabolic inhibitor) or cytochalasin D (endocytosis inhibitor) uptake was impeded and only plasma membrane labeling was detected. These results indicate that human ovarian carcinoma cells were internalising TAT-liposomes via endocytosis. It was also shown that binding of the TAT-liposomes can be reduced by addition of either of the polyanion dextran sulfate or heparin, suggesting a role for the cell surface proteoglycans. Altogether, this study showed that TAT-liposomes do not have an advantageous mechanism of cellular entry over targeted delivery systems. And the encapsulated drug will still be exposed to the degrading environment of late endosomes and lysosomes. However, the TAT-mediated enhancement of cellular binding and uptake could be beneficial for certain drug targeting applications.

Endocytosis is a broad term indicating several different pathways of cellular uptake, which include clathrin- and caveolae-dependent uptake, macropinocytosis and others (12). To differentiate between the different pathways and to investigate whether a specific route

plays a role in the cellular uptake of drug delivery tools like CPP and CPP conjugates, inhibitors of different endocytic pathways have been used.

Chapter 5 explored the influence of compounds used as macropinocytosis inhibitors on the subcellular localisation of endocytic organelles and the intracellular distribution of CPPs. Amiloride and its more effective derivative 5-(*N*-ethyl-*N*-isopropyl)amiloride (EIPA) were used because of their ability to reduce macropinocytotic uptake (13, 14). The literature reports that these compounds also influence the uptake of the CPPs TAT and R8, which consequently suggests that macropinocytosis might be involved as cellular uptake mechanism (15-17). In this chapter, we demonstrated that incubation with even relatively low concentrations of amiloride or EIPA altered the morphology and subcellular localisation of early, late endosomes and lysosomes in HeLa cells. The early and late endocytotic vesicles appeared to be enlarged and accumulated in the perinuclear region in contrast to smaller vesicles distributed throughout the cytoplasm of the non-treated controls. The effect of EIPA on distribution of endocytic organelles was also reflected in the change of localisation of fluorescent L-R8 in live HeLa cells. Cytotoxicity studies of amiloride and EIPA in the leukaemic KG1a cell line demonstrated no cytotoxic effect of amiloride at all tested concentrations, while EIPA started to be cytotoxic at concentrations over 100 μM. No additional cytotoxicity was observed when KG1a cells were treated with L-R8 or TAT after the incubation with EIPA or amiloride. Despite the lack of cytotoxicity, KG1a cells treated with EIPA followed by fluorescent TAT or L-R8 incubation demonstrated severe redistribution of the fluorescent R8 and TAT from vesicular to presence in the cytosol at higher concentrations EIPA. Furthermore, morphological aberrations were also visible, suggesting toxicity. Therefore, caution should be given to the interpretation of data using this type of inhibitors.

Most CPP research makes use of fluorescent conjugates of CPP or CPP-cargo. The cellular uptake is assessed by techniques such as flow cytometry and fluorescence microscopy. Tunneman *et al.* showed that a fluorescent conjugate of TAT and the recombinase protein Cre (TAT-Cre) could solely be visualised in intracellular vesicles. Even when an endosomal escape-enhancing peptide combined with TAT (TAT-HA2) was simultaneously incubated, no TAT-Cre could be detected in the cytoplasm or nucleus. However, when the recombinase activity of the Cre protein was measured, a significant increase could be measured. The protein Cre acts in the nucleus and although no TAT-Cre could be visualised with microscopy, this more sensitive assay showed that a small but significant amount of TAT-Cre was able to reach the nucleus. If this portion escaped from endosomes or was directly translocated over the plasma membrane needs to be determined (7). Other studies also using read-out systems different from fluorescence microscopy showed that CPP-protein conjugates are able to reach their intracellular target site and show activity (5, 18, 19).

For future application of CPP as drug delivery tools, more research needs to be done to identify the cellular uptake mechanism(s). Furthermore, the parameters which define the

uptake mechanism should be identified. Alteration of these parameters should be explored to select the desired uptake mechanism to make that particular CPP suitable as delivery tool. However, it should be realised that coupling of CPP to larger cargoes like liposomes can strongly change the cellular uptake mechanism.

II. PHOTOCHEMICAL INTERNALISATION TO IMPROVE INTRACELLULAR DRUG DELIVERY

Photochemical internalisation (PCI) is a photochemical technology to release drug molecules from endocytic vesicles and has already been successfully used for drug delivery purposes. Amphiphilic photosensitisers localise in the plasma membrane upon addition to cells and upon endocytosis they accumulate primarily in endosomal membranes. Illumination activates the formation of highly reactive oxygen species which cause damage to the endosomal membrane with subsequent release of material present in the endosomal lumen into the cytoplasm without extensive cell death (reviewed in (20)). Successful endosomal release of a variety of (macro)molecules and particles, including (immuno)toxins, oligonucleotides and particulates for gene delivery has been demonstrated (21-26). **Chapter 6** describes the first study on the use of PCI to optimise the delivery of liposomally targeted proteins. Three different liposome formulations were investigated: two types of targeted liposomes, one with an anti-epidermal growth factor receptor antibody at the distal end of the PEG-shield (EGFR-L) and the other with a positively charged bilayers (DOTAP-L) and as control, non-targeted pegylated liposomes (PEG-L). As a model protein, saporin, was encapsulated into the liposomes. Saporin is a member of the family of ribosome-inactivating proteins (RIP) and when delivered into the cytosol highly cytotoxic. However, saporin lacks a cell-binding domain and is not capable of escaping from the endosomes. Therefore, it relies on a drug delivery vehicle to get efficiently delivered into the cytosol (27). The results in this chapter showed that both targeted liposome formulations do significantly enhance the target cell binding and the uptake in vitro by the EGFR-positive OVCAR-3 cells compared to non-targeted liposomes. However, cytotoxicity of liposomal saporin was not observed except when PCI was additionally applied. The targeted saporin-loaded liposomes showed a strong superior cytotoxic effect over the non-targeted liposomes, whereas the latter were as inefficient as free saporin after PCI. The positively charged DOTAP-liposomes showed better tumour-cell killing properties than EGFR-targeted liposomes, which most likely can be explained by their enhanced binding and higher degree of intracellular delivery of saporin. It was shown that increased cytotoxicity could be attained with by increasing the illumination time. At short illumination times, most of the cytotoxic effect was attributed to the saporin which escaped from the endosomes, while with a longer illumination times cell death was for a large part (50%) caused by the photodynamic therapy (PDT) effect, due to the action of the photosensitiser and light alone. PCI aims to successfully deliver molecules into the cytosol without

extensive cell death. However, in case of cancer therapy application, the additional PDT effect arising with longer illumination times can be beneficial as it will strengthen the anti-tumour effect.

The exact mechanism of photochemically induced endosomal membrane rupture is unknown. Damage to the endosomal membrane causing release of molecules present in the endosomes to the cytosol is described, however, no data is available which molecules (lipids/proteins) within the endosomal membrane are damaged and if this impairment is reversible. The 'light-before' approach (PCI is applied before the 'to-be-delivered' molecule is added to the cells (28)) has been successfully applied, suggesting that PCI causes some irreversible or slowly reversible damage. Characterisation of the effects of PCI at the subcellular level could be helpful for further development, optimisation and better understanding of the technique.

In vivo application of PCI remains challenging. First, the applied light needs to reach the target site. Unfortunately light has a limited penetration depth; for clinical application far red-light absorbing photosensitisers are most useful, with an estimated effective penetration depth of 2 cm (20). Furthermore, progress is being made in laser and fibre technology which gives opportunities to illuminate almost any site within the human body (29). A second in vivo application aspect is that drug and photosensitiser have been administered separately in most studies described so far (in vitro and in vivo). It would be very favourable to have simply one delivery system for both the photosensitiser and the drug. The preparation of such a system has been recently described by Nishima *et al*. A ternary complex including photosensitiser and a DNA/polymer complex showed up to a 100-fold photochemical enhancement of transgene expression in vitro and in vivo (30). Liposomes would be an attractive carrier for both photosensitiser and drug; the photosensitiser should be incorporated in the liposomal bilayers, while the drugs can be entrapped in the aqueous interior of the liposomes. Delivery of photosensitisers by liposomes has already been described in literature (31) and although not described in this thesis, preliminary studies have been perfomed showing that the photosensitiser used in our studies can be efficiently embedded in the liposomal bilayer. Future studies need to address the possibility for liposomes to deliver both photosensitiser and drug.

III. TARGETED INTRACELLULAR BORON DELIVERY FOR BORON NEUTRON CAPTURE THERAPY

A major challenge in the field of boron neutron capture therapy (BNCT) is the relatively large number of boron atoms required to be delivered to tumour cells for successful therapy. The subcellular localisation of the boron atoms is also very important: the closer to the nucleus the more effective the cell-killing effect will be.

The use of EGFR-targeted liposomes (EGFR-L) for BNCT was evaluated using two human tumour cell lines (OVCAR-3 and A431). Both cell lines are considered EGFR positive, but

results in **chapter 7** showed that they express the EGFR to a different extent. Earlier studies in our laboratory have demonstrated that the EGFR-L can be used succesfully to target drugs to OVCAR-3 cells despite their relatively basal EGFR expression. OVCAR-3 cells bind and internalise EGFR-L more efficiently than non-targeted PEG-L (**chapter 6** and (32)). However, although flow cytometry experiments showed enhanced binding of boron-loaded EGFR-L to OVCAR-3 cells compared to boron-loaded PEG-L, a significant enhancement of cell-associated boron after incubation with EGFR-L versus PEG-L in OVCAR-3 was not observed. This is in contrast to similar studies with A431, where EGFR-L did show superior binding and uptake of encapsulated boron over PEG-L most likely due to the higher EGFR expression. This difference in targeting effect of EGFR-L between A431 and OVCAR-3 cells is in good agreement with our BNCT findings that EGFR-L performed only slightly better than PEG-L in case of OVCAR-3 cells, while EGFR-L are performing much better than PEG-L with in case of A431 cells. This could be of major importance for potential future clinical application; EGFR expression differs between different tumours and even within one tumour the expression might be heterogeneous (33).
The in vivo use of targeted liposomes for BNCT has been described in two studies. Both studies showed that intravenously administered targeted liposomes are not superior over non-targeted liposomes in delivering boron to tumours (34, 35). Although, it is likely that the intracellular localisation of boron encapsulated in targeted liposomes may have been higher as compared to PEG-liposomes lacking the targeting ligand, the BNCT effect appeared not to be improved (35). Further investigations are needed to study liposomal boron delivery at the cellular and subcellular levels.
Unfortunately, the cellular retention of our internalised liposomal boron was not optimal. The cells cleared the small borane salt used in our studies quickly. Already after 1 hr, 50% or less of the cellular boron was removed, with only a fraction left 4 hrs after removal of the liposomes. For further application, increased cellular retention would be favourable. Encapsulation of other boron-containing molecules into liposomes with better cellular retention may yield stronger BNCT activity.

CONCLUSION

In conclusion, this thesis has investigated novel ways to improve intracellular drug delivery by using targeted liposomes. The results show that improvement indeed is possible. In particular, the use of the photochemical internalisation technology shows promise for in vivo application in the near future. The use of both cell-penetrating peptides and the BNCT approach needs further fundamental investigation in vitro before success in the in vivo situation can be expected.

REFERENCES

1. G. P. Dietz and M. Bahr. Delivery of bioactive molecules into the cell: the Trojan horse approach. *Mol Cell Neurosci.* **27:** 85-131 (2004)
2. M. Lundberg and M. Johansson. Positively charged DNA-binding proteins cause apparent cell membrane translocation. *Biochem Biophys Res Commun.* **291:** 367-71 (2002)
3. J. P. Richard, K. Melikov, E. Vives, C. Ramos, B. Verbeure, M. J. Gait, L. V. Chernomordik and B. Lebleu. Cell-penetrating peptides: A re-evaluation of the mechanism of cellular uptake. *J Biol Chem.* (2002)
4. C. Cohen-Saidon, H. Nechushtan, S. Kahlon, N. Livni, A. Nissim and E. Razin. A novel strategy using single chain antibody to show the importance of Bcl-2 in mast cell survival. *Blood.* **5** (2003)
5. M. Peitz, K. Pfannkuche, K. Rajewsky and F. Edenhofer. Ability of the hydrophobic FGF and basic TAT peptides to promote cellular uptake of recombinant Cre recombinase: a tool for efficient genetic engineering of mammalian genomes. *Proc Natl Acad Sci U S A.* **99:** 4489-94 (2002)
6. D. J. Mitchell, D. T. Kim, L. Steinman, C. G. Fathman and J. B. Rothbard. Polyarginine enters cells more efficiently than other polycationic homopolymers. *J Peptide Res.* **56:** 318-25 (2000)
7. G. Tunnemann, R. M. Martin, S. Haupt, C. Patsch, F. Edenhofer and M. C. Cardoso. Cargo-dependent mode of uptake and bioavailability of TAT-containing proteins and peptides in living cells. *Faseb J.* **20:** 1775-84 (2006)
8. J. R. Maiolo, M. Ferrer and E. A. Ottinger. Effect of cargo molecules on the cellular uptake of arginine-rich cell-penetrating peptides. *Biochem Biophys Acta.* **1712:** 161-72 (2005)
9. V. P. Torchilin, R. Rammohan, V. Weissig and T. S. Levchenko. TAT peptide on the surface of liposomes affords their efficient intracellular delivery even at low temperature and in the presence of metabolic inhibitors. *Proc Natl Acad Sci U S A.* **98:** 8786-91 (2001)
10. Y. L. Tseng, J. J. Liu and R. L. Hong. Translocation of liposomes into cancer cells by cell-penetrating peptides penetratin and tat: a kinetic and efficacy study. *Mol Pharmacol.* **62:** 864-72 (2002)
11. E. Vives, P. Brodin and B. Lebleu. A truncated HIV-1 Tat protein basic domain rapidly translocates through the plasma membrane and accumulates in the cell nucleus. *J Biol Chem.* **272:** 16010-7 (1997)
12. S. D. Conner and S. L. Schmid. Regulated portals of entry into the cell. *Nature.* **422:** 37-44 (2003)
13. O. Meier, K. Boucke, S. V. Hammer, S. Keller, R. P. Stidwill, S. Hemmi and U. F. Greber. Adenovirus triggers macropinocytosis and endosomal leakage together with its clathrin-mediated uptake. *J Cell Biol.* **158:** 1119-1131 (2002)
14. M. A. West, M. S. Bretscher and C. Watts. Distinct endocytic pathways in epidermal growth factor-stimulated human carcinoma A431 cells. *J Cell Biol.* **109:** 2731-2739 (1989)
15. J. S. Wadia, R. V. Stan and S. F. Dowdy. Transducible TAT-HA fusogenic peptide enhances escape of TAT-fusion proteins after lipid raft macropinocytosis. *Nat Med.* **10:** 310-315 (2004)
16. I. Nakase, M. Niwa, T. Takeuchi, K. Sonomura, N. Kawabata, Y. Koike, M. Takehashi, S. Tanaka, K. Ueda, J. C. Simpson, A. T. Jones, Y. Sugiura and S. Futaki. Cellular uptake of arginine-rich peptides: roles for macropinocytosis and actin rearrangement. *Mol Ther.* **10:** 1011-22 (2004)
17. I. M. Kaplan, J. S. Wadia and S. F. Dowdy. Cationic TAT peptide transduction domain enters cells by macropinocytosis. *J Control Release.* **102:** 247-253 (2005)
18. N. Watanabe, T. Iwamoto, K. D. Bowen, D. A. Dickinson, M. Torres and H. J. Forman. Bio-effectiveness of Tat-catalase conjugate: a potential tool for the identification of H2O2-dependent cellular signal transduction pathways. *Biochem Biophys Res Commun.* **303:** 287-293 (2003)
19. U. Kilic, E. Kilic, G. P. Dietz and M. Bahr. Intravenous TAT-GDNF is protective after focal cerebral ischemia in mice. *Stroke.* **34:** 1304-1310 (2003)
20. A. Hogset, L. Prasmickaite, P. K. Selbo, M. Hellum, B. O. Engesaeter, A. Bonsted and K. Berg. Photochemical internalisation in drug and gene delivery. *Adv Drug Deliv Rev.* **56:** 95-115 (2004)
21. K. Berg, P. K. Selbo, L. Prasmickaite, T. E. Tjelle, K. Sandvig, J. Moan, G. Gaudernack, O. Fodstad, S. Kjolsrud, H. Anholt, G. H. Rodal, S. K. Rodal and A. Hogset. Photochemical internalization: a novel technology for delivery of macromolecules into cytosol. *Cancer Res.* **59:** 1180-3 (1999)
22. P. K. Selbo, G. Sivam, O. Fodstad, K. Sandvig and K. Berg. Photochemical internalisation increases the cytotoxic effect of the immunotoxin MOC31-gelonin. *Int J Cancer.* **87:** 853-9 (2000)
23. P. K. Selbo, K. Sandvig, V. Kirveliene and K. Berg. Release of gelonin from endosomes and lysosomes to cytosol by photochemical internalization. *Biochim Biophys Acta.* **1475:** 307-13 (2000)

24. B. O. Engesaeter, A. Bonsted, K. Berg, A. Hogset, O. Engebraten, O. Fodstad, D. T. Curiel and G. M. Maelandsmo. PCI-enhanced adenoviral transduction employs the known uptake mechanism of adenoviral particles. *Cancer Gene Ther.* **12:** 439-48 (2005)
25. A. Hogset, L. Prasmickaite, M. Hellum, B. O. Engesaeter, V. M. Olsen, T. E. Tjelle, C. J. Wheeler and K. Berg. Photochemical transfection: a technology for efficient light-directed gene delivery. *Somat Cell Mol Genet.* **27:** 97-113 (2002)
26. M. Folini, K. Berg, E. Millo, R. Villa, L. Prasmickaite, M. G. Daidone, U. Benatti and N. Zaffaroni. Photochemical internalization of a peptide nucleic acid targeting the catalytic subunit of human telomerase. *Cancer Res.* **63:** 3490-4 (2003)
27. F. Stirpe. Ribosome-inactivating proteins. *Toxicon.* **44:** 371-83 (2004)
28. L. Prasmickaite, A. Hogset, P. K. Selbo, B. O. Engesaeter, M. Hellum and K. Berg. Photochemical disruption of endocytic vesicles before the delivery of drugs: a new strategy for cancer therapy. *Br J Cancer.* **86:** 652-657 (2002)
29. T. J. Dougherty, C. J. Gomer, B. W. Henderson, G. Jori, D. Kessel, M. Korbelik, J. Moan and Q. Peng. Photodymanic therapy. *J Natl Cancer Inst.* **90:** 889-905 (1998)
30. N. Nishiyama, A. Iriyama, W. D. Jang, K. Miyata, K. Itaka, Y. Inoue, H. Takahashi, Y. Yanagi, Y. Tamaki, H. Koyama and K. Kataoka. Light-induced gene transfer from packaged DNA enveloped in dendrimeric photosensitizer. *Nat Mater.* **4:** 934-41 (2005)
31. A. S. Derycke and P. A. de Witte. Liposomes for photodynamic therapy. *Adv Drug Deliv Rev.* **56:** 17-30 (2004)
32. E. Mastrobattista, G. A. Koning, L. Van Bloois, A. C. Filipe, W. Jiskoot and G. Storm. Functional Characterization of an Endosome-disruptive Peptide and Its Application in Cytosolic Delivery of Immunoliposome-entrapped Proteins. *J Biol Chem.* **277:** 27135-43 (2002)
33. T. M. Allen. Ligand-targeted therapeutics in anticancer therapy. *Nat Rev Cancer.* **2:** 750-63 (2002)
34. X. Q. Pan, H. Wang and R. J. Lee. Boron delivery to a murine lung carcinoma using folate receptor-targeted liposomes. *Anticancer Res.* **22:** 1629-1633 (2002)
35. K. Maruyama, O. Ishida, S. Kasaoka, T. Takizawa, N. Utoguchi, A. Shinohara, M. Chiba, H. Kobayashi, M. Eriguchi and H. Yanagie. Intracellular targeting of sodium mercaptoundecahydrododecaborate (BSH) to solid tumors by transferrin-PEG liposomes, for boron neutron-capture therapy (BNCT). *J Control Release.* **98:** 195-207 (2004)

Appendices

Color Figures

Nederlandse samenvatting

Dankwoord

Curriculum Vitae

List of publications

List of abbreviations

COLOR FIGURES

Chapter 3, Figure 1

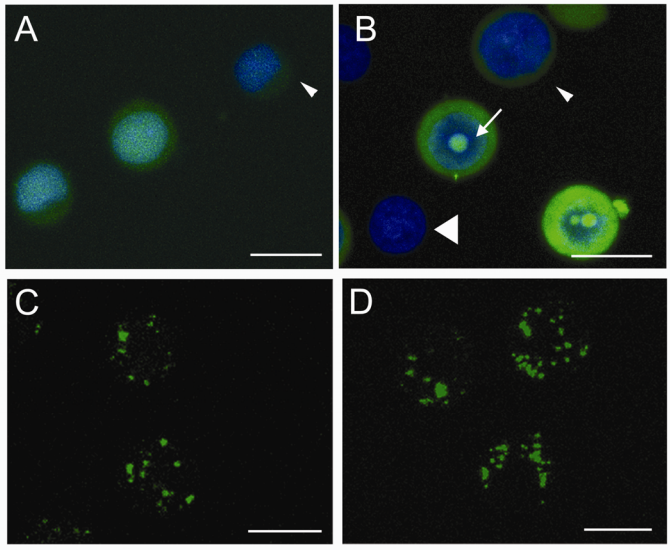

Figure 1. Cellular distribution of L- and D-R8-Alexa488 in KG1a cells at 4 and 37°C (A-D) KG1a cells were incubated for 1 h with 2 µM L- (A, C) or D-R8-Alexa488 (B, D) at either 4°C (A-B) or 37°C (C-D), prior to analysis by confocal microscopy. Shown are maximum projections of 35 z-stacks (~ 500 nm/ and 2 to 4 s/section) for each condition. A and B were also labeled with DRAQ5 dye as described in experimental. Arrows in B indicate peptide labeling of nucleolus, small arrowhead show a cell showing low peptide labeling, large arrowhead shows a cell with undetectable levels of peptide fluorescence. Scale bars 10 µm.

Chapter 4, Figure 2

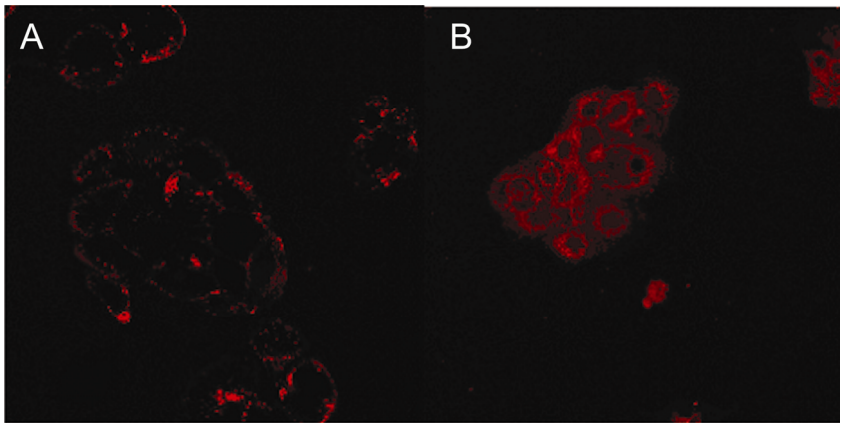

Figure 2. Fixation induced redistribution of liposomal label. OVCAR-3 cells were incubated for 1 hr at 37°C with TAT-liposomes labeled with Rho-PE and either visualised without fixation (A) or after fixation with 4% formaldehyde (B).

Chapter 4, Figure 3

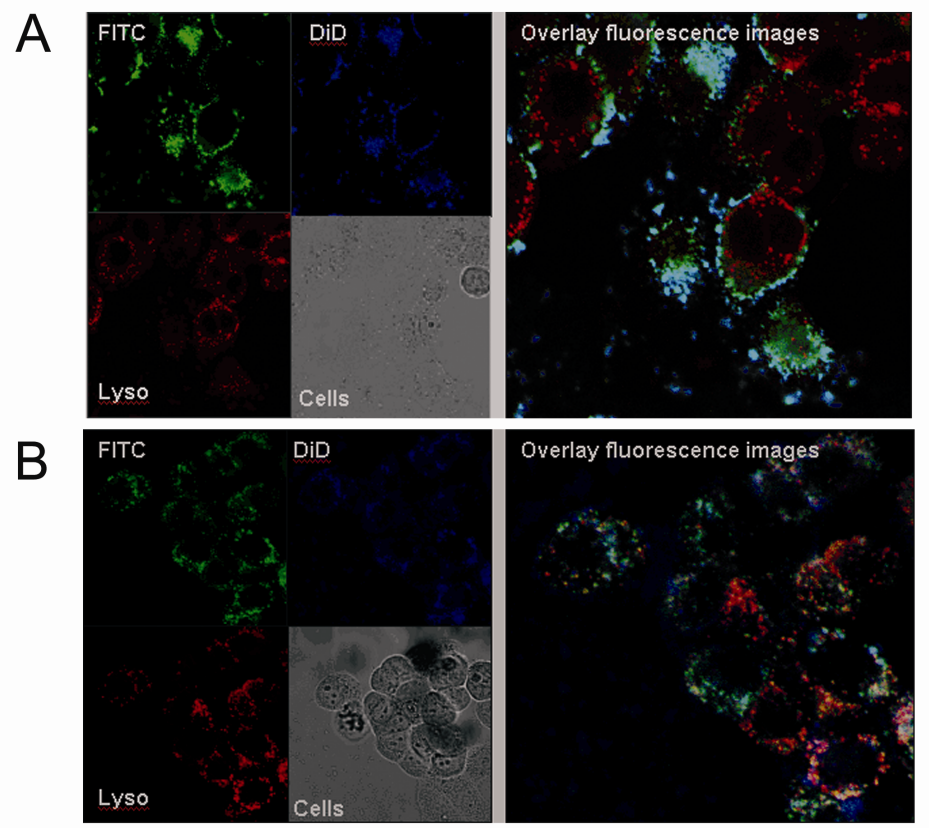

Figure 3. Intracellular localisation of TAT-liposomes. OVCAR-3 cells were incubated with 150 nmol of TAT-liposomes for 1 hr and directly visualised (A) or subsequently incubated for 23 hours with liposome-free medium (B). Endosomes and lysosomes were stained 30 minutes prior to visualisation with Lysotracker Red. In the right panels the different confocal images are electronically merged.

Chapter 5, Figure 1

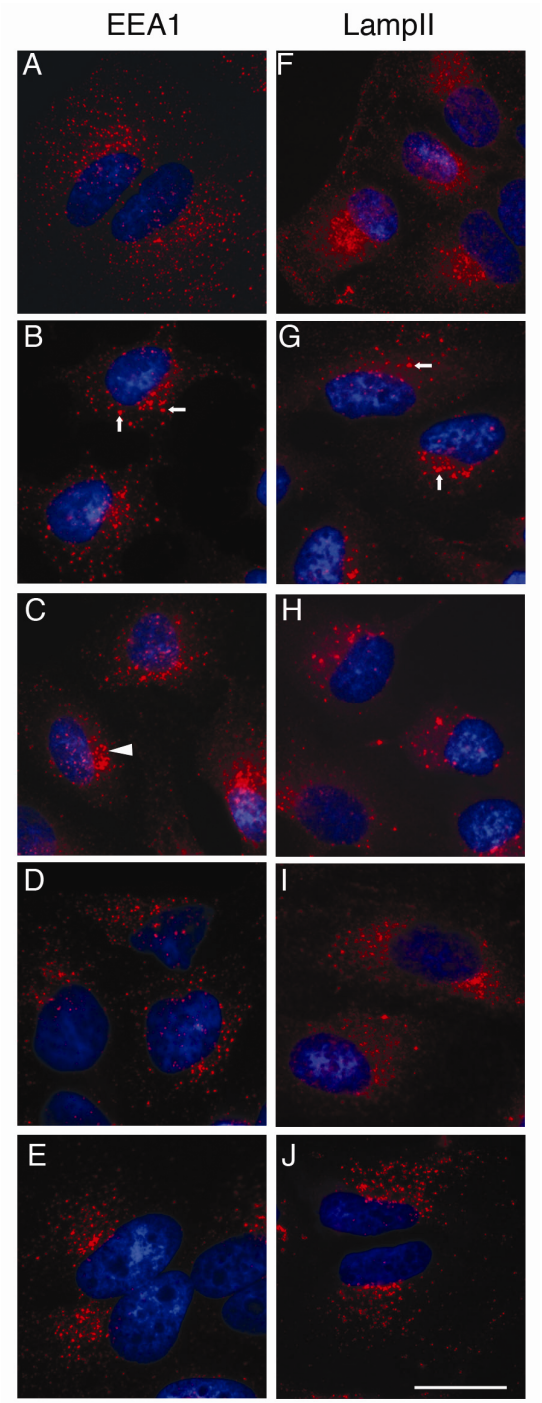

Figure 1. Effects of EIPA and amiloride on subcellular distribution of early and late organelles of endocytic pathways. HeLa cells were incubated in the presence of DMSO diluent (A and F), 50 µM EIPA (B-C and G-H) or 50 µM amiloride (D-E and I-J) for 1 (B, D, G and I) or 2.5 hours (C, E, H and J). The cells were then fixed, labeled with antibodies against EEA1 or LampII and then Alexa594 conjugated secondary anti-mouse antibodies and analysed by fluorescence microscopy. The nuclei in A-J were labeled with Hoechst 33342. Arrows show enlarged EEA1 and LampII vesicles in EIPA treated cells. Arrowheads show accumulation of vesicles in a perinuclear region. Scale bar 20 µm.

Chapter 5, Figure 3

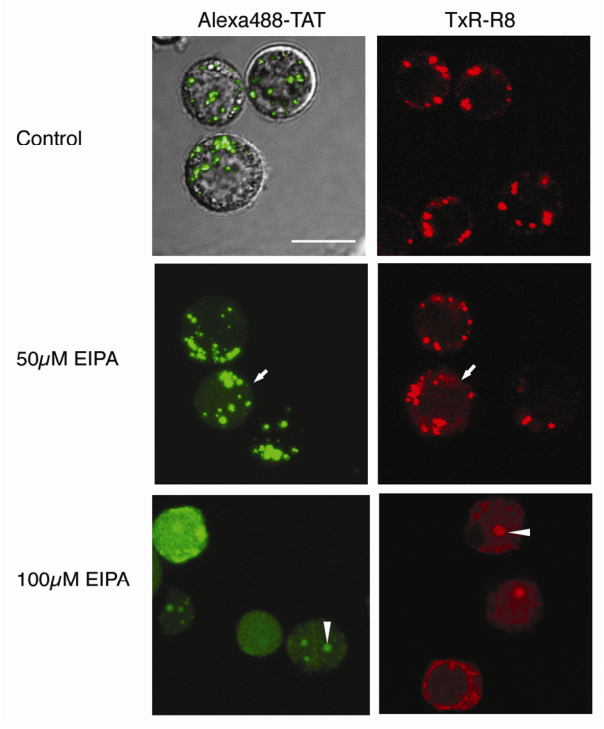

Figure 3. Subcellular distribution of Alexa488-TAT and TxR-R8 in EIPA-treated KG1a cells. KG1a cells were preincubated in the absence (control) or in the presence of 50 or 100 μM EIPA for 30 minutes prior to addition of 3 μM Alexa488-TAT or 1 μM TxR-R8. After 1 h the cells were washed and imaged by live cell confocal microscopy. All images are Z-stacked images from 15-20 sections of ~ 0.5 μm. Top left shows an overlay of peptide distribution against a phase image of the cells. Arrows show cells with cytosolic fluorescence, arrowhead shows peptide labeled nucleolus.

Chapter 7, Figure 5

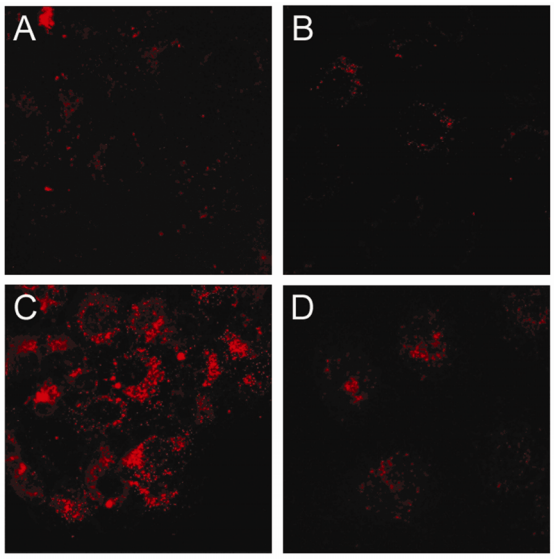

Figure 5. Intracellular distribution of liposomes. OVCAR-3 (A and B) or A431 (C and D) were incubated with fluorescently labeled EGFR-L (A and C) and PEG-L (B and D) for 24 hr at 37ºC. The cells were washed, fixed and analysed with confocal microscopy.

NEDERLANDSE SAMENVATTING VOOR LEKEN

Met behulp van de toenemende kennis in de biotechnologie en moleculaire biologie van de laatste jaren zijn er ook een groter aantal geneesmiddelen en geneesmiddel-aangrijpingspunten ontdekt. Deze aangrijpingspunten bevinden zich vaak in bepaalde compartimenten van de cel, ook wel cel-organellen genaamd. Om effectief te werken, moet het geneesmiddel dan ook dit aangrijpingspunt in de cel weten te bereiken.

Cellen zijn omgeven door een celmembraan, welke er voor zorgt dat stoffen niet zomaar de cel binnen kunnen komen. Dit is natuurlijk een voordeel in het geval van schadelijke stoffen, maar voor geneesmiddelen kan dit een groot nadeel zijn. Met name 'nieuwe generatie' geneesmiddelen, zoals eiwitten en DNA, bezitten eigenschappen die transport over de celmembraan tegenwerken. Dit resulteert vervolgens in een lage effectiviteit van het betreffende geneesmiddel.

Om ervoor te zorgen dat dergelijke geneesmiddelen beter cellen kunnen binnendringen, kan gebruik gemaakt worden van dragersystemen. Een veel gebruikt dragersysteem is het liposoom. Een liposoom is een heel klein vetbolletje dat bestaat uit een dubbele laag van fosfolipiden en cholesterol die een water-compartiment omsluiten. Fosfolipiden zijn zogenaamde amfifiele moleculen, die bestaan uit zowel een 'waterlievend' als een 'watervrezend' deel. Omdat de 'watervrezende' groepen van de fosfolipiden het liefst dichtbij elkaar in de buurt zitten en zo min mogelijk in aanraking willen komen met water, zal er in een waterige oplossing een liposoom ontstaan. Dit is voor deze fosfolipiden de meeste gunstige rangschikking, waarbij 'watervrezende' gedeelten naar elkaar toe wijzen en zich in de bilaag bevinden, terwijl de 'waterlievende' gedeelten naar buiten wijzen. In het binnenste van een liposoom kunnen geneesmiddelen ingesloten worden die ook van water houden, terwijl in de bilaag tussen de watervrezende staarten van de fosfolipiden, vetoplosbare geneesmiddelen gestopt kunnen worden.

De grootte van een liposoom kan erg verschillen, van tientallen nanometers (een nanometer is één miljoenste deel van een millimeter) tot enige micrometers (een micrometer is één duizendste deel van een millimeter). Als liposomen als geneesmiddel-dragersysteem gebruikt worden, ligt de grootte meestal tussen 75 en 200 nm. De grootte is namelijk erg belangrijk, omdat te grote liposomen niet op de plaats van werking terecht kunnen komen. Zie in figuur 1 een schematische weergave van een liposoom.

Om er voor te zorgen dat liposomen herkend worden door specifieke cellen, bijvoorbeeld kankercellen, en op die manier specifieker hun geneesmiddel kunnen afgeven, worden er zogenaamde targeting liganden aan de buitenkant van een liposoom gekoppeld. Dergelijke liposomen worden 'getargette' liposomen genoemd.

Opname van liposomen door cellen gebeurt via een proces dat endocytose heet. Tijdens dit proces, wat continue plaats vindt, stulpt de celmembraan in. Deze instulpingen vormen blaasjes in de cel die endosomen en in een later stadium lysosomen worden genoemd.

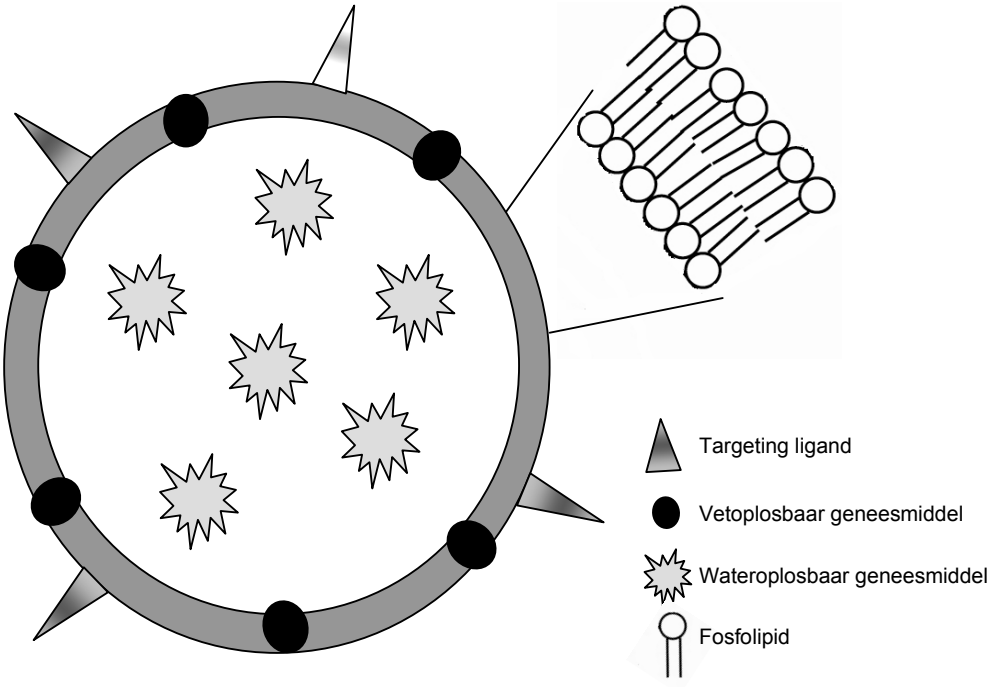

Figuur 1. Schematische weergave van een liposoom

Helaas bevinden veel aangrijpingspunten van geneesmiddelen zich niet in de endosomen en/of lysosomen. Omdat na endocytose het geneesmiddel zich in zo'n endosoom blaasje bevindt en dus eigenlijk nog steeds niet met andere cel-onderdelen in aanraking komt, moet het liposomale geneesmiddel dus uit het endosoom ontsnappen. Daarbij komt nog dat in lysosomen stoffen zitten het liposoom en het geneesmiddel afbreken.

Hoofdstuk 2 beschrijft welke strategieën in ons laboratorium zijn en/of worden onderzocht om liposomaal geneesmiddel uit het endosoom te laten ontsnappen. Een van de strategieën is afgekeken van het griepvirus. Dit virus kan heel efficiënt uit het endosoom ontsnappen om zo griep te veroorzaken. Door gebruik te maken van bepaalde componenten van dit virus, kunnen we dit nabootsen en zo liposomale geneesmiddelen te bevrijden uit het endosoom. Andere strategieën maken gebruik van cel-penetrerende peptiden (CPP) of fotochemische internalisatie. Deze laatste twee technieken staan in dit proefschrift centraal en worden hieronder uitgebreid besproken.

I. CEL-PENETRERENDE PEPTIDEN

In plaats van geneesmiddelen uit het endosoom te laten ontsnappen, zou het nog gemakkelijker zijn als er geen endocytose zou plaatsvinden, maar dat het geneesmiddel direct over het celmembraan heen de cel ingaat. Zoals al eerder gezegd, is dit niet

weggelegd voor alle geneesmiddelen omdat ze daar niet de juiste eigenschappen voor bezitten. Ook liposomen en het ingesloten geneesmiddel gaan niet zo de cel binnen. Als we nu een bepaald signaal aan het geneesmiddel of liposomen kunnen koppelen zou dit wellicht mogelijk gemaakt kunnen worden. Nu zijn er uit de literatuur dergelijke signalen bekend: zogenaamde cel-penetrerende peptiden, afgekort CPP. Deze molekulen zijn bekend geworden omdat zij niet via endocytose door cellen worden opgenomen, maar direct over het plasma membraan kunnen 'transloceren'. Het mooie hieraan is dat als een ander molecuul (geneesmiddel) of zelfs een deeltje (liposoom) aan zo'n CPP gekoppeld wordt, deze ook niet via endocytose opgenomen wordt. Helaas is er nog niet veel bekend over het werkingsmechanisme van deze CPP en bestaat er ook veel controverse over de translocatie mogelijkheden. Er zijn ook aanwijzingen dat deze CPP toch via endocytose opgenomen worden.

In **hoofdstuk 3** hebben wij daarom gekeken naar het gedrag van het CPP octa-arginine (R8). Verschillende parameters zijn gevarieerd tijdens de experimenten, zoals de temperatuur en de concentratie R8. Het bleek dat de manier waarop de leukemie cellen die we in deze experimenten gebruikten R8 opnamen, veranderde met verschillende parameters. Zo was de zogenoemde translocatie sterk actief bij lage temperaturen (4 – 19°C), terwijl bij hogere temperaturen (30-37°C) endocytose de overhand had. Ook kon de opname route veranderen van endocytose naar translocatie als de concentratie R8 verhoogd werd. Duidelijk werd, dat de opname van deze CPP dus niet eenduidig is en afhangt van een samenspel van factoren, wat het wel lastig maakt om deze moleculen te gebruiken voor het afleveren van geneesmiddelen.

In **hoofdstuk 4** is gekeken of het ook mogelijk is om een heel liposoom over het celmembraan te transloceren als er een CPP aan de buitenkant van dit liposoom gekoppeld zit. Met behulp van microscopische technieken toonden we aan in levende cellen dat de liposomen 'helaas' via endocytose opgenomen worden. Wel lieten we zien dat deze zogenoemde CPP-liposomen wel in veel hogere mate door de cellen opgenomen worden en dat dit komt door affiniteit voor bepaalde moleculen aan het oppervlak van de cel. Helaas kunnen we endocytose van liposomen dus niet voorkomen door er een CPP aan te koppelen.

In **hoofdstuk 5** lieten we zien dat het gebruik van specifieke endocytose remmers, een grote impact kan hebben op de resultaten van het experiment. Endocytose kan opgesplitst worden in verschillende typen opname-routes. In dit hoofdstuk werd gebruik gemaakt van remmers die specifiek één van de verschillende routes kunnen blokkeren. Dit is erg handig om het effect van een bepaalde route te bestuderen. Zeker in het kader van het CPP onderzoek, waarbij veel onduidelijkheid bestaat over het cellulaire opname mechanisme van CPP.

In dit hoofdstuk hebben we gebruik gemaakt van amiloride en een derivaat hiervan, EIPA. We lieten zien dat als cellen behandeld zijn met EIPA en amiloride, de distributie van endosomen en lysosomen binnen een cel verandert. Ook zagen we dat het CPP R8, ook gebruikt in hoofdstuk 3, na behandeling met EIPA, ook een volledige andere distributie binnen de cel had en dit terwijl met standaard toxiciteits testen geen waarneembaar effect te zien was. Deze resultaten laten zien dat voorzichtige interpretatie van de data gewenst is als er gebruik gemaakt wordt van remmers in combinatie met CPP.

II. FOTOCHEMISCHE INTERNALISATIE

Een recent ontwikkelde techniek, fotochemische internalisatie genoemd, maakt gebruik van lichtgevoelige stoffen, fotosensitisers, die na bestraling met licht van een bepaalde golflengte in een 'aangeslagen' toestand komen. Wanneer deze fotosensitisers terug vallen van hun 'aangeslagen' naar hun normale toestand, komt er energie vrij. Deze energie activeert zuurstofmoleculen tot zuurstofradicalen die vervolgens beschadigingen kunnen aanbrengen. Beschadigingen worden alleen aangebracht aan moleculen in dichte nabijheid van de gevormde zuurstofradicalen. Als er nu voor gezorgd wordt dat een fotosensitiser zich in of vlakbij het membraan van het endosoom bevindt, zal de beschadiging plaatsvinden aan het endosoom-membraan. Als gevolg van de beschadiging, kunnen stoffen (zoals het liposomale geneesmiddel) die zich in het endosoom bevinden, vrijkomen. Voor een schematische weergave van het principe van fotochemische internalisatie wordt verwezen naar figuur 5 in hoofdstuk 1.

In **hoofdstuk 6** hebben wij aangetoond, dat deze techniek inderdaad erg efficiënt werkt voor het afleveren van liposomale eiwit-geneesmiddelen in het cytoplasma van cellen. Het model- eiwit saporine, wat in dit hoofdstuk gebruikt werd, moet om zijn celdodende werking uit te oefenen, in het cytoplasma van een cel terecht komen. Door saporine in getargette liposomen in te sluiten werd het mogelijk om meer saporine in de cel te krijgen, maar het celdodende effect van saporine bleek zeer gering. Echter met de toepassing van de fotochemische internalisatie techniek kwam de celdodende werking van saporine volop tot uiting. De combinatie van getargette liposomen en fotochemische internalisatie bleek vele tientallen malen effectiever dan vrij saporine of saporine in niet getargette liposomen in combinatie met fotochemische internalisatie. Al met al geven deze resultaten aan dat de gecombineerde toepassing van getargette liposomen en de fotochemische internalisatie techniek veelbelovend is.

III. BORON NEUTRON CAPTURE THERAPY

Boron neutron capture therapy (BNCT) is een speciale soort van radiotherapie voor de behandeling van kanker. Het element borium komt in de natuur voor als twee isotopen, borium-10 en borium-11 welke verschillen in het aantal neutronen dat zij bezitten. Door het

borium-10 isotoop te bestralen met een bron van neutronen onstaat er een reactie, welke resulteert in de vorming van radioactieve deeltjes (zie figuur 6 in hoofdstuk 1). Deze radioactieve deeltjes kunnen kankercellen doden. Ze hebben zoals dat heet, een korte dracht, wat betekent dat ze alleen gevaar opleveren voor de cellen waarin deze deeltjes gevormd worden. De grote uitdaging van deze therapie zit hem in de grote hoeveelheid borium-atomen die afgeleverd moeten worden in de kankercel om te resulteren in een effectieve therapie. Om deze grote hoeveelheid borium-atomen af te kunnen leveren, hebben wij gebruik gemaakt van 'getargette' liposomen. Deze liposomen zijn zo ontworpen dat ze binden aan een groeifactor receptor die vooral op tumor-cellen in hoge mate aanwezig is. Daarbij moet wel gezegd worden dat ondanks het feit, dat deze receptor op kankercellen verhoogd aanwezig is, dit voor de verschillende typen kanker behoorlijk kan verschillen.

In **hoofdstuk 7** is bestudeerd of getargette liposomen een geschikt geneesmiddel-dragersysteem zijn voor BNCT. We hebben het gebruik van de getargette liposomen vergeleken met liposomen die geen tumorcel-gericht targeting ligand bezitten. Daarnaast hebben we het effect bestudeerd in geval van twee verschillende typen kankercellen, die verschillen in de mate waarin zij de groeifactor receptor bezitten. We hebben aangetoond dat boron inderdaad in voldoende hoeveelheid afgeleverd kan worden bij de kankercellen die de groeifactor receptor in grote hoeveelheden bezitten, terwijl dat niet zo is in het geval van kankercellen met weinig groeifactor receptoren. Dit kan van groot belang zijn voor de klinisch toepassing van getargette liposomen voor BNCT, omdat tumoren verschillen in de mate waarin ze de groeifactor receptor bezitten.

CONCLUSIE

In dit proefschrift zijn verschillende strategieen bestudeerd om met behulp van getargette liposomen afgifte van een geneesmiddel in de cel te verbeteren.

Het is gebleken dat het koppelen van cel-penetrerende peptide aan een liposoom niet resulteert in celmembraan translocatie maar in opname via endocytose van liposomen, terwijl met alleen peptide ook translocatie waargenomen kan worden.

Het gebruik van fotochemische internalisatie in combinatie met getargette liposomen is een succesvolle benadering om te komen tot intracellulaire afgifte van liposomale geneesmiddelen.

Bij BNCT hangt het succes van getargette liposomen af van de mate waarmee de kankercel de target receptor tot expressie brengt.

DANKWOORD

The scientific mind does not so much provide the right answers as ask the right questions
Claude Levi-Strauss

Ik ben veel dank verschuldigd aan de vele mensen die de juiste vragen wisten te stellen en mij daarnaast ook hebben gestimuleerd om dit te doen. Voor jullie dit dankwoord!

Ik zou graag willen beginnen met het bedanken van mijn promotor, Prof. dr. Gert Storm. Beste Gert, ondanks jouw enorme drukke tijdschema heb je wel de tijd gevonden om alles na te kijken en te corrigeren. Tijdens het onderzoek heb je me veel vrijheid en ruimte gegeven om mij te ontplooien. Dank hievoor!
Mijn tweede promotor, Prof. dr. Wim Jiskoot. Beste Wim, ik ben erg blij dat jij bij mijn project betrokken bent geweest. Jouw kritische kijk heeft mij altijd scherp gehouden en ik heb heel veel van je geleerd.
My co-promotor, Dr. Arwyn Jones. Dear Arwyn, it was a great pleasure to work in your lab. I learned loads from your enthusiasm and enormous creativity, and additionally Adobe Photoshop is no mystery anymore! I certainly also enjoyed the Welsh culture like the Eisteddfod, rugby and the beers! Diolch yn fawr iawn.
Wijze vragen werden ook gesteld door Prof. dr. Wim Hennink, Prof. dr. Daan Crommelin, Heren, hartelijk bedankt voor jullie raad en kennis.

Dr. Koning, beste Gerben, ik ben je grote dank verschuldigd. Naast dat je in het begin in Utrecht veel geïnvesteerd hebt om mijn project goed te laten draaien, heb je ook toen je naar Delft ging altijd grote betrokkenheid getoond. Jouw interesse en optimistische kijk op het onderzoek hebben vele van mijn onderzoeksdipjes verkleind!
Dr. Krijger, Gerard, ik heb de samenwerking voor het BNCT altijd als heel prettig ervaren en er is dan ook een mooi hoofdstuk van gekomen. Hartelijk dank voor je adviezen! Ula en Olav, heel veel dank voor het meten van het eindeloos aantal samples op de ICP. Voor de uiteindelijke bestralingsstudies zijn we uitgeweken naar het Joint Research Center in Petten en daar werden we fantastisch geholpen door Dr. Raymond Moss and Sander Nievaart.
Ook wil ik graag de inzet van Dr. Roland Pieterse en Dr. Chantal Appeldoorn even noemen. Helaas hebben de door jullie gesynthetiseerde boron-conjugaten geen plekje meer in dit boekje gekregen.

An important part of my research was not possible without the collaboration with PCI Biotech. A special thanks goes to Dr. Anders Høgset. Your interest, suggestions and your always kind and enthusiastic emails are much appreciated.

De hulp van Jack, Laura, Richard en Anko van het Centrum voor cellulaire beeldvorming heeft een grote bijdrage geleverd aan de kwaliteit van de plaatjes in dit proefschrift. Dank!

Dr. John Kruijtzer wil ik graag bedanken voor het synthetiseren van verscheidene peptides.

Zo kom je vanzelf bij je collega's! Naast al de colloquia, werkbesprekingen en proeven, was er ook genoeg tijd voor gezelligheid. Van kerstdiners, 'getting drunk for free' op de borrels , dansen in Tivoli en koffiepauzes! Iedereen – nu echt teveel om op te noemen - heeft er dan ook voor gezorgd dat ik niet met tegenzin naar mijn werk ging.
Zeker in het lab op Z509 was het dikke pret. Marieke en Cor: zonder jullie was het werk zeker veel minder leuk geweest en ben dus blij dat ik een lab met jullie gedeeld heb. Marieke, alvast heel erg bedankt dat je de 'promotie' ervaring nogmaals met mij wilt delen, deze keer als paranimf en helemaal super dat je daarvoor terug komt uit San Francisco! Cor, naast de gezelligheid op het lab was je ook altijd bereid om te helpen bij proeven. Geen liposomen batch of dierproef was je teveel. Daardoor kon zelfs het Utrecht-werk doorgaan toen ik in Cardiff was! Dank je wel.
Ik zou graag een aantal mensen nog even willen noemen: Adriënne, Martin en Marcel. Door jullie was het celkweek lab altijd goed georganiseerd en konden proeven zonder moeite uitgevoerd worden. Jullie flexibiliteit als ik weer eens niet zo heel goed gepland had, heb ik ook enorm gewaardeerd. Wijze raad en ondersteuning kwam ook zeker van Raymond en Enrico, bedankt heren. Barbara en Lidija, jullie hulp bij het invullen van alle papieren was essentieel, heel erg bedankt.

Ook mijn studenten hebben het nodig werk verzet. Ook al is er niet veel in het proeschrift gekomen, het heeft zeker zin gehad. Ricardo, you were my first student and I appreciated your hard-working mentality. Good luck with your own PhD. Magali en Ellen, ook allebei gekozen voor een carriere in de wetenschap. Zet hem op, dames!

My stay in Cardiff was a great success both scientifically and socially. The Galenos network is greatly acknowledged for the financial support and I would like to thank Dr. Mark Gumbleton for his help as Galenos coordinator in Cardiff.
A special thanks goes to Neal: you were great in the lab (and outside)! Elaine, Kerri, Lucile, Jing, Kaz, Sian, Sam, Verena, Simon, Chris, Matt, Danielle, Cath, Fran, Wendy, Alison, Baolu and Maria: Thanks for making me feel at home in and outside the lab from week one onwards!

Naast wetenschappelijke gesprekken heb je ook tijd nodig om dit alles te relativeren. Ik wil dan ook graag al mijn vriendjes en vriendinnetjes van buiten het onderzoek van harte bedanken voor al onze gezellige uitjes. Lieve cordial-genootjes, vriendinnetjes van het

Maartens, BFW-vriendjes en vriendinnetjes, basketballers en alle anderen: hopelijk volgen er nog vele gezellige feestjes en weekendjes weg.

Lieve papa, mama en Jur: ook al was het jullie niet altijd even duidelijk wat ik nu in dat lab aan het doen was, jullie hebben mij altijd gestimuleerd en gesteund. Mam, ik weet dat je blij bent dat ik de wetenschap ben ingegaan en Papa, jij bent trots dat er in Fretz-familie iemand de beta-hoek is opgegaan!
Ook mijn schoonfamilie staat altijd voor me klaar. Lieve Marja, Eddy, Evelien en Alex bedankt. Eef, helemaal te gek dat je vandaag mijn paranimf wilt zijn.

Mijn allerliefste vriendje, lieve Emiel, het was voor jou ook niet altijd makkelijk, zeker niet de laatste tijd. Ik vind het geweldig dat je met mij mee gegaan bent naar Wales en onthoud wel: jij bent diegene die mijn dagen tot een feestje maakt. Elke dag opnieuw. En dat is het allerbelangrijkste!

Dikke kus,

Marjan

CURRICULUM VITAE

Marjan Fretz werd geboren op 5 mei 1978, te ‘s Gravenhage. In 1996 werd het VWO diploma behaald aan het Sint Maartens-college te Voorburg. In datzelfde jaar begon zij met de studie Bio-Farmaceutische Wetenschappen aan de Universiteit Leiden. Van mei 2000 tot mei 2001 liep zij stage bij de Disciplinegroep Farmaceutische Technologie van het Leiden/Amsterdam Center for Drug Research (Universiteit Leiden) onder begeleiding van Dr. I.M. van der Lubben, Dr. J.C. Verhoef en Prof. H.E. Junginger. Tijdens deze stage werd onderzoek verricht naar chitosan en tri-methyl chitosan micropartikel deeltjes voor nasale vaccinatie. Een tweede onderzoekstage van 3 maanden (mei 2001 – september 2001) werd uitgevoerd binnen het farmaceutische concern AstraZeneca in Södertalje, Zweden onder begeleiding van Dr. C. Wadell. Zij heeft daar de expressie van P-glycoproteine in humaan en varkens mucosa onderzocht. In december 2001 behaalde zij het doctoraal diploma om vervolgens in februari 2002 te beginnen als Aio bij de Disciplinegroep Biofarmacie en Farmaceutische Technologie van het Utrecht Institute for Pharmaceutical Sciences (Universiteit Utrecht). Onder begeleiding van Prof. dr. G. Storm en Prof. dr. W. Jiskoot heeft zij onderzoek gedaan naar de ontwikkeling van liposoom systemen voor intracellulaire afgifte van geneesmiddelen. Met een Marie Curie/Galenos Fellowship heeft zij in het kader van haar promotie onderzoek van februari 2006 tot februari 2007 onderzoek gedaan aan de Welsh School of Pharmacy (Cardiff University) onder begeleiding van Dr. A.T. Jones. De resulaten van haar promotieonderzoek zijn beschreven in dit proefschrift.

Marjan Fretz was born on May the 5th of 1978 in The Hague, The Netherlands. She attended the Sint-Maartens college secondary school in Voorburg from 1990 to 1996, after which she started to study Bio-Pharmaceutical Sciences at the Leiden University. From May 2000 till May 2001 she preformed an undergraduate research project at the Division of Pharmaceutical Technology of the Leiden/Amsterdam Center for Drug Research (Leiden University) under supervision of Dr. I.M. van der Lubben, Dr. J.C. Verhoef and Prof. H.E. Junginger. Chitosan and tri-methyl chitosan microparticles were investigated as nasal vaccine carrier systems. A second research project was performed at AstraZeneca (Södertalje, Sweden) from May 2001 till September 2001 under supervision of Dr. C. Wadell. P-glycoprotein expression was evaluated in human and porcine nasal mucosa. In December 2001 she graduated as a MSc in Bio-Pharmaceutical Sciences. In February 2002 she started as a PhD student at the Department of Pharmaceutics of the Utrecht Institute for Pharmaceutical Sciences under supervision of Prof. dr. G. Storm and Prof. dr. W. Jiskoot. Her PhD project dealt with strategies to improve intracellular delivery by targeted liposomes. With a Marie Curie/Galenos Fellowship she stayed, as part of her PhD, from February 2006 till February 2007 at the Welsh School of Pharmacy (Cardiff University, UK) under supervision of Dr. A.T. Jones. The results of her PhD research are described in this thesis.

LIST OF PUBLICATIONS

From this thesis

M.M. Fretz, G.A. Koning, E. Mastrobattista, W. Jiskoot and G. Storm. OVCAR-3 cells internalize TAT-peptide modified liposomes by endocytosis. *Biochimica Biophysica Acta* 1665: 48-56 (2004)

M.M. Fretz, E. Mastrobattista, G.A. Koning, W. Jiskoot and G. Storm. Strategies for cytosolic delivery of liposomal macromolecules. *International Journal of Pharmaceutics.* 298: 305-309 (2005)

M.M. Fretz, J. Jin, R. Conibere, N.A. Penning, S. Al-Taei, G. Storm, S. Futaki, T. Takeuchi, I. Nakase and A.T. Jones. Effect of Na^+/H^+ exchanger inhibitors on subcellular localisation of endocytic organelles and intracellular dynamics of protein transduction domains HIV-TAT peptide and octaarginine. *Journal of Controlled Release.* 116: 247-254 (2006)

M.M. Fretz, A. Høgset, G.A. Koning, W. Jiskoot and G. Storm. Cytosolic delivery of liposomally targeted proteins induced by photochemical internalization. *Pharmaceutical Research.* Accepted for publication.

M.M. Fretz, N.A. Penning, S. Al-Taei, S. Futaki, T. Takeuchi, I. Nakase, G. Storm and A.T. Jones. Temperature, concentration and cholesterol dependent translocation of L- and D-octaarginine across the plasma and nuclear membrane of CD34+ leukaemia cells. *Biochemical Journal*. Accepted for publication.

M.M. Fretz, G.C. Krijger, U.D. Woroniecka, V.A. Nievaart, W. Jiskoot, R. Moss, G.A. Koning and G. Storm. Targeted liposomes for boron neutron capture therapy (BNCT): importance of target receptor density. *Manuscript in preparation.*

Other publications

I.M. Van der Lubben, G. Kersten, **M.M. Fretz**, C. Beuvery, J.C. Verhoef and H.E. Junginger. Chitosan microparticles for mucosal vaccination against diphtheria: oral and nasal efficacy studies. *Vaccine.* 21: 1400-1408 (2003)

A.M. Funhoff, C.F. van Nostrum, M.C. Lok, **M.M. Fretz**, D.J.A. Crommelin and W.E. Hennink. Poly(3-guanidinopropyl methacrylate): a novel cationic polymer for gene delivery. *Bioconjugate Chemistry* 15: 1212-2220 (2004)

G.A. Koning, **M.M. Fretz**, U.D. Woroniecka, G. Storm and G.C. Krijger. Targeting liposomes to tumor endothelial cells for neutron capture therapy. *Applied Radiation and Isotopes* 61: 963-967 (2004)

G.C. Krijger, **M.M. Fretz**, U.D. Woroniecka, O.M. Steinebach, W.Jiskoot, G. Storm and G.A.Koning. Tumor cell and tumor vasculature targeted liposomes for neutron capture therapy. *Radiochimica Acta*. 93: 589-593 (2005)

S. Oliveira, **M.M. Fretz**, A. Høgset, G. Storm and R.M. Schiffelers. Photochemical internalization enhances silencing of epidermal growth factor receptor trough improved endosomal escape of siRNA. *Biochimica Biophysica et Acta.* Accepted for publication

Selected abstracts

M.M. Fretz, G.A. Koning, W. Jiskoot and G. Storm. Cellular uptake of TAT-liposomes by OVCAR-3 cells: evaluation of the utake mechanism. Poster presentation at the Liposome Advances 2003, London, UK, December 2003

M.M. Fretz, G.C. Krijger, V.A. Nievaart, U.D. Woroniecka, W. Jiskoot, R. Moss, G.A. Koning and G. Storm. Targeted liposomes for boron neutron capture therapy of tumors. Selected for oral presentation at the Student Poster Highlights Session at the Annual Meeting of the Controlled Release Society, Miami, USA, June 2005

M.M. Fretz, N.A. Penning, S. Al-Taei, G. Storm, S. Futaki and A.T. Jones. Effect of temperature on the intracellular distribution of cell-penetrating peptides. Oral presentation and poster at the Biochemical Focused meeting: Cellular delivery of therapeutic macromolecules, Cardiff, UK, August 2006

LIST OF ABBREVIATIONS

ADEPT	Antibody-directed Enzyme-Prodrug therapy
$AlPcS_{2a}$	Aluminium phtalocyanine
ANOVA	Analysis of Variance
BNCT	Boron Neutron Capture Therapy
BPA	Borono-phenylalanine
BSH	Mercaptoundecahydrododecaborate
CHEMS	Cholesteryl hemisuccinate
CHOL	Cholesterol
CPP	Cell-penetrating peptides
CVPDT	Cell Viability after PDT
DHDB	Dodecahydrododecaborate
DiD	1,1'-dioctadecyl-3,3,3',3'-tetramethylindodicarbocyanine perchlorate
DMSO	Dimethyl sulfoxide
DOPE	Dioleoyl phosphatidyl ethanolamine
DOTAP	Dioleoyl trimethylammonium-propane
DPPC	Dipalmitoyl phosphatidylcholine
DSPE	Distearoyl phosphatidylethanolamine
DSPG	Dipalmitoyl succinyl glycerol
DTA	A-domain of diphtheria toxin
EEA1	Early Endosome Antigen-1
EGF	Epidermal growth factor
EGFR	Epidermal growth factor receptor
EIPA	5-(N-ethyl-N-isopropyl) amiloride
EPC	Egg phosphatidylcholine
EPR	Enhanced permeability and retention
FACS	Fluorescence activated cell sorter
FCS	Foetal calf serum
HBS	Hepes buffered saline
HER2	Human EGF-like receptor no.2
HPMA	N-(2-hydroxylpropyl)methacrylamide
ICP-OES	Inductively coupled plasma-optical emission spectroscopy
LampII	Lysosome Associated Membrane Protein-II
LET	Linear energy transfer
LLO	Listeriolysin O
mAb	Monoclonal antibody
MβCD	Methyl-β-cyclodextrin
MWCO	Molecular Weight Cut Off

NLS	Nuclear Localisation Signal
OA	Oleic acid
PBS	Phosphate buffered saline
PCI	Photochemical internalisation
PDT	Photodynamic therapy
PEG	poly(ethylene)glycol
PEI	poly(ethyleneimine)
PFA	Paraformaldehyde
PHC	N-palmitoyl homocysteine
PI	Propidium iodide
PTD	Protein transduction domain
PS	Photosensitiser
R8	Octaarginine
RES	Reticulo-endothelial system
RIP	Ribosome inactivating proteins
Rho-PE	Lissamine Rhodamine B-labeled glycerophosphoethanolamine
SATA	N-succinimidyl-S-acetylthioacetate
SFM	Serum free medium
TCV	Total Cell Viability
Tf	Transferrin
$TPPS_{2a}$	Mesotetraphenylporphine
TxR-PE	Texas Red-1,2-dihexadecanoyl-sn-glycero-3-phoshoethanolamine